12-14-2015

Hydroxy Polybenzimidazoles for High Temperature Fuel Cells and the Solution Polymerization of Polybenzimidazole

Kayley Fishel
University of South Carolina - Columbia

HYDROXY POLYBENZIMIDAZOLES FOR HIGH TEMPERATURE FUEL CELLS AND THE SOLUTION POLYMERIZATION OF POLYBENZIMIDAZOLE

by

Kayley Fishel

Bachelor of Science
University of Pittsburgh at Greensburg, 2011

Submitted in Partial Fulfillment of the Requirements

For the Degree of Doctor of Philosophy in

Chemistry

College of Arts and Sciences

University of South Carolina

2015

Accepted by:

Brian Benicewicz, Major Professor

Chuanbing Tang, Committee Member

Hui Wang, Committee Member

John Weidner, Committee Member

Lacy Ford, Senior Vice Provost and Dean of Graduate Studies

DEDICATION

In loving memory of my grandfather, William Loutsenhizer.

ACKNOWLEDGEMENTS

First and foremost I would like to thank my research advisor, Dr. Brian Benicewicz, for all of his guidance and support on my research projects. His knowledge and enthusiasm for polymer science and chemistry has greatly inspired me and I am sincerely grateful for all of the opportunities I have had while working in his group.

I would like to thank the chair of my committee, Dr. Chuanbing Tang, for his guidance and for taking an interest in my research over the last 4.5 years. I have also enjoyed being a part of his group's many fun outings. Next, I would like to thank Dr. Hui Wang and Dr. John Weidner for being a part of my committee and for providing me with guidance and valuable suggestions on my research.

I would like to thank the Benicewicz group members, both past and present, for all of their help, suggestions, and friendship. I would especially like to thank Max, Xin, Guoqing, and Alex for taking me under their wings when I first joined the group. I will never forget the many fun times we've had. I'd also like to thank Andrew Pingitore for being a great lab mate and friend. I can't imagine having to "brute force" a project like that with anyone else and I'll remember the laughs we had throughout the process. I'd like to thank the Tang group members for their support and help along the way. I look forward to continuing our friendships in the future.

Next, I would like to thank my husband who has been my greatest competition and biggest fan. I appreciate your love, support, and feedback on my work. I also

appreciate you listening to my practice-talks many times over. I'd like to thank my parents, brother, and aunt for always supporting and encouraging me and my dogs, Holly and Benji, who took turns keeping my lap warm as I wrote.

Finally, I would like to acknowledge the funding support and collaboration with BASF and PBI Performance Products.

ABSTRACT

In this dissertation, two different hompolymers of polybenzimidazole (PBI) containing hydroxyl functional units were synthesized via the PPA Process to produce gel membranes. These polymers and their phosphoric acid doped membranes were characterized to further explore structure-property relationships in functionalized PBI's. Fuel cell performance of the doped membranes was evaluated and compared to previously reported PBI membrane chemistries. Copolymers of p-OH PBI and para-PBI were prepared at five different copolymer compositions to examine the effects of hydroxy content on membrane properties and compared to the respective homopolymers. The reactivity of the hydroxy groups and the formation of phosphate bridges were important in the final properties of the doped membranes.

A new method for producing high inherent viscosity (IV) PBI directly in organic solution was studied. Initially, small molecule studies were performed in order to find appropriate chemical functionalities that allow for the formation of benzimidazole in dimethyl acetamide (DMAc). Once appropriate chemical functionalities were identified, polymerization studies were conducted to determine the critical variables for the synthesis of high molecular weight polymers. Insights on the mechanism of polymerization and complete benzimidazole ring closure were important for developing a method to produce PBI at high molecular weight and at high polymer concentrations that are relevant for the processing of films, coatings and fibers. Finally the synthesis of PBI

analogs containing an ether linkage was explored. These polymers were synthesized via the new solution polymerization method to demonstrate the utility of the method for different monomer and polymer structures. Thermal studies were performed on the ether-PBI analogs to understand the effect of the ether linkage on the potential processability of polymers.

TABLE OF CONTENTS

LIST OF TABLES

LIST OF FIGURES

LIST OF SYMBOLS

T_g glass transition temperature

wt% weight percent

List of Abbreviations

AFC ..... Alkaline Fuel Cell

DMAc ..... N,N-dimethylacetamide

DMF ..... N,N-dimethylformamide

DMSO ..... Dimethylsulfoxide

DPIP ..... Diphenylisophthalate

DSC ..... Differential Scanning Calorimetry

HTPEMFC ..... High Temperature Polymer Electrolyte Membrane Fuel Cell

IV ..... Inherent Viscosity

MEA ..... Membrane Electrode Assembly

NMP N-methyl-2-pyrrolidone

NMR ..... Nuclear Magnetic Resonance

PA ..... Phosphoric Acid

PAFC ..... Phosphoric Acid Fuel Cell

PA/PRU ..... Phosphoric Acid/Polymer Repeat Unit

PBI ..... Polybenzimidazole

PEEK ..... Polyetheretherketone

PEM ..... Proton Exchange Membrane

PPA ..... Polyphosphoric Acid

SOFC ..... Solid Oxide Fuel Cell

TAB ..... 3,3',4,4'-Tetraaminobiphenyl

TGA ..... Thermogravimetric Analysis

THF ..... Tetrahydrofuran

CHAPTER 1

GENERAL INTRODUCTION

REPRINTED IN PARTIAL WITH PERMISSION FROM SPRINGER INTERNATIONAL PUBLISHING.

* Fishel, K. J., Qian, G., Benicewicz, B.C. *PBI Membranes Via the PPA Process*; Springer International Publishing, 2016.

1.1 Fuel Cells.

The need for energy has exponentially increased as technology continues to evolve and the world population continues to grow. Due to the ever-rising demand for energy and the finite resources available, it is no surprise that alternative energy sources are needed. As costs have risen for developing and converting fossil resources to power and fuel, non-fossil options have become more attractive and economically competitive for their potential renewable and environmental benefits.[1] Alternative energy sources are considered to be energy sources that have no harmful consequences associated with them unlike fossil fuels and nuclear energy. British Petroleum and Royal Dutch Shell, two of the world's largest oil companies, estimate that by 2050, one-third the world's energy will need to be produced from alternative energy sources due to the growing population and the limited quantities of fossil fuels.[2] Several types of alternative energy sources such as solar energy, biomass energy, wind energy, geothermal energy, and hydroelectric energy, are currently being employed, however; they only account for the production of a small portion of the world's energy. One major area of interest for energy generation is from fuel cells.

In 1801, Humphry Davy first discussed the concept of a fuel cell and by 1839, William Grove, a lawyer and scientist, had developed the first fuel cell.[3] Fuel cells are electrochemical devices that convert chemical energy from fuel into electrical energy with the use of an oxidant.[4] These devices offer many advantages over other energy conversion devices, such as batteries and combustion engines. These advantages include no environmental risks, such as pollution, a broad selection of fuels, no need for recharging, and a high energy conversion efficiency (no Carnot cycle limitations).[5-7] Due to all of the benefits, fuel cells are of high interest as a clean, efficient energy source.

Though fuel cell technology is constantly evolving, Grove's model is still the basis for the electrochemical reactions. A typical hydrogen fuel cell consists of an electrolyte layer sandwiched between anode and cathode electrodes.[6] Hydrogen is split at the anode into protons and electrons. The electrons travel around an external circuit and the protons travel through the electrolyte layer. At the cathode side, the protons and electrons react with oxygen to form water. The reactions are shown below:

$$\text{Anode: } 2H_2 \rightarrow 4H^+ + 4e^-$$

$$\text{Cathode: } O_2 + 4e^- + 4H^+ \rightarrow 2H_2O$$

$$\text{Overall: } 2H_2 + O_2 \rightarrow 2H_2O$$

Many types of fuel cells have been developed based on various factors, such as, electrolyte materials, side reactions, and target applications. Fuel cells can be categorized based on electrolyte materials as follows: proton exchange membrane fuel cell (PEMFC), alkaline fuel cell (AFC), phosphoric acid fuel cell (PAFC), molten carbonate fuel cell (MCFC), and solid oxide fuel cell (SOFC). Detailed descriptions and discussions on these fuel cells can be found elsewhere.[4,8-10]

1.2 Proton Exchange Membrane Fuel Cells (PEMFC).

Proton exchange membrane fuel cells, also known as, polymer electrolyte membrane fuel cells, were first invented in the late 1950s by Willard Thomas Grubb at General Electric (GE). Another researcher at GE, Leonard Niedrach, refined the PEMFC by using platinum as a catalyst on the membrane.[8] PEMFCs have since gained much attention as promising candidates for portable power, transportation, and residential power generator applications.[11-13] These fuel cells typically contain a solid electrolyte

complex which gives many advantages over fuel cells that do not, such as, AFCs and PAFCs. Some of the advantages include: higher conductivities, a suppressed corrosion effect, and prevention of reactant gas crossover compared to liquid electrolytes. One advantage PEMFCs offer over other high temperature fuel cells, like SOFCs and MCFCs, is a fast startup time, making them suitable for applications like portable devices and automobiles.[6]

Figure 1.1 demonstrates the operational scheme of a PEMFC. Similar to the hydrogen fuel cell previously described, the hydrogen is split into protons and electrons at the anode. The electrons travel through an external circuit and the protons are transported through the polymer electrolyte membrane. Protons and electrons combine with oxygen at the cathode to produce water and heat.

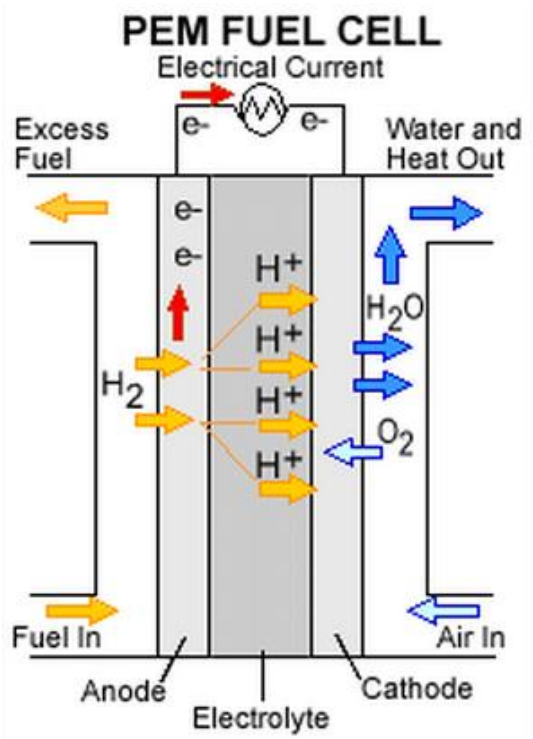

Figure 1.1: The basic operation of a fuel cell using hydrogen as fuel and air as oxidant[14]

The heart of the PEMFC is the membrane electrode assembly (MEA), which consists of the anode electrode, the polymer electrolyte membrane, and the cathode electrode. The MEA is then built into the fuel cell with other components such as: graphite plates, gas diffusion layers, gaskets, and endplates, as seen in Figure 1.2.

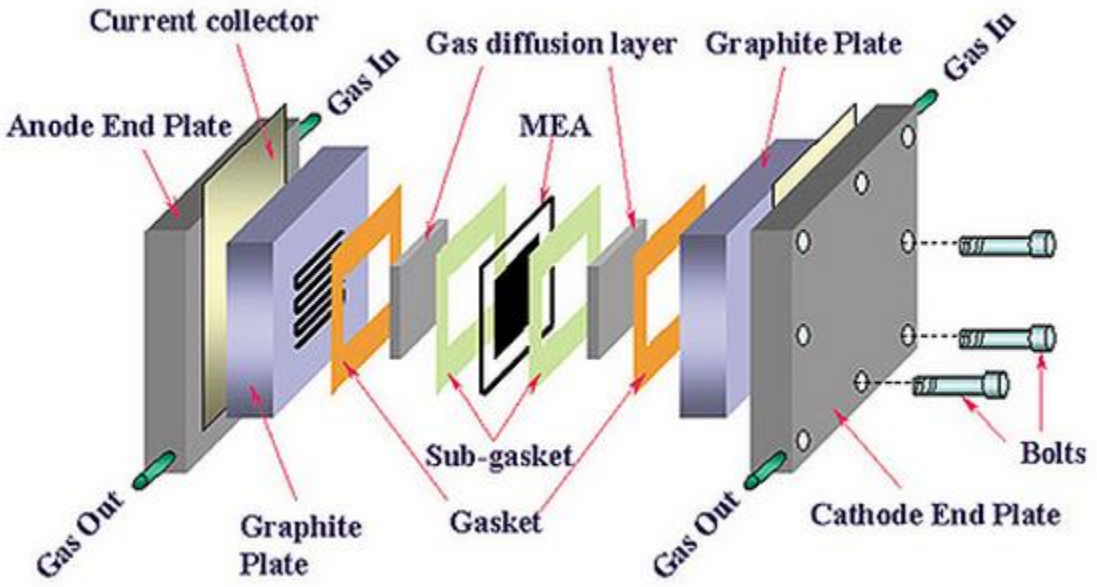

Figure 1.2: Fuel cell components

The efficiency of a PEMFC is largely dependent on the materials and their arrangements within the cell. Various types of catalysts, membranes, electrodes, and dopants can all be used under different operational conditions within the fuel cell.

The components of the fuel cell largely affect the temperature at which the fuel cell operates. Cells that use membranes containing low boiling point electrolytes, such as water, typically operate at 60-80 °C and large heat exchangers are required to ensure the electrolyte is not boiled off. This results in a complex system consisting of extra components and controls to maintain operation. Another issue associated with fuel cells that operate at low temperatures is the need for an extremely pure fuel source. If reformate impurities are present within the fuel source, they competitively and

irreversibly bind to and poison the catalyst. Once the catalyst is poisoned, fuel cell performance drops dramatically.

Some of the disadvantages associated with operating PEMFCs at low temperatures can be overcome when operating at high temperatures (120-200 °C). To operate at high temperatures, electrolytes with high boiling points, such as phosphoric acid and sulfuric acid, are employed. Smaller heat exchangers can be used since there is less risk of boiling off the electrolyte resulting in a less complex design than seen with low temperature PEMFCs. A large advantage of high temperature operation is the reversible binding of reformate impurities to the catalyst. For this reason, less pure fuel sources can be used without risking the performance of the fuel cell. Having the ability to use less pure fuel sources leads to lower costs associated with reformation. Faster electrode kinetics and operating abilities of the fuel cell also improve at high temperatures.[16] The research reported herein will focus on polybenzimidazole-based high temperature PEMFCs.

1.3 Polybenzimidazoles.

Polybenzimidazoles (PBI) are a class of heterocyclic polymers that were first invented in 1959.[17] The general structure of PBI can be seen in Figure 1.3. Since then a variety of polybenzimidazoles has been synthesized, however, aromatic polybenzimidazoles have gained the most attention due to their thermal stability and chemical resistance.

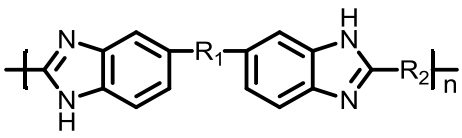

Figure 1.3: General Structure of Polybenzimidazole

In the early 1960s, polybenzimidazole fibers were synthesized in a joint effort of the United States Air Force Materials Laboratory with Dupont and the Celanese Research Company. Poly(2,2'-*m*-phenylene-5,5'-bibenzimidazole), or meta-PBI, as seen in Figure 1.4, was one of the first PBI chemistries to be heavily investigated. This polymer is not only thermally stable, chemically resistant, and non-flammable, but can be spun into fibers, which has led to its use in fireman coats and astronaut space suits.

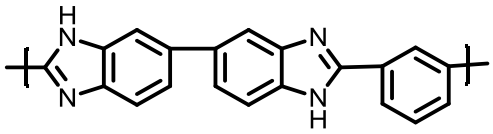

Figure 1.4: Meta-PBI

Acid-imbibed polybenzimidazoles are excellent membranes to be used in high temperature PEMFCs. These membranes are efficient proton conductors and are able to withstand the high operating temperatures. The thermal stability of these PBIs is attributed to the rigid, aromatic structure of the backbone.[18] The acid acts as the electrolyte allowing the protons to be transported from the anode to the cathode and the membrane acts as a barrier that prevents gas crossover. The acid electrolyte and the PBI membrane interact through the proton donor and acceptor sites along the backbone of the polybenzimidazole. This complex forms a network through which protons can be transported. The phosphoric acid transports protons using a Grotthuss-type mechanism which enables the protons to "hop" from the anode to cathode. The high conductivity and thermal stability of phosphoric acid and sulfuric acid make them great electrolytes for use in high temperature applications. It is vital for PBI to be doped with electrolyte as PBI itself has a negligible conductivity.

1.4 Synthesis of Polybenzimidazole.

Polybenzimidazoles are synthesized through a polycondensation reaction. A variety of methods to synthesize PBI has been reported; however, two are commonly employed and industrially used. The reaction of 3,3',4,4'-tetraaminobiphenyl (TAB) and terephthalic acid monomers are polymerized in PPA to produce para-PBI, as shown in Scheme 1.1. Polyphosphoric acid acts as both an acid catalyst and the solvent for the reaction.[16] This synthetic route is used by BASF to produce Celtec-P, a polymer electrolyte membrane. Polymerizations conducted in PPA have shown excellent results for fuel cell membrane synthesis and will be discussed in depth later.

Scheme 1.1: Synthesis of Para-PBI via Polycondensation of TAB and Terephthalic Acid

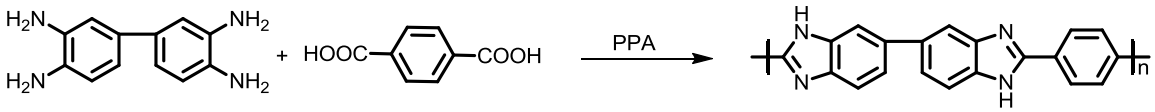

Scheme 1.2 shows the method used by PBI Performance Products to synthesize meta-PBI by the condensation of TAB and diphenylisophthalate (DPIP) which is subsequently used to produce fibers. The polymerization is conducted through a two-step melt/solid process which generates phenol and water as byproducts.[19] The solid polymer can then be dissolved in a dimethyl acetamide/ lithium chloride mixture and spun into high performance fibers. Though these two methods are the most commonly utilized, other synthetic pathways to PBI have been reported.

The synthesis of benzimidazole and its derivatives are well-known and can be applied to difunctional systems for polymers, however, the solubility limitations of these

aromatic chains needs to be taken into account. PBI contains both donor and acceptor sites that allow for specific interactions with polar solvents, however, PBI is practically insoluble in most organic solvents. In 1974, meta-PBI was synthesized through a mixed solvent system of sulfolane and phenyl sulfone. The product was confirmed and inherent viscosities up to 0.69 dL/g were achieved, however, polymerizations were performed at low concentrations.[20] In another report, ortho-esters were reacted with a tetra-amine in dimethyl sulfoxide (DMSO) at 100 °C to produce polybenzimidazole, however, only low molecular weight polymer could be achieved.[21] The synthesis of PBI has also been performed in Eaton's Reagent[22] (phosphorous pentoxide in methane sulfonic acid) and through Higashi phosphorylation,[23] though neither of these methods is as commonly used as the first two methods.

Scheme 1.2: Synthesis of Meta-PBI via Melt/Solid Polymerization

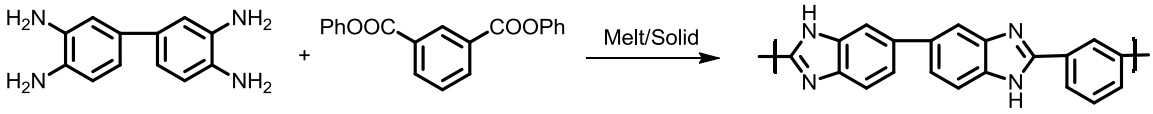

1.5 Methods of Membrane Preparation.

Polyphosphoric acid (PPA) has long been used as a polymerization solvent. Its ability to be used at high temperatures and lack of side reactions and tar formation in the presence of organics has proven useful in polymer syntheses that require high temperatures for condensations, ring closure and aromaticity formation[24]. Thermally stable polymers, such as polybenzothiazoles, polyquinazolines, and polybenzimidazoles, have all been successfully synthesized in PPA.[25,26] PBI polymer and fibers have typically been produced through a two-step melt/solid polycondensation processes and spun from solutions of DMAc at concentrations over 20 wt % polymer as reported by Celanese and

Conciatori et al.[25,27] Although the solubility of PBI in PPA would not allow for this high wt % of polymer to be dissolved for fiber production, PBI has sufficient solubility in PPA in order to produce films. For this reason, PPA is used as the polymerization solvent in both the conventional method of film formation and in the PPA Process. The methods through which polybenzimidazole membranes are processed have been found to greatly affect the properties and morphology of the membrane. Differences in acid loading, conductivity, mechanical properties, inherent viscosity, and fuel cell performance have been shown to vary depending on the synthesis and processing method. Two methods of processing have been shown to produce greater conductivity than the conventional imbibing method. Recent reviews by Savinell, Bjerrum, Li, Benicewicz, and Schmidt discuss polybenzimidazole membranes for fuel cells prepared by many different methods.[28,29] Though all methods will be briefly covered, the work presented hereafter will focus on the preparation, properties and fuel cell performance of acid-doped membranes made by a unique sol-gel method termed the PPA Process.

1.5.1 Conventional Method.

The conventional acid imbibing method consists of a multi-step process in which the polymerization takes place in an organic solvent such as dimethyl acetamide (DMAc) that may contain lithium chloride (LiCl). The solution is then cast as a film and the solvents are allowed to evaporate. Once solvent has evaporated, the PBI film is washed with water to remove residual DMAc and LiCl and is then doped with phosphoric acid (PA) by means of an acid bath. The full process is schematically shown in Figure 1.5.[30]

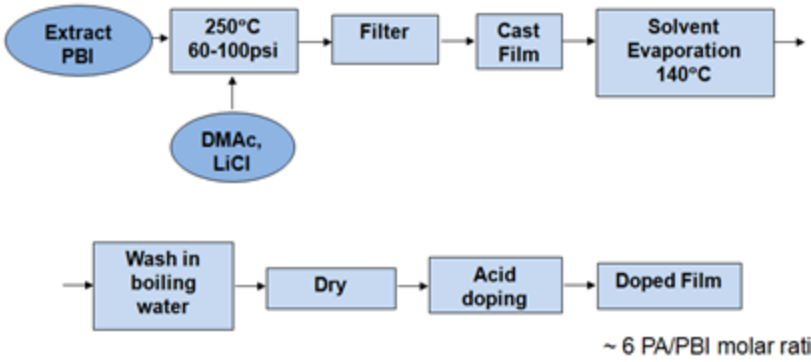

Figure 1.5: Conventional Imbibing Process of PBI Membranes with PA

1.5.2 Porous PBI.

Another method of imbibing PBI with PA was published in 2004. In this method, a porous PBI film is created by casting a solution containing PBI and a porogen (phthalates or phosphates) onto a glass plate. The film is dried and the porogen-plasticizer is removed by soaking the membrane in methanol.[31] The membrane is then removed from the methanol and completely dried. Once dried, the porous membrane is immersed in a concentrated phosphoric acid solution for four days and is dried via blotting, as shown in Figure 1.6. This process is both tedious and time consuming.

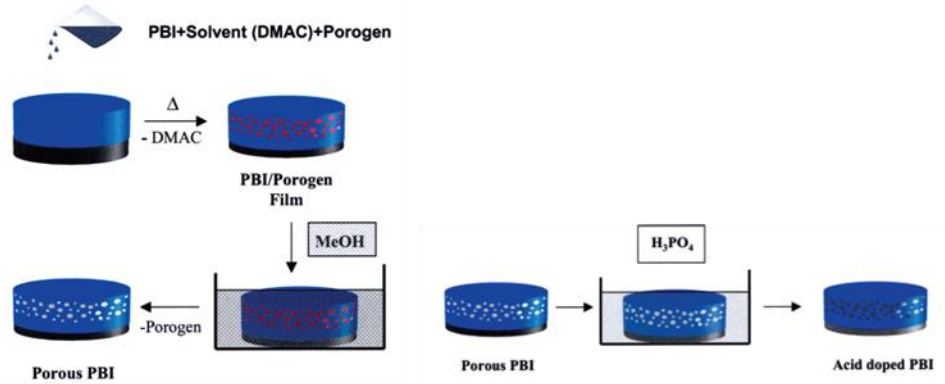

Figure 1.6: Imbibing Process of Porous PBI with PA[31]

Although PBI membranes were imbibed with PA through these methods, the membranes from these processes demonstrated poor mechanical properties at high PA

doping levels. Due to the substandard properties of these membranes, they exhibited high rates of PA loss during fuel cell operation, poor mechanical properties, or failed to operate altogether.[16,31]

1.5.3 The Sol-Gel Process.*

In 2005, Benicewicz et al. (in cooperation with BASF Fuel Cell GmbH) reported a new method for producing polybenzimidazole films imbibed with phosphoric acid.[16] This process, termed the PPA Process, represents a sol-gel process that utilizes polyphosphoric acid (PPA) as both the polymerization medium and the casting solvent for PBI polymers. In the PPA Process, dicarboxylic acids and tetramines such as 3,3',4,4'-tetraaminobiphenyl (TAB) (or AB type monomers) are polymerized in PPA between 195 and 220 °C to produce high molecular weight PBI polymers. After polymerization, the PPA solution containing PBI is directly cast onto glass plates or other suitable substrates. Since both PBI and PPA are hygroscopic, moisture from the surrounding environment readily hydrolyzes the PPA to phosphoric acid (PA). A sol-to-gel transition can occur which is attributed to the change in the nature of the solvent, i.e., many PBIs show higher solubility in PPA and poorer solubility in phosphoric acid. This process encompasses many favorable attributes. For example, high molecular weight polymer (typically determined through inherent viscosity measurements) can be readily produced using the PPA Process. Since the process does not use organic solvents for the polymerization or casting steps, the PPA process eliminates the cost of such solvents, worker exposure, and solvent recovery and disposal costs. Also, separate unit operations for imbibing are not needed as the solvent is transformed into the dopant as part of the process. Acid-doped PBI membranes produced through the PPA Process also

demonstrate greater mechanical properties with greater acid loadings and higher conductivities than membranes formed through other methods.[16]

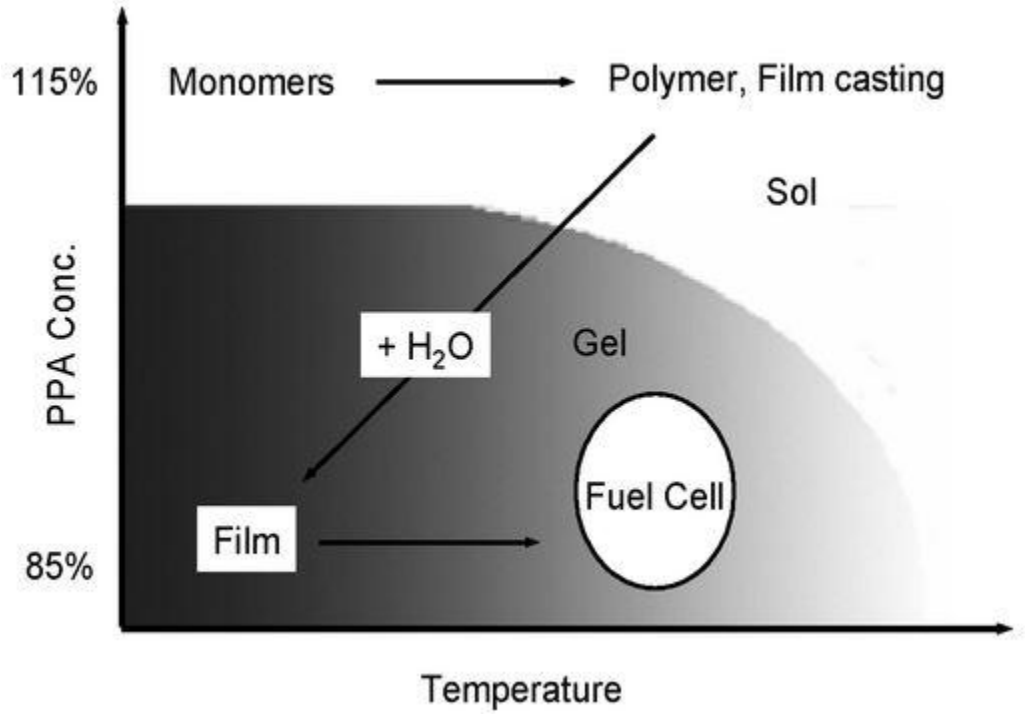

Figure 1.7: The Sol-Gel State Diagram[16]

Figure 1.7 provides a summary of the multiple chemical and physical transformations that occur in the PPA process. Preliminary simulations by Padmanabhan and Kumar of the phase behavior and formation of a physical gel from semiflexible polymer chains provides some insights into the process.[32,33] Increases in chain stiffness of semiflexible polymer chains will increase chain association in solution and are likely to play a role in the formation of reversible gels with liquid crystalline-like order. Molecular dynamics simulations have also indicated that chain stiffness, depth and rate of the temperature change, and the additional quench provided by the solvent quality (via PPA hydrolysis) result in the transformation of a homogeneous solution into a trapped, three dimensional network of nematic-like bundles forming a percolated gel as shown in

Figure 1.8. Many of the predictions from these simulations are consistent with the observations made over the past 10-15 years.

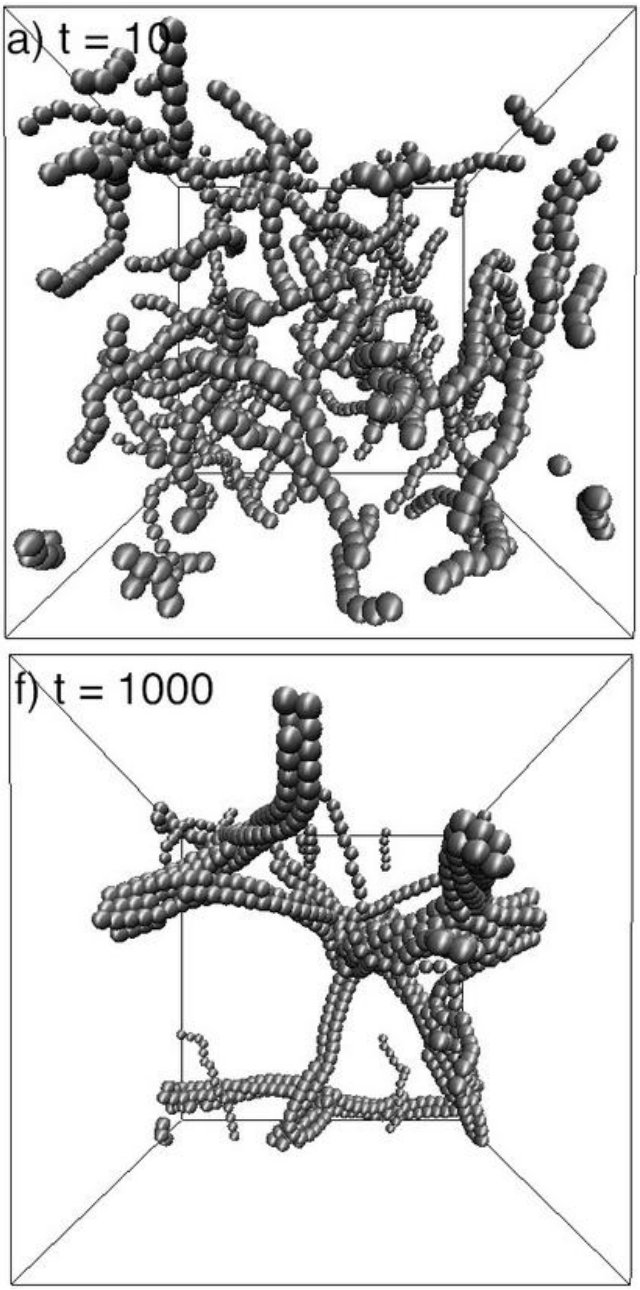

Figure 1.8: Simulation of a) isotropic homogenous solution of polymer chains and f) dynamically arrested network of nematic-like bundles after thermally quenching the system [33]

1.5.4 Direct Acid Casting.

Researchers at Case Western Reserve University reported a method for casting PBI films directly from acid solutions.[34] This Direct Acid Casting method was performed by initially dissolving PBI in trifluoroacetic acid (TFA). Phosphoric acid was then added to create a single-phase solution which was filtered and cast onto untreated glass plates. The film was heated at 140 °C for 15 minutes in air. Finally, the film was removed from the glass plate and heated in a vacuum oven overnight to produce a dry film. Just as PBI prepared through the PPA Process exhibits different properties than PBI prepared through the conventional imbibing method, PBI films produced from Direct Acid Casting also display unique properties. It was commonly observed that PBI films prepared through conventional imbibing are tougher and stronger than those prepared by Direct Acid Casting.[35] It was reported that PBI of high inherent viscosity must be used for films cast from TFA to produce films of reasonable strength.[35]

1.5.5 Conductivities and Acid Content.

Since the processing method greatly affects the properties of the PBI films, differences in phosphoric acid content and conductivities vary among the PPA Process, Direct Casting, and traditional casting from DMAc even with identical PBI chemistry. When meta-PBI was cast from DMAc and doped in PA baths, conductivities ranged from 0.01-0.05 S/cm.[30,34] Savinell et al. found that by casting from trifluoroacetic acid rather than DMAc, conductivities for meta-PBI membranes could reach as high as 0.083 S/cm.[34] This is a significant increase from the traditional casting/imbibing method and demonstrates the influence the processing method has on the membrane properties, such as conductivity. Conductivities for meta-PBI can be significantly increased when membranes are prepared through the PPA Process. Perry et al. reported conductivities for

meta-PBI membranes made via the PPA Process of 0.13 S/cm.[30] This is nearly a 3-fold improvement from films cast from DMAc and almost double the conductivity of films cast from trifluoroacetic acid. The PPA Process produces membranes that contain more acid than those prepared from conventional imbibing. Acid loadings of 14-26 moles PA/ moles polymer repeat unit (PRU) were reported for meta-PBI membranes prepared through the PPA Process and 6-10 moles PA/PRU when prepared by conventional DMAc casting and PA imbibing.[36] Additionally, the membranes prepared by the conventionally imbibed technique and PPA Process exhibited fundamentally different responses of ionic conductivity on acid doping level.

1.6 Variations in PBI Chemistry.

The properties of the polymer gel film are not only affected by processing and morphology, but also by the chemistry of the PBI polymers. The chemistry of the polymer affects acid doping levels, conductivities, mechanical properties, and the polymer solids content. Many PBI chemistries can be synthesized through the PPA Process by varying the chemistry of the monomers and the combination of monomers used. The ability to prepare and process many different PBI chemistries using the PPA Process is a great advantage because it is less restricted by polymer solubility issues. The properties of these PBI membranes have been thoroughly studied to evaluate structure-property relationships and ultimately to enhance their properties for use in HT-PEM fuel cells. Table 1.1 shows the properties of various chemistries of homopolymers prepared using the PPA Process.

Table 1.1: Properties of various chemistries of PBI prepared through the PPA Process.

PBI chemistry	Structure of Polymer Repeat Unit	Monomer Charges (wt %) Tested via PPA Process	Inherent Viscosity ranges (dL/g)	~Membrane Acid loading (mols PA/mol PRU)	Conductivity (S/cm) @ 180 °C	Ref
Meta-PBI	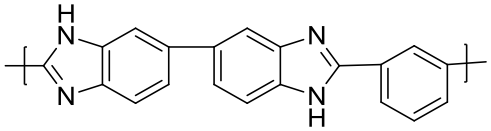	2-12	0.8-2.3	14-26	0.13	[37]
Para-PBI	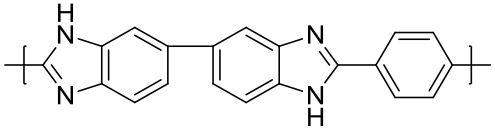	1-5	0.3-2.9	30-40	0.25	[38]
Sulfonated-PBI	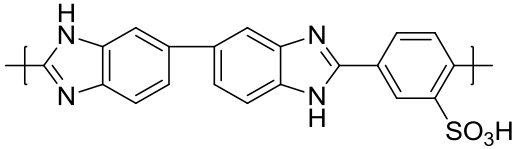	2.48-7.4	1.03-1.71	28-53	0.33	[39]
AB-PBI	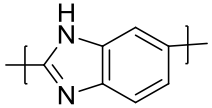	N/A	≤ 10.0	22-35	N/A	[40]
i-AB-PBI	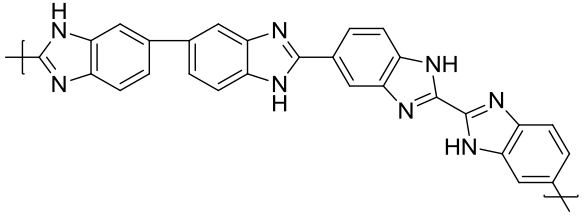	2.9-8.2	1.0-3.1	24-37	0.2	[41]

2,5-pyridine PBI	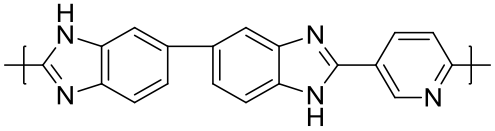	4-18*	0.8-3.1	15-25	0.22	[42]
3,5-pyridine PBI	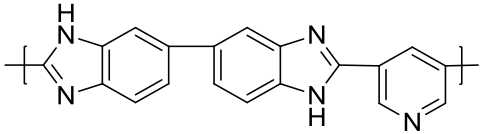	4-20*	0.6-3.1	N/A	N/A	[42]
2,6-pyridine PBI	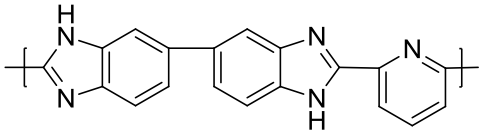	~7*	0.2-1.3	8-10	0.1	[42]
2,4-pyridine PBI	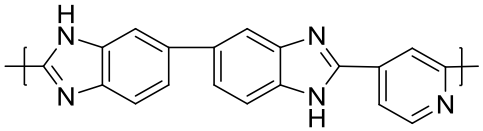	~7*	0.3-1.00	N/A	N/A	[42]

N/A= film was too unstable to test, *= Polymer concentration

1.7 Research Objectives.

The objectives of the projects discussed in this dissertation focus on new chemistries of polybenzimidazole, as well as a new method to synthesize high molecular weight PBI's in an organic solvent. New PBI polymers were synthesized and characterized in order to form structure-property relationships and to better understand how to prepare polymers with specific properties. A new synthetic approach that allows for the polymerization of high molecular weight PBI's under commercially relevant conditions is also reported.

1.7.1 Hydroxy-PBI Homopolymers and Copolymers.

It is well known that by altering the chemistry of a polymer, you can greatly change the polymer's properties. In previous work, a PBI chemistry containing hydroxyl functional units along the backbone had demonstrated interesting properties compared to PBIs of other chemistries, such as high conductivity and low compliance creep.[43] Chapter 2 discusses two novel hydroxy-PBI analogs that were synthesized in order to further explore structure-property relationships in hydroxyl containing PBI's that had the potential to be used in high temperature PEMFCs. These new hydroxyl functionalized PBI chemistries contained only one hydroxy group per repeat unit and also examined the role of chain stiffness on properties. The formation of phosphate bridges and phosphate-ester linkages during the polymerization in polyphosphoric acid and in the final cast membranes was also investigated. Characterization of the polymers and cast membranes was conducted to establish structure-property relationships and fuel cell performance was evaluated to determine if these new chemistries would be good candidates as the electrolyte membrane in fuel cells.

PBI copolymer systems have shown interesting properties in the past and have been used as a convenient method to modify membrane properties. For this reason, Chapter 3 focuses on the preparation and characterization of a copolymer series of p-OH PBI and para-PBI at five different ratios and was compared to each homopolymer. The films' properties were assessed to correlate copolymer composition with the mechanical properties, conductivity, and overall fuel cell performance. By performing this study at a constant monomer concentration but varying copolymer composition, the isolated effects of copolymer composition on membrane properties were studied.

1.7.2 Solution Polymerization of PBI.

Many polymerization methods for polybenzimidazole have been previously reported; however, a synthetic technique to produce high molecular weight PBI directly in an organic solvent had not been reported. Chapter 4 discusses a method to produce high IV meta-PBI directly in DMAc solutions. This is an important advancement in the synthesis of this polymer, as PBI fibers are spun commercially from DMAc. This work discusses the synthetic approaches that were taken to develop monomers with proper functionalities to produce benzimidazole directly in DMAc. Several key variables were explored in these polymerizations studies. In the first part of this chapter, small molecule studies were performed in order to determine the chemical functionalities that could successfully produce benzimidazole directly in DMAc in a reasonable amount of time and with little or no side products. Once monomers with appropriate functionalities were identified, the polymerization concentration was carefully studied to determine the appropriate concentration ranges that produced high IV PBI. Additional experiments

were conducted to identify reaction conditions that affected ultimate molecular weight and were explained in terms of a polymerization mechanism for this polymerization.

Since the previously discussed solution polymerization method is not limited to the synthesis of just meta-PBI, this method was used to produce PBI analogs that contain ether linkages. PBI's containing an ether linkage were of great interest due to the increased backbone flexibility. As previously discussed, fully aromatic PBIs have excellent thermal properties which leads to many advantages in high temperature applications, however, fully aromatic PBIs are extremely difficult to process due to their high Tg's. Chapter 5 discusses the synthesis of novel monomers to produce two ether PBI chemistries via the new solution polymerization method. The resulting ether-PBIs were then characterized with a specific focus on their thermal properties and compared to meta-PBI also produced via the solution polymerization.

1.8 References.

(1) In *Hard Truths: Facing the Hard Truths about Energy*; National Petroleum Council: 2007, p 89.

(2) In *http://www.altenergy.org/* 2015.

(3) Grove, W. R. *London and Edinburgh Philosophical Magazine and Journal of Science* **1839**, *14*, 127.

(4) Hirschenhofer, J. H., Stauffer, D.B., Engleman, R.R., Klett, M.G., In *Fuel Cell Handbook*; 4 ed.; EG&G Technical Services, I., Ed.; Parsons Corporation: Reading, PA, 1998; Vol. 4, p 1.

(5) Yeager, E. *Science* **1961**, *134*, 1178.

(6) Larminie, J., Dicks, A., McDonald, M., In *Fuel Cell Systems Explained*; Wiley Chichester: Hoboken, NJ, 2003; Vol. 2, p 433.

(7) Srinivasan, S. *From Fundamentals to Applications*; 1 ed.; Springer, 2006.

(8) Carter, D., Ryan, M., Wing, J. The Fuel Cell Industry Review. *Fuel Cell Today: History* [Online Early Access]. Published Online: 2012. http://www.fuelcelltoday.com/about-fuel-cells/history.

(9) Appleby, A. J. *Journal of Power Sources* **1990**, *29*, 3.

(10) Bacon, F. T. *Electrochimica Acta* **1969**, *14*, 569.

(11) Böddeker, K. W., Peinemann, K. V., Nunes, S. P., *Journal of Membrane Science* **2001**, *185*, 1.

(12) Costamagna, P., Srinivasan, S., *Journal of Power Sources* **2001**, *102*, 253.
(13) Costamagna, P., Srinivasan, S., *Journal of Power Sources* **2001**, *102*, 242.
(14) NIST www.NIST.com.
(15) White, D. M., Takekoshi, T., Williams, F. J., Relles, H. M., Donahue, P. E., Klopfer, H. J., Loucks, G. R., Manello, J. S., Matthews, R. O., Schluenz, R. W. *Journal of Polymer Science: Polymer Chemistry Edition* **1981**, *19*, 1635.
(16) Xiao, L., Zhang, H., Scanlon, E., Ramanathan, L. S., Choe, E., Rogers, D., Apple, T., Benicewicz, B.C., *Chemistry of Materials* **2005**, *17*, 5328.
(17) Brinker, K. C., Cameron, D. D., Robinson, I. M., U.S. Patent #2904537, 1959.
(18) Wainright, J. S., Wang, J. T., Weng, D., Savinell, R. F., Litt, M., *Journal of The Electrochemical Society* **1995**, *142*, L121.
(19) Sandor, R. B. *PBI (Polybenzimidazole): Synthesis, Properties, and Applications* **1990**, *2*, 25.
(20) Hedberg, F. L., Marvel, C. S. *Journal of Polymer Science: Polymer Chemistry Edition* **1974**, *12*, 1823.
(21) Dudgeon, C. D., Vogl, O. *Journal of Polymer Science: Polymer Chemistry Edition* **1978**, *16*, 1831.
(22) Jouanneau, J., Mercier, R., Gonon, L., Gebel, G., *Macromolecules* **2007**, *40*, 983.
(23) Yamazaki, N., Higashi, F., *Journal of Polymer Science: Polymer Letters Addition* **1974** *12*, 185.
(24) Popp, F., McEwen, W., *Chemical Reviews* **1959**, *58*, 321.
(25) Yang H *Aromatic high-strength fibers*; John Wiley and Sons: New York, 1989.
(26) Cassidy P *Thermally stable polymers*; Marcel Dekker, Inc.: New York, 1980.
(27) Conciatori A, Buckley A, Stuetz D, *Polybenzimidazole fibers*; Marcel Dekker: New York, 1985.
(28) Molleo, M., Schmidt, T., Benicewicz, B.C. In *Encyclopedia of Sustainability, Science and Technology*; Meyers, R. A., Ed.; Springer Science + Business Media LLC: New York, 391-431, 2013.
(29) Li Q, Jennsen J, Savinell R, Bjerrum, *Progress in Polymer Science* **2009**, *34*, 449.
(30) Perry, K. A., More, K.L, Payzant, A., Meisner, R.A., Sumpter, B.G., Benicewicz, B.C. *Journal of Polymer Science Part B: Polymer Physics* **2014**, *52*, 26.
(31) Mecerreyes, D., Grande, H., Miguel, O., Ochoteco, E., Marcilla, R., Cantero, I., *Chemistry of Materials* **2004**, *16*, 604.
(32) Padmanabhan, V., Kumar, S., Yethiraj, A., *The Journal of Chemical Physics* **2008**, *128*.
(33) Padmanabhan, V., Kumar, S., *The Journal of Chemical Physics* **2011**, *134*.
(34) Savinell, R., Litt, M., US Patent #6,099,988, 2000.
(35) Ma, Y., Wainright, J., Litt, M., Savinell, R., *Journal of The Electrochemical Society* **2004**, *151*, A8.
(36) Perry, K. A., More, K.L, Payzant, A., Meisner, R.A., Sumpter, B.G., Benicewicz, B.C. *Journal of Polymer Science Part B: Polymer Physics* **2014**, *52*, 26.

(37) Mader, J., Xiao, L., Schmidt, T., Benicewicz, B.C., In *Fuel Cells II*; Scherer, G., Ed.; Springer Berlin Heidelberg: 2008; Vol. 216, p 63.

(38) Yu, S., Zhang, H., Xiao, L., Choe, E. W., Benicewicz, B. C. *Fuel Cells* **2009**, *9*, 318.

(39) Mader, J., Benicewicz, B.C., *Macromolecules* **2010**, *43*, 6706.

(40) Yu, S. In *Ph. D. Thesis, Rensselaer Polytechnic Institute*; Doctor of Philosophy: 2006.

(41) Gulledge, A., Gu, B., Benicewicz, B. *Journal of Polymer Science Part A: Polymer Chemistry* **2012**, *50*, 306.

(42) Xiao, L., Zhang, H., Jana, T., Scanlon, E., Chen, R., Choe, E., Ramanathan, L., Yu, S., Benicewicz, B.C., *Fuel Cells* **2005**, *5*, 287.

(43) Yu, S., Benicewicz, B.C. *Macromolecules* **2009**, *42*, 8640.

CHAPTER 2

SYNTHESIS AND CHARACTERIZATION OF TWO NOVEL MONOHYDROXY POLYBENZIMIDAZOLES FOR HIGH TEMPERATURE POLYMER ELECTROLYTE MEMBRANE FUEL CELL APPLICATIONS

2.1 Abstract.

Two novel polybenzimidazole (PBI) homopolymers, poly(2,2'-(2-hydroxy-1,4-phenylene)5,5'-bibenzimidazole (p-OH PBI) and poly(2,2'-(5-hydroxy-m-phenylene)-5,5-bibenzimidazole (m-OH PBI), each containing a single hydroxyl group per repeat unit, were synthesized and characterized. Previous work investigated a para-oriented PBI analog that contained two hydroxyl groups per repeat unit. This polymer demonstrated high conductivity but had limited solubility in polyphosphoric acid (PPA) due crosslinks formed by phosphate bridges between hydroxyl units. These new hydroxy-containing PBIs were evaluated to determine if high conductivities could be maintained while simultaneously increasing the solubility of the polymer by lowering the number of potential phosphate bridges. Polymer films were tested for acid content, conductivity, mechanical properties, and overall fuel cell performance. From the data, structure-property relationships were formed and membranes were evaluated for use in high temperature fuel cell applications.

2.2 Introduction.

Through the evolution of technology and with the rapid increase in global population, the demand for energy has exponentially increased. High-Temperature Polymer Electrolyte Membrane Fuel Cells (HTPEMFCs) have gained increasing attention due to their abilities to efficiently produce clean energy without many of the problems observed with low temperature devices. Faster electrode kinetics, reduced catalyst poisoning due to reversible binding, and simplified design are all benefits seen in high temperature devices (>120 °C).[1] Polybenzimidazoles (PBI) imbibed with phosphoric acid have long been known to be excellent candidates as the polymer

electrolyte membrane in HTPEMFCs due to their affordability and excellent performance. These gel membranes demonstrate high ionic conductivities, thermal and oxidative stability, and relatively no osmotic drag.[2-4]

Polybenzimidazole films imbibed with phosphoric acid have been produced through various methods. The traditional method of film formation involves dissolving the PBI in an appropriate solvent, typically dimethyl acetamide (DMAc) with LiCl or trifluoroacetic acid, and casting the film.[3,5,6] The PBI film can then be placed in a phosphoric acid (PA) bath for imbibing. Meta-PBI is the most commonly synthesized chemistry of polybenzimidazole produced through the traditional method due to the commercial availability of the polymer and the solubility limitations associated with these solvents.[7] Meta-PBI films doped with PA produced via this method have reportedly demonstrated conductivities ranging from 0.01-0.05 S/cm.[8,9]

A new method of synthesizing PBI films imbibed with PA was reported by Benicewicz et al. in 2005.[10] This process, termed the Sol-Gel Process or PPA Process, polymerizes PBI directly in polyphosphoric acid (PPA) at high temperatures (195-220°C). The hot solution is taken and cast directly onto glass plates using a Gardner blade. The PPA (an excellent solvent for PBI) is hydrolyzed to PA (a poor solvent for PBI) from the moisture in the air, thereby, inducing the solution to gel transition. The result is a PBI membrane already imbibed with phosphoric acid. This method has many benefits compared to the traditional method of synthesis, such as, fewer steps and less solvent exposure for workers. Not only is the process beneficial, the resulting membranes prepared through the PPA Process demonstrate better properties than those prepared via the conventional method. Higher acid loadings, increased conductivity, and better

mechanical properties are all a result of the PPA Process.[8,10] One of the greatest advantages this method has over the traditional method is the ability to produce new chemistries of PBI since the solubility limits associated with PBI in DMAc and trifluoracetic acid do not apply to this process. For this reason, many chemistries of PBI have been synthesized via this method in order to form structure-property relationships to target property improvements.[11-13]

In 2009, Yu et al. reported the synthesis of Poly(2,2'-(2,5-dihydroxy-1,4-phenylene)5,5'-bibenzimidazole) (2OH-PBI) via the PPA Process.[7] These membranes demonstrated interesting properties attributed to the chemistry of the polymer. Previous reports have suggested that rigid-rod polymers containing hydroxyl units and nitrogen-containing heterocycles can strongly hydrogen bond and form network structures.[14-17] These 2OH-PBI films had higher acid loadings and demonstrated significantly higher conductivity than traditional para-PBI prepared via the PPA Process (0.35 S/cm vs 0.27 S/cm).[7,10] Though this new chemistry led to improvement in conductivity and an overall good fuel cell performance, the 2OH-PBI demonstrated a lower solubility in PPA than para-PBI, leading to membranes with lower polymer solids and lower tensile properties. The low solubility is attributed to the formation of the phosphate bridges which cause crosslinking between chains which are formed during polymerization at high temperatures in PPA.[7] The hydroxyl units along the backbone can form phosphate bridges between hydroxyl units, thereby, crosslinking the chains. Small molecule studies and other reports of polymerizations done in PPA have confirmed the formation of phosphate-ester linkages and phosphate bridges between hydroxyl units.[18]

This new work focuses on the synthesis and characterization of two novel PBI homopolymers, each containing one hydroxyl unit per polymer repeat unit, in order to form structure-property relationships. Since 2OH-PBI, shown in Figure 2.1, demonstrated high conductivities but low solubilities in PPA, the properties of polymers containing one less hydroxyl unit per polymer repeat unit were investigated to understand how conductivity and solubility would be affected. Polymer membranes were characterized through various methods to determine if they are suitable candidates for polymer electrolyte membranes in HTPEMFCs. These novel polymers, poly(2,2'-(2-hydroxy-1,4-phenylene)5,5'-bibenzimidazole (p-OH PBI) and poly(2,2'-(5-hydroxy-m-phenylene)-5,5-bibenzimidazole (m-OH PBI), are shown in Scheme 2.1.

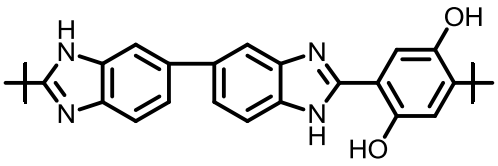

Figure 2.1: Structure of 2OH-PBI

Scheme 2.1: Synthesis of p-OH PBI and m-OH PBI

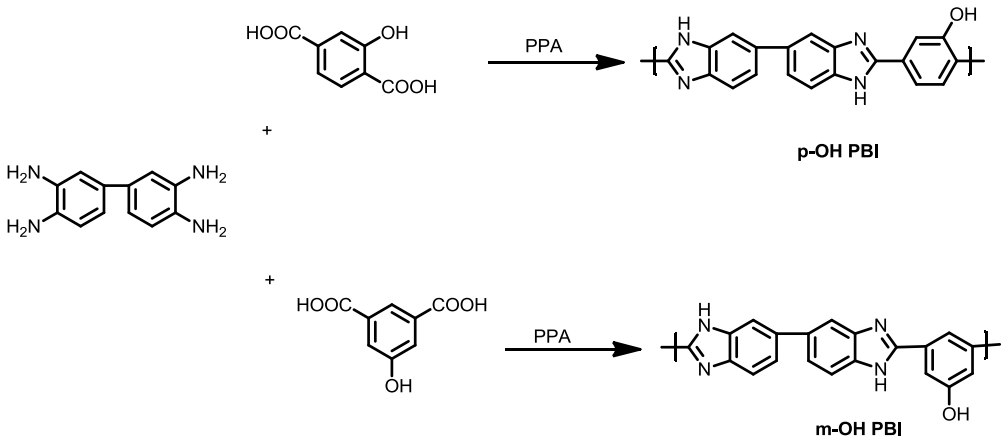

2.3 Experimental Section.

2.3.1 Materials. TAB (3,3',4,4'-tetraaminobiphenyl, polymerization grade) was obtained from Celanese Ventures, GmbH. Polyphosphoric Acid (PPA, 116%) was donated by BASF. 5-hydroxyisophthalic acid (97%) and 2-bromoterephthalic acid (95%) were purchased from Sigma Aldrich. Ammonium hydroxide, sulfuric acid, hydrochloric acid, acetic acid, sodium hydroxide, n-methyl-2-pyrrolidone (NMP), dimethyl sulfoxide (DMSO), and sodium acetate were purchased from Fisher Scientific. Copper powder (98%, 160 mesh) was purchased from Acros. All chemicals were used as received unless otherwise stated.

2.3.2 Synthesis of 2-hydroxyterephthalic acid. Sodium acetate (25.3g, 0.308mol), sodium hydroxide (7.87g, 0.197mol), 2-bromoterephthalic acid (20.42g, 0.083mol), copper powder (0.49g, 0.77mmols) and distilled water (250mL) were charged to a 500mL 3-neck round bottom flask equipped with a stir bar, a nitrogen inlet, a reflux condenser, and a glass stopper. The reaction was allowed to heat at reflux for 4 days. Upon cooling to room temperature, copper powder was removed by vacuum filtration. Filtrate was collected and acidified to a pH of 2 by adding hydrochloric acid drop-wise. Upon acidification, white precipitate began to crash out. Precipitate was collected through vacuum filtration and washed with acetic acid. Product was recrystallized in NMP, washed with water, and dried under vacuum at 150°C. The yield was 12.9 g (85% yield). Product was confirmed through ^{1}H-NMR (300 MHz, DMSO-d6) δ 13.1 (s, 1H), 8.1 (d, 1H), 7.9 (d, 1H), 7.5 (d, 1H), 4.0 (s, 1H) and elemental analysis C=53.02%, H=3.34%.

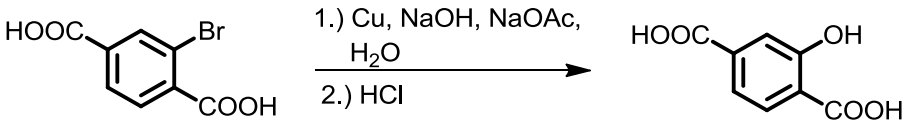

2.3.3 Polymer and Membrane Preparation. *Synthesis of p-OH PBI.* TAB (3,3',4,4'-tetraaminiobiphenyl) (1.892g, 8.83mmol) and 2-hydroxyterephthalic acid (1.609g, 8.83mmol) were placed in a 250 mL resin kettle in a nitrogen atmosphere glove box followed by the addition of 96.5g of PPA. The resin kettle was equipped with a nitrogen inlet, a mechanical stirrer, and a nitrogen outlet. Using a programmable temperature control with ramp and soak features and a silicone oil bath, the polymerization was conducted at 195-220°C for 3-9 hours. During this time, the monomer dissolved and later a dark, viscous polymer solution had formed. A small amount of the polymer was poured into water and isolated as a brown solid. The solid was then chopped using a blender, then neutralized using ammonium hydroxide. Residual salts from the neutralization were then removed by washing the polymer powders with water. Powders were then placed in the vacuum oven to dry at 180°C for 24 hours.

2.3.4 Synthesis of m-OH PBI. TAB (3,3',4,4'-tetraaminobiphenyl) (3.235g, 15.1mmol) and 5-hydroxyisophthalic acid (2.750g, 15.1mmol) were placed in a 250 mL resin kettle in a nitrogen atmosphere glove box followed by the addition of 94.0g of PPA. The resin kettle was equipped with a nitrogen inlet, a mechanical stirrer, and a nitrogen outlet. Using a programmable temperature control with ramp and soak features and a silicone oil bath, the polymerization was conducted at 195-220°C for hours 20-30 hours. During this time, the monomer dissolved and later a dark, viscous polymer solution had formed. A small amount of the polymer was poured into water and isolated as a brown solid. The

solid was then chopped using a blender and neutralized using ammonium hydroxide. Residual salts from the neutralization were then removed by washing the polymer powders with water. Powders were then placed in the vacuum oven to dry at 180°C for 24 hours.

2.4 Characterization Techniques.

2.4.1 Inherent Viscosity. Inherent viscosities (IV) of the polymer powders were measured at a concentration of 0.2 g/dL in concentrated sulfuric acid (96%) at 30°C using a Cannon Ubbelohde viscometer. Samples were prepared by dissolving the dried polymer powders in sulfuric acid using a mechanical shaker. Reported IV values are an average of three separate measurements and were calculated as previously reported.[19]

2.4.2 Thermal Analysis. Thermal gravimetric analysis (TGA) of dried polymer samples was conducted using a TA Instruments Q5000 with nitrogen flow rates of 25mL/min and a heating rate of 10 ˚C/min.

2.4.3 Elemental Analysis. All samples were sent to Midwest Microlabs for elemental testing. The workups of the samples sent out for testing are discussed in the results.

2.4.4 Titrations. The composition of acid-doped PBI membranes was determined by measuring the relative amounts of polymer solids, water, and acid in the film. The phosphoric acid (PA) content was determined by titrating a sample of membrane with standardized sodium hydroxide solution (0.1 N) using a Metrohm 716 DMS Titrino autotitrator. The sample was washed with water and dried under vacuum at 180°C overnight. The dried sample was then weighed to determine polymer solids content for

the membrane. The amount of water was calculated by subtracting the weights of polymer and PA from the initial PBI membrane sample weight.

2.4.5 Conductivity. Ionic conductivities were measured using a four-probe through-plane bulk measurement using an AC Zahner IM6e impedance spectrometer that scanned a frequency range from 1 Hz to 100 KHz. A rectangular sample of membrane was placed in a polysulfone cell with four platinum wire current collectors. Two outer electrodes set 6.0 cm apart supplied current to the cell, while the two inner electrodes 2.0 cm apart on opposite sides of the membrane measured the voltage drop. To ensure a through-plane bulk measurement of the membrane ionic conductivity, the two outer electrodes were placed on opposite sides of the membrane and the two inner electrodes were arranged in the same manner. The membrane sample was heated over 100°C for over 2 hours to ensure water was removed before reporting conductivity data. Conductivity was calculated from the recorded resistance using the equation: $\sigma = D/(LBR)$ where D is the distance between the two test current electrodes, L and B are the thickness and width of the film, respectively, and R is the resistance value measured.

2.4.6 Tensile Testing. The tensile properties of the membranes were tested at room temperature using an Instron Model 5543A system with a 10 N load cell and crosshead speed of 5 mm/min. Dog-bone shaped specimens were cut according to ASTM standard D683 (Type V specimens) and preloaded to 0.1 N prior to testing.

2.4.7 Compression Creep Testing. Compression creep testing was performed using a dynamic mechanical analyzer (TA Instruments, model RSAIII) using the testing method and conditions as previously reported by Chen et al.[20]

2.4.8 Membrane Electrode Assembly. The membrane electrode assemblies (MEA) were prepared by hot pressing the acid-doped membrane between an anode electrode and a cathode electrode at 150 °C for 90-150 seconds using 4500 lbs of force and compressing to 80% its original thickness. Electrodes were received from BASF Fuel Cell, Inc. with 1.0 mg/cm^2 platinum (Pt) catalyst loading. Anode electrodes contained only Pt as the catalyst, while the cathode electrodes contained a BASF Fuel Cell standard cathode Pt alloy. The active area of the electrodes was 45.15 cm^2.

2.4.9 Fuel Cell Testing. Fuel cell fabrication was conducted by assembling the cell components as follows: end plate: anode current collector: anode flow field: MEA : cathode flow field: cathode current collector: end plate. Gaskets were used on both sides of the MEA to control compression. Following assembly, the cell was evenly clamped to 50 inlbs of pressure. Fuel cell performance was measured on 50 cm^2 (active area 45.15 cm^2) single stack fuel cells using test stations obtained from Plug Power or purchased from Fuel Cell Technologies. Polarization curves were obtained at various temperatures (120-180 °C) with hydrogen and air at a constant stoich of H_2 (λ=1.2) /air (λ=2.0) with no external humidification. Fuel cells were operated for at least 100 hours (break-in period) at 0.2 A/cm^2 at 180 °C before measurement of polarization curves.

2.5 Results and Discussion

Both the p-OH PBI and the m-OH PBI were synthesized in polyphosphoric acid (PPA) via the PPA Process. The p-OH PBI was synthesized at a range of monomer concentrations, 2-5 wt%, in order to determine the optimal concentration to obtain high IV polymer. Monomer concentrations of 2.5-3.5 wt% yielded high IV polymer which

resulted in stable films that were easily characterized. The polymerization performed at 4 wt% monomer charge quickly became viscous and was casted after a short time at the final polymerization temperature. The film easily cracked and was unstable for characterization which can be attributed to the low IV of the polymer. The polymerization conducted at 5 wt% monomer charge was too viscous to cast after only a few hours at final temperature. The IV of the polymer was tested and was found to be low, 0.59 dL/g, even though the solution was very viscous at 220 °C. This is commonly seen in PBI polymerizations as they approach their solubility limits. The highest IV obtained, 2.04 dL/g, was found at a monomer charge of 3.5 wt%, making this the ideal concentration to perform polymerizations targeting high IVs. Monomer concentrations higher than 3.5 wt% resulted in solubility issues, even at high temperatures. Inherent viscosities for p-OH PBI are shown in Figure 2.2. Polymerizations were conducted in a ramp/soak method and held at a final temperature of 195-220 °C for 3-9 hours. Viscosity had to be closely monitored for casting as the solution quickly became viscous and difficult to cast. Upon casting the hot solution, films were placed the humidity chamber where the polyphosphoric acid was hydrolyzed to phosphoric acid, thereby inducing the solution to gel transition. Resulting stable films were strong and red in color. The p-OH PBI was able to be polymerized at a slightly higher monomer concentration than 2-OH PBI (3.5 wt% vs 3.0 wt%). Though p-OH does not demonstrate a great difference in solubility compared with 2-OH PBI, the slight difference could be due to fewer cross-links between chains since the polymer repeat unit contains only one hydroxyl unit rather than two.

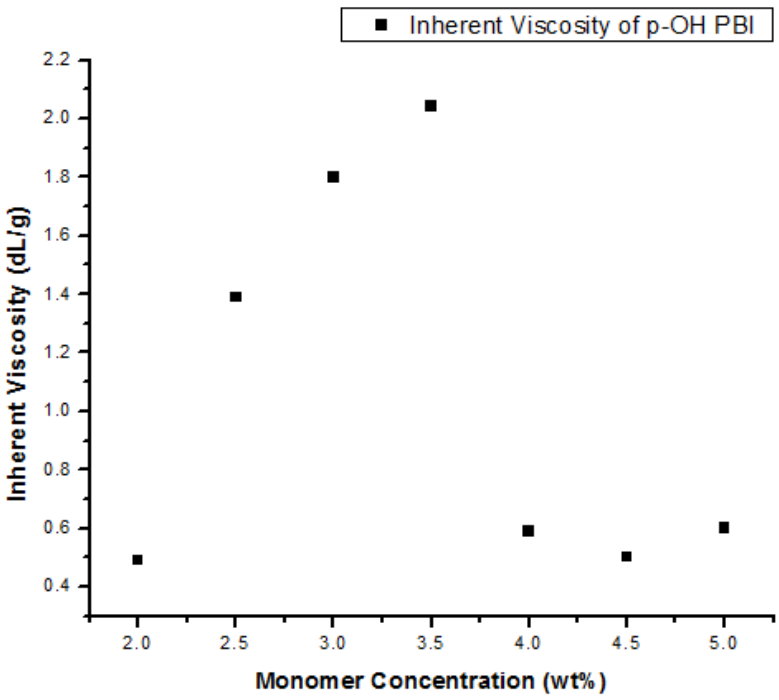

Figure 2.2: Inherent viscosity as a function of monomer concentration for p-OH PBI

m-OH PBI. Polymerizations were also conducted at a range of monomer concentrations, 5.0-7.5 wt%, to determine optimal concentration to obtain high IV PBI as shown in Figure 2.3. Polymerizations conducted at 5.0 and 5.5 wt% monomer charge initially resulted in low IV, non-film forming, polymer. A polymerization at 5.5 wt% monomer charge was redone, this time for a longer time, and resulted in a higher IV polymer that formed a stable film. Polymerizations were conducted at 6.0 wt% for varying times to ultimately increase IV. Polymerizations conducted with monomer charges higher than 6.0 wt% demonstrated solubility issues and had low IVs at an appropriate casting viscosity. The ideal monomer charge was found to be 6.0 wt% at which the highest IV was obtained. Polymerizations were performed using a ramp/soak temperature profile and held at a final polymerization temperature, 195-220°C, for 10-30 hours before casting. The resulting high-IV films were mechanically stable and red in color. These polymerizations showed a greater solubility in PPA than p-OH PBI and 2-

OH PBI. This is to be expected as the meta-oriented backbone is less rigid than the para-oriented backbone. This is also supported by previously reported data on meta and para-PBI synthesized via the PPA Process which suggests meta-PBI can be polymerized with nearly double the monomer concentration as para-PBI.[12,21]

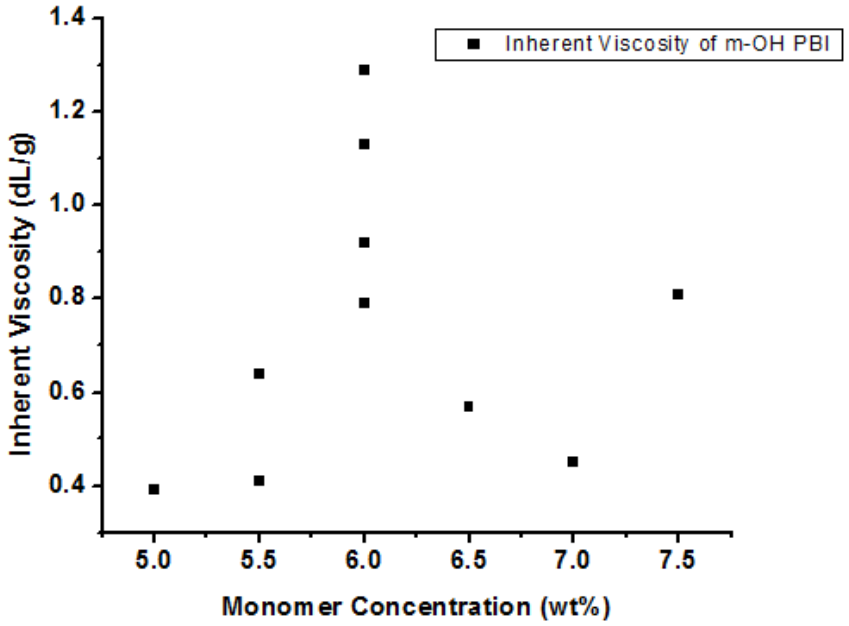

Figure 2.3: Inherent viscosity as a function of monomer concentration for m-OH PBI

Basic workup of polymer powders. To better understand the phosphate-ether linkages and phosphate bridges which were believed to be contributing to the high viscosity of the polymer solution, polymer powders of both p-OH PBI and m-OH PBI were used for investigation. Since polymer powders are obtained by heating the chopped polymers in water to kick out phosphoric acid, followed by neutralization with ammonium hydroxide as previously stated in the experimental section, all free phosphoric acid should have been removed during the neutralization. The only remaining

phosphorous would be the phosphorous that is covalently bound as phosphate bridges or phosphate-esters between hydroxyl units along the PBI backbone. Phosphate bridges would also lead to a higher inherent viscosity due to the increased rigidity of the cross-linked structure and a higher Mark-Houwink coefficient. To test for phosphate bridges, a sample of each of the polymer powders was heated at reflux in a DMSO/water mixture with 0.02M of sodium hydroxide for 24 hours to hydrolyze any phosphate bridges as previously reported.[7] Upon washing and drying the samples, inherent viscosities were run on both the neat polymer powders and the powders that went through the basic workup. These results are shown in Table 2.1. The inherent viscosities of both polymers decreased slightly but not as much as one might expect if many phosphate bridges were present. To further characterize the polymer powders, both the neat powders and the powders that were hydrolyzed were tested using elemental analysis to determine the amount of phosphorous present within the samples. The results of the elemental analysis are shown in Table 2.2. In the p-OH PBI samples, the amount of phosphorous seen in the neat sample was significantly higher than the amount seen in the sample after the basic workup. The neat sample was found to have a ratio of 31.14 equiv. carbon to 1.0 equiv. phosphorous. After hydrolysis of phosphate bridges and phosphate esters, the ratio of carbon atoms to phosphorous atoms was found to be 332.14 to 1.0 indicating there was a large amount of covalently bound phosphorous. The m-OH PBI powders roughly saw a 50% decrease in the amount of phosphorous after basic workup. The neat powders had a ratio of 17.88 equiv. carbon to 1.0 equiv. phosphorous. Upon the basic workup, the ratio of carbon to phosphorous changed to 35.5 equiv. carbon to 1.0 equiv. phosphorous. The change in the amount of phosphorous in both p-OH PBI and m-OH PBI shows that

initially there is much phosphorous in the sample, however, since IV did not drastically change after the basic workup, it can be hypothesized that there are many phosphate-ether linkages and few phosphate bridges. The difference in these structures are shown in Figure 2.4.

Table 2.1: Inherent Viscosities of powders before and after hydrolysis

Polymer sample	I.V. of neat powder (dL/g)	I.V. of powder after basic workup (dL/g)
p-OH PBI	2.04	1.95
m-OH PBI	0.72	0.67

Table 2.2: Elemental analysis of polymer powders in weight %

Sample	C (%)	H (%)	N (%)	P (%)
p-OH PBI (Neat)	52.30	4.52	12.18	4.23
p-OH PBI (after basic workup)	55.81	4.29	13.5	0.45
m-OH PBI (Neat)	53.71	4.74	12.08	7.75
m-OH PBI (after basic workup)	44.88	4.40	12.95	3.18

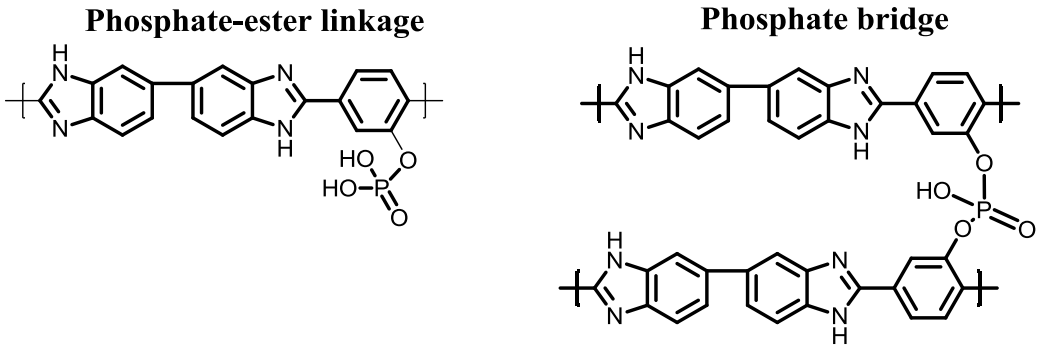

Figure 2.4: Phosphate-ester linkage and phosphate bridge structures

Thermal gravimetric analysis (TGA) was performed on the dried p-OH and m-OH PBI powders to determine the thermal stabilities of these polymers. Weight loss below 200 °C is attributed to water loss. Both homopolymers demonstrated high decomposition temperatures, ~600 °C, as shown in Figure 2.5.

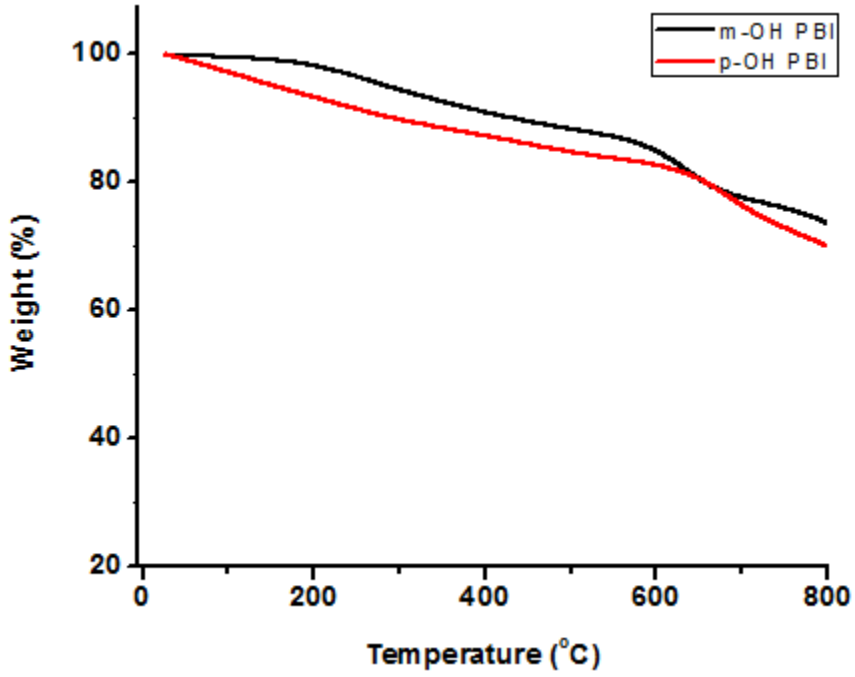

Figure 2.5: TGA of p-OH and m-OH PBI in nitrogen

Titrations were performed on both homopolymers to determine the composition of the membrane as shown in Table 2.3. The amount of phosphoric acid in the membrane was determined through titration with 0.1N sodium hydroxide solution. The p-OH PBI, which was found to have an acid loading of 36.5 moles PA/ moles polymer repeat unit (PRU), demonstrated a greater acid loading than both m-OH PBI and the previously reported 2OH-PBI which had 19.1 moles PA/PRU and 25.4 moles PA/PRU,[7]

respectively. The larger acid loading of the p-OH PBI than the m-OH PBI can be attributed to the more rigid backbone of the polymer allowing for a greater acid uptake. This effect is also seen when comparing the acid loading of para PBI to meta PBI. Both p-OH and m-OH PBI demonstrate higher acid loadings than their counterparts that do not contain hydroxyl units—para PBI (30 moles PA/PRU)[21] and meta PBI (14 moles PA/PRU)[12]. This demonstrates the effect the hydroxyl units have on the acid content of the films.

Table 2.3: Summary of membrane composition for p-OH PBI and m-OH PBI

Polymer	Acid Doping Level (PA/PRU.)	Polymer content (%)	PA content (%)	Water content (%)
p-OH PBI	36.5	4.5	49.9	45.6
m-OH PBI	19.1	9.6	56.3	34.1

Proton conductivity is an important factor when choosing a fuel cell membrane. Since there are many benefits to operating fuel cells at high temperatures without humidification, such as faster electrode kinetics, high tolerance to gas impurities, and no water management issues, it was important to ensure water was not contributing to the reported conductivity. In order to ensure water was not a factor, conductivity tests were performed in a programmable oven at a range of temperatures (up to 180 °C), and the sample was cooled down under vacuum before starting a second run in which the conductivity was measured from 20-180 °C. Cooling under vacuum is important since PBI is hygroscopic and demonstrates hydrogen bonding between the N-H groups along the backbone and water. Figure 2.6 shows the conductivities of p-OH PBI and m-OH PBI

with 2OH-PBI included for comparison. The p-OH PBI showed a similar, but slightly higher conductivity than 2-OH PBI and the m-OH PBI fell below these two. The difference in conductivities between the p-OH PBI and m-OH PBI could be attributed to both the difference in structure of the polymer backbone and the difference in acid doping levels. Also, the meta-oriented PBI could have exhibited solubility issues in PA at high temperatures resulting in a lower conductivity. The high conductivity demonstrated by p-OH PBI reaffirms that high conductivity can still be maintained even when one less hydroxyl unit/repeat unit is present.

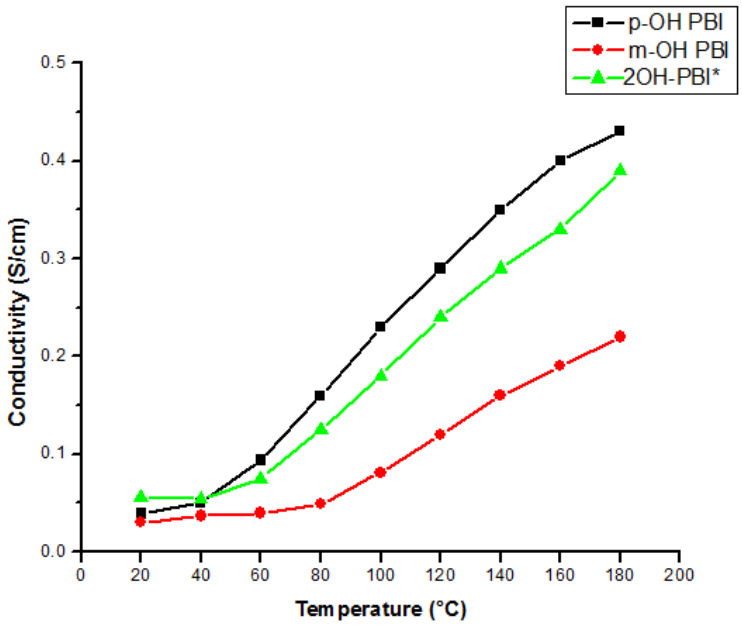

Figure 2.6: Conductivities of hydroxy PBIs.*Included for comparison[7]

The tensile properties of the membranes were evaluated to ensure the films were mechanically stable and could be handled during MEA preparation. Tensile data is shown in Table 2.4. Even though both polymer samples were similar in IV, it can be seen that the m-OH PBI sample had greater tensile properties than the p-OH membrane. The m-OH PBI had ~1.5x the tensile strength and ~5x greater the strain at break than that of p-

OH PBI. The difference in tensile properties can be attributed to the greater polymer content, over twice as much, within the m-OH PBI membrane than the p-OH membrane.

Table 2.4: Tensile properties of p-OH PBI and m-OH PBI

Polymer	Wt% Polymer	Tensile Strength (MPa)	Strain at Break (mm/mm)	Young's Modulus (MPa)
p-OH PBI	4.5	0.29	0.52	0.93
m-OH PBI	9.6	0.43	2.62	1.12

Polybenzimidazoles have been known to undergo creep when placed under compressive loads at elevated temperatures, like those during fuel cell operation. Membrane creep can lead to membrane thinning, loss of close contact with the electrodes, and can ultimately cause fuel cell degradation.[20] Many factors influence the creep resistance of a polymer networks, such as: chain rigidity, molecular weight, and physical crosslinks with in the network.[20] Recently, Chen et al. published a study on the creep of various polybenzimidazole chemistries.[20] Since the chemical structure of the PBI membrane plays a large role in the polymer's resistance to creep, both p-OH PBI and m-OH PBI were examined. Creep testing was performed using similar conditions to that of fuel cell testing to best assess how the membrane would handle stress during operation. Figure 2.7 shows the compliance of the p-OH and m-OH PBI membranes. It can be seen that the p-OH PBI sample has a slightly higher compliance and creep than that of m-OH PBI. This can be explained by the greater amount of polymer solids the m-OH PBI sample contains compared to the p-OH PBI sample. The final polymer contents in the samples that underwent compliance creep testing were found to have solids contents of

8.77 wt% in the p-OH PBI film and 27.37 wt% in the m-OH PBI film. The ability of p-OH PBI to still maintain a low creep even though it is low in polymer content can be attributed to its para-oriented backbone. When rigid para-oriented chains are bent or stretched, they contain more elastic energy than would be seen in a meta-oriented backbone.[20] While meta-oriented polymers exhibit greater solubility and can form films with higher polymer content, the meta-orientation of the chains are more flexible than those of the para-oriented chains leading to an increased tendency to creep. Therefore, if both p-OH PBI and m-OH PBI samples contained similar polymer contents, the p-OH PBI film would most likely have a lower creep.

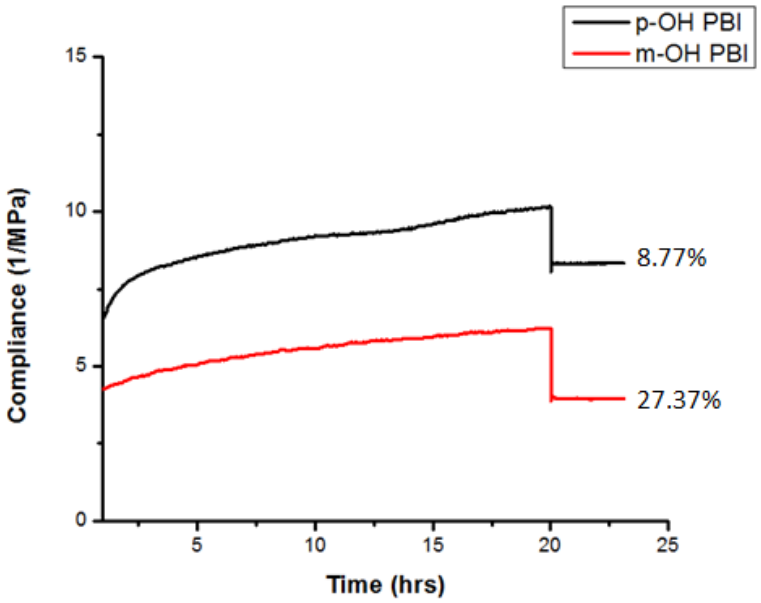

Figure 2.7: Compliance data of p-OH PBI and m-OH PBI

Fuel cell performance was evaluated with the p-OH PBI and m-OH PBI membranes using hydrogen and air, as seen in Figure 2.8 A and B. Polarization curves were run over range of temperatures, 120-180 °C, and at various current densities. The fuel cell testing performed using the p-OH PBI membrane could successfully operate a

fuel cell up to 1.0 A/cm^2 even at the lowest tested temperature of 120 °C without any external humidification. Fuel cell testing performed using the m-OH PBI membrane showed a lower overall performance than that of the p-OH membrane. The highest current density that the m-OH PBI membrane could operate at was 0.8 A/cm^2 at 180 °C. A current density of 0.7 A/cm^2 could be achieved at 160 °C and above. The fuel cell could only operate up to 0.4 A/cm^2 when run at temperatures of 120 °C and 140 °C. The subpar fuel cell performance of m-OH PBI compared to p-OH PBI could be attributed to a few factors. The conductivity of the m-OH PBI is significantly lower than that of the p-OH PBI which could be one factor leading to a lesser fuel cell performance. Also, poor overall performance could have been caused by solubility issues of the m-OH PB in PA at high temperatures or pinholes within the film that formed during casting.

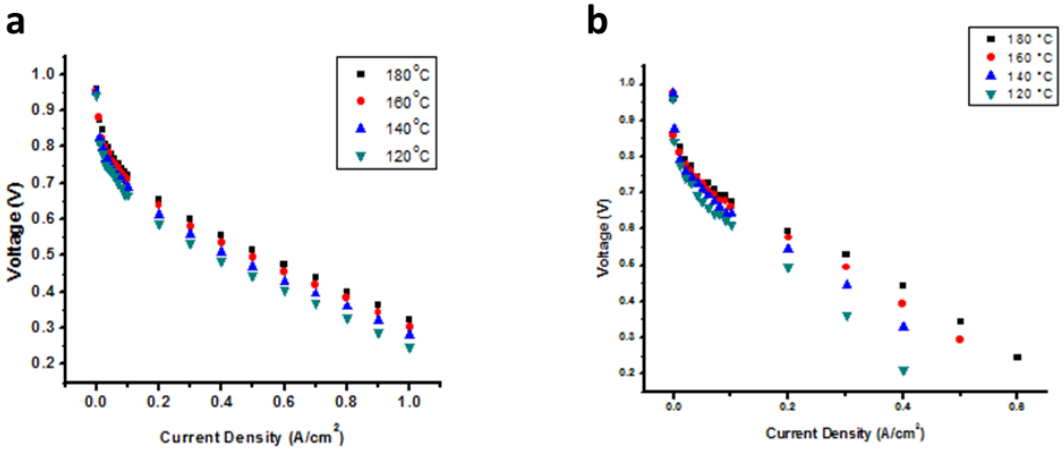

Figure 2.8: Polarization curves of a.) p-OH PBI and b.) m-OH PBI

2.6 Conclusion.

Two novel hydroxyl-containing polybenzimidazole homopolymers were synthesized and characterized to determine their potential as membranes for HTPEMFCs. Both chemistries were synthesized via the PPA Process from a hydroxy-diacid and TAB. Optimal polymerization concentrations were determined by studying the effect monomer concentration has on the inherent viscosity and elemental analysis was conducted to understand the amount and the role of phosphorous within the films. Both polymers were able to be polymerized at higher monomer concentrations than that of the previously reported 2-OH PBI. By studying the powders, both neat and hydrolyzed, it was determined that there are some phosphate bridges and a great amount of phosphate-ester linkages.

Higher acid loadings were seen within both p-OH and m-OH PBIs than those seen in para and meta PBI indicating the importance of the hydroxyl unit on the acid content. p-OH PBI had a higher acid content and conductivity than that of the m-OH PBI and the previously reported 2OH-PBI. The m-OH PBI membrane demonstrated better mechanical properties, both tensile and creep, than the p-OH PBI membrane though both films were mechanically stable enough to perform fuel cell testing. This difference in mechanical properties is largely attributed to the greater polymer content within the m-OH membrane.

Fuel cell testing was performed at a range of temperatures and current densities. The m-OH PBI was successful at all temperatures when run at a current density of 0.2 A/cm^2 or lower, however, above this current density, the fuel cell began having

performance issues. The fuel cell containing the p-OH PBI membrane was successful at the range of temperatures and current densities tested and is considered to be a promising candidate for use in fuel cells.

2.7 Acknowledgement.

The authors acknowledge the financial support from BASF.

2.8 References.

(1) Yang, C., Costamagna, P., Srinivasan, S., Benziger, J., Bocarsly, A. B., *Journal of Power Sources* **2001**, *103*, 1.

(2) Xiao, L., Zhang, H., Jana, T., Scanlon, E., Chen, R., Choe, E. W., Ramanathan, L. S., Yu, S., Benicewicz, B. C., *Fuel Cells* **2005**, *5*, 287.

(3) Savinell, R., Yeager, E., Tryk, D., Landau, U., Wainright, J., Weng, D., Lux, K., Litt, M., Rogers, C. *Journal of The Electrochemical Society* **1994**, *141*, L46.

(4) Wainright, J. S., Wang, J. T., Weng, D., Savinell, R. F., Litt, M., *Journal of The Electrochemical Society* **1995**, *142*, L121.

(5) Weng, D., Wainright, J. S., Landau, U., Savinell, R. F., *Journal of The Electrochemical Society* **1996**, *143*, 1260.

(6) Samms, S. R., Wasmus, S., Savinell, R. F., *Journal of The Electrochemical Society* **1996**, *143*, 1225.

(7) Yu, S., Benicewicz, B.C., *Macromolecules* **2009**, *42*, 8640.

(8) Perry, K., More, K., Payzant, A., Meisner, R. A., Sumpter, B.G., Benicewicz, B.C., *Journal of Polymer Science Part B: Polymer Physics* **2014**, *52*, 26.

(9) Savinell, R. L., M. U.S. Patent #6,099,988, 2000.

(10) Xiao, L., Zhang, H., Scanlon, E., Ramanathan, L. S., Choe, E.W., Rogers, D., Apple, T., Benicewicz, B.C., *Chemistry of Materials* **2005**, *17*, 5328.

(11) Molleo, M., Schmidt, T., Benicewicz, B.C. In *Encyclopedia of Sustainability, Science and Technology*; Meyers, R. A., Ed.; Springer Science + Business Media LLC: New York, 391-431, 2013.

(12) Mader, J., Xiao, L., Schmidt, T. J., Benicewicz, B. C. *Advances in Polymer Science*; Springer-Verlag, 2008

(13) Seel, D. C., Benicewicz, B. C., Xiao, L., Schmidt, T. J., *High-Temperature Polybenzimidazole-Based Membranes*, 2009.

(14) Sikkema, D. J. *Polymer* **1998**, *39*, 5981.

(15) Klop, E. A., Lammers, M., *Polymer* **1998**, *39*, 5987.

(16) Jenkins, S., Jacob, K. I., Kumar, S., *Journal of Polymer Science Part B: Polymer Physics* **2000**, *38*, 3053.

(17) Tomlin, D. W., Fratini, A. V., Hunsaker, M., Wade, A. W., *Polymer* **2000**, *41*, 9003.

(18) Tan, L., Arnold, F. E., Dang, T. D., Chuah, H. H., Wei, K. H., *Polymer* **1994**, *35*, 3091.

(19) Mader, J. A., Benicewicz, B.C., *Macromolecules* **2010**, *43*, 6706.
(20) Chen, X., Qian, G., Molleo, M., Benicewicz, B.C., Ploehn, H.J., *Journal of Polymer Science Part B: Polymer Physics* **2015**, 1527.
(21) Yu, S., Zhang, H., Xiao, L., Choe, E. W., Benicewicz, B. C. *Fuel Cells* **2009**, *9*, 318.

CHAPTER 3

SYNTHESIS AND CHARACTERIZATION OF A COPOLYMER SERIES OF P-OH PBI AND PARA-PBI FOR HIGH TEMPERATURE POLYMER ELECTROLYTE MEMBRANE FUEL CELL APPLICATIONS

3.1 Abstract.

A copolymer series consisting of poly(2,2'-(2-hydroxy-1,4-phenylene)5,5'-bibenzimidazole (p-OH PBI) and poly(2,2'-(1,4-phenylene)5,5'-bibenzimidazole (para-PBI) was successfully synthesized in polyphosphoric acid (PPA). These two PBI analogs were chosen for this copolymer study due to the excellent fuel cell performance of para-PBI, the high conductivity of p-OH PBI, and the low creep seen in para-oriented PBI polymers. After polymer synthesis and film formation, copolymer membranes were characterized to determine if these chemistries would be good candidates as the polymer electrolyte membrane in high temperature polymer electrolyte membrane fuel cells. Five ratios of p-OH PBI/para-PBI were evaluated and compared to each other and their homopolymer counterparts in order to form structure-property relationships.

3.2 Introduction.

Polymer electrolyte membrane fuel cells have gained much attention over the last few decades as efficient energy conversion devices for both mobile and stationary applications.[1,2] Perfluorosulfonic acid membranes, which contain water as the electrolyte, have commonly been used as the polymer electrolyte membrane, however, the temperature at which these fuel cells operate is limited by the potential evaporation of the electrolyte. Since operation is restricted to low temperatures (< 100°C), these fuel cells require large heat exchangers and have a low tolerance to fuel impurities. In contrast, polybenzimidazole membranes imbibed with phosphoric acid are able to operate at high temperatures (> 120 °C), thereby increasing tolerance to fuel impurities, improving electrode kinetics, and eliminating humidification requirements.[1-5]

The conventional method of preparing acid imbibed polybenzimidazole membranes is a lengthy, multi-step process in which the polymer is first synthesized in

polyphosphoric acid (PPA), dissolved in an organic solvent, cast into a film, heated for solvent evaporation, and soaked in a PA bath.[6-9] Another, more efficient method of producing acid imbibed PBI membranes, termed the PPA Process, involves polymerizing PBI in PPA and casting a film directly from the hot polymer solution. The PPA is then hydrolyzed from moisture in the air to PA, thereby, inducing the solution-to-gel transition. Since the film is already imbibed with PA, there is no need for any additional steps. Membranes prepared via the PPA Process have shown higher conductivities, a larger acid content, better mechanical properties, and overall better fuel cell performance than PBI membranes prepared through the conventional method.[10,11]

Another advantage seen with the PPA Process is the ability to produce many variations of polybenzimidazole since the solubility limitations associated with PBI in dimethyl acetamide (DMAc) do not apply to this process. This great advantage has led to the synthesis of many PBI chemistries which have been studied extensively to form structure-property relationships within these membranes.[10,12-17] Further structure-property relationships have been evaluated through copolymer systems prepared via the PPA Process.[2,18]

In previous studies, both para-PBI and p-OH PBI homopolymers were evaluated as polymer electrolyte membranes for high temperature fuel cells. Para-PBI was found to have a good conductivity and demonstrated excellent fuel cell performance,[2] while p-OH demonstrated excellent conductivity and a mediocre fuel cell performance. Both homopolymers demonstrated a low compliance creep which can be attributed to their para-oriented backbones.[19] This study looks to investigate a copolymer system of p-OH PBI and para-PBI prepared via the PPA Process in order to determine structure-property

relationships between the copolymers and the previously reported homopolymers. The synthesis of this copolymer system can be seen in Scheme 1.

Scheme 1: Synthesis of p-OH/Para PBI Copolymers

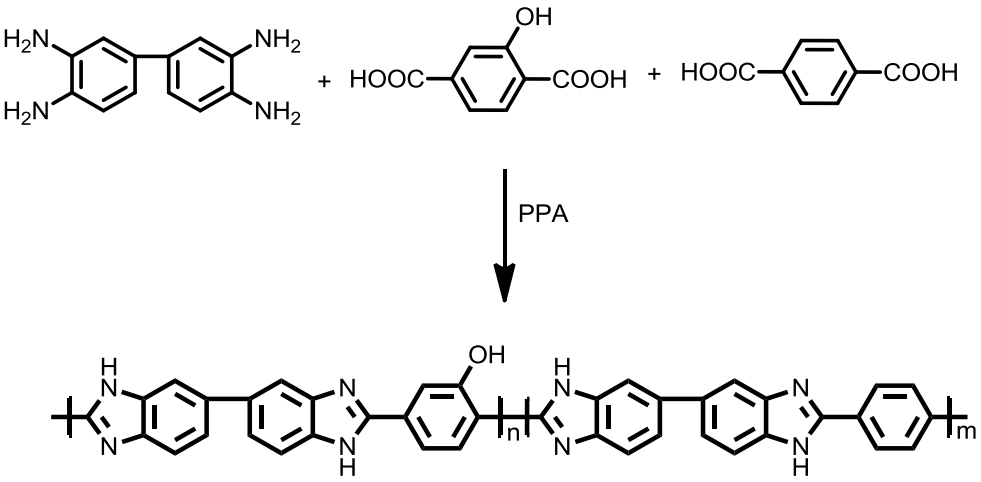

3.3 Experimental Section

3.3.1 Materials. TAB (3,3',4,4'-tetraaminobiphenyl, polymerization grade) was obtained from Celanese Ventures, GmbH. Terephthalic acid (TA, 99+%) was purchased from Amoco. Polyphosphoric Acid (PPA, 116%) was donated by BASF. 2-bromoterephthalic acid (95%) was purchased from Sigma Aldrich. Ammonium hydroxide, sulfuric acid, hydrochloric acid, acetic acid, sodium hydroxide, n-methyl-2-pyrrolidone (NMP), dimethyl sulfoxide (DMSO), and sodium acetate were purchased from Fisher Scientific. Copper powder (98%, 160 mesh) was purchased from Acros. All chemicals were used as received unless otherwise stated.

3.3.2 Synthesis of 2-hydroxyterephthalic acid. Sodium acetate (25.3g, 0.308mol), sodium hydroxide (7.87g, 0.197mol), 2-bromoterephthalic acid (20.42g, 0.083mol), copper powder (0.49g, 0.77mmols) and distilled water (250mL) were charged to a

500mL 3-neck round bottom flask equipped with a stir bar, a nitrogen inlet, a reflux condenser, and a glass stopper. The reaction was allowed to heat at reflux for 4 days. Upon cooling to room temperature, copper powder was removed by vacuum filtration. Filtrate was collected and acidified to a pH of 2 by adding hydrochloric acid drop-wise. Upon acidification, white precipitate began to crash out. Precipitate was collected through vacuum filtration and washed with acetic acid. Product was recrystallized in NMP, washed with water, and dried under vacuum at 150°C. The yield was 12.9 g (85% yield). Product was confirmed through ^{1}H-NMR (300 MHz, DMSO-d6) δ 13.1 (s, 1H), 8.1 (d, 1H), 7.9 (d, 1H), 7.5 (d, 1H), 4.0 (s, 1H) and elemental analysis C=53.02%, H=3.34%.

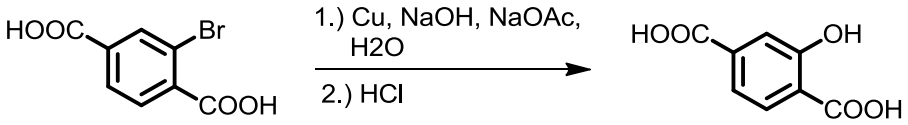

3.3.4 Polymer and Membrane Preparation. *Synthesis of p-OH-r-para PBI*. TAB (3,3',4,4'-tetraaminiobiphenyl), 2-hydroxyterephthalic acid, and terephthalic acid, were placed in a 250 mL resin kettle in a nitrogen atmosphere glove box followed by the addition of 96.5 g of PPA. The mole ratio of TAB to diacid was 1:1 and gave an overall monomer charge of ~3.5 wt%. The amount of each diacid was adjusted to the ratios reported below in Table 1. The resin kettle was equipped with a nitrogen inlet, a mechanical stirrer, and a nitrogen outlet. Using a programmable temperature control with ramp and soak features and a silicone oil bath, the polymerization was conducted at 195-220°C for 13-50 hours. During this time, the monomer dissolved and later a dark, viscous polymer solution had formed. A small amount of the polymer was poured into water and isolated as a brown solid. The solid was chopped using a blender, then neutralized using

ammonium hydroxide. Residual salts from the neutralization were then removed by washing the polymer powders with water. Powders were then placed in the vacuum oven to dry at 180°C for 24 hours.

3.4 Characterization Techniques.

3.4.1 Inherent Viscosity. Inherent viscosities (IV) of the polymer powders were measured at a concentration of 0.2 g/dL in concentrated sulfuric acid (96%) at 30°C using a Cannon Ubbelohde viscometer. Samples were prepared by dissolving the dried polymer powders in sulfuric acid using a mechanical shaker. Reported IV values are an average of three separate measurements and were calculated as previously reported.[13]

3.4.2 Elemental Analysis. All samples were sent to Midwest Microlabs for elemental testing.

3.4.3 Titrations. The composition of acid-doped PBI membranes was determined by measuring the relative amounts of polymer solids, water, and acid in the film. The phosphoric acid (PA) content was determined by titrating a sample of membrane with standardized sodium hydroxide solution (0.1 N) using a Metrohm 716 DMS Titrino autotitrator. The sample was washed with water and dried under vacuum at 180°C overnight. The dried sample was then weighed to determine polymer solids content for the membrane. The amount of water was calculated by subtracting the weights of polymer and PA from the initial PBI membrane sample weight.

3.4.4. Conductivity. Ionic conductivities were measured using a four-probe through-plane bulk measurement using an AC Zahner IM6e impedance spectrometer that scanned a frequency range from 1 Hz to 100 KHz. A rectangular sample of membrane was placed in a polysulfone cell with four platinum wire current collectors. Two outer electrodes set

6.0 cm apart supplied current to the cell, while the two inner electrodes 2.0 cm apart on opposite sides of the membrane measured the voltage drop. To ensure a through-plane bulk measurement of the membrane ionic conductivity, the two outer electrodes were placed on opposite sides of the membrane and the two inner electrodes were arranged in the same manner. The membrane sample was heated over 100°C for over 2 hours to ensure water was removed before reporting conductivity data. Conductivity was calculated from the recorded resistance using the equation: $\sigma = D/(LBR)$ where D is the distance between the two test current electrodes, L and B are the thickness and width of the film, respectively, and R is the resistance value measured.

3.4.5 Tensile Testing. The tensile properties of the membranes were tested at room temperature using an Instron Model 5543A system with a 10 N load cell and crosshead speed of 5 mm/min. Dog-bone shaped specimens were cut according to ASTM standard D683 (Type V specimens) and preloaded to 0.1 N prior to testing.

3.4.6 Compression Creep Testing. Compression creep testing was performed using a dynamic mechanical analyzer (TA Instruments, model RSAIII) using the testing method and conditions as previously reported by Chen et al.[19]

3.4.7 Membrane Electrode Assembly. The membrane electrode assemblies (MEA) were prepared by hot pressing the acid-doped membrane between an anode electrode and a cathode electrode at 150 °C for 90-150 seconds using 4500 lbs of force and compressing to 80% its original thickness. Electrodes were received from BASF Fuel Cell, Inc. with 1.0 mg/cm^2 platinum (Pt) catalyst loading. Anode electrodes contained only Pt as the catalyst, while the cathode electrodes contained a BASF Fuel Cell standard cathode Pt alloy. The active area of the electrodes was 45.15 cm^2.

3.4.8 Fuel Cell Testing. Fuel cell fabrication was conducted by assembling the cell components as follows: end plate: anode current collector: anode flow field: MEA : cathode flow field: cathode current collector: end plate. Gaskets were used on both sides of the MEA to control compression. Following assembly, the cell was evenly clamped to 50 inlbs of pressure. Fuel cell performance was measured on 50 cm^2 (active area 45.15 cm^2) single stack fuel cells using test stations obtained from Plug Power or purchased from Fuel Cell Technologies. Polarization curves were obtained at various temperatures (120-180 °C) with hydrogen and air at a constant stoich of H_2 (λ=1.2) /air (λ=2.0) with no external humidification. Fuel cells were operated for at least 100 hours (break-in period) at 0.2 A/cm^2 at 180 °C before measurement of polarization curves.

3.5 Results and Discussion.

All polymerizations were conducted at ~3.5 wt% monomer charge with varying ratios of 2-hydroxyterephthalic acid to terephthalic acid, shown in Table 3.1. This concentration was decided upon since the optimal concentration of the p-OH hompolymer was previously found to be 3.5 wt%. This concentration is also suitable for para-PBI as it reaches high IV at 3.5 wt% monomer charge and loses solubility after 4.0 wt% monomer charge.[10] Concentration was kept consistent in each copolymerization to eliminate the variable of concentration and to focus on the effect of chemistry. All solutions were cast once the solution appeared to have the proper viscosity for casting a film. It was important to carefully watch the solution viscosity of the polymerizations containing a greater amount of hydroxy-character as they easily became too viscous to cast. This is a common occurrence with hydroxy PBI since it can be for phosphate-ester linkages and phosphate bridges between chains at high temperatures in PPA. Upon hydrolysis of the PPA to PA, the film containing a 50:50 mixture of hydroxy and para

character appeared opaque as if it had phase separated. This could be due to the solubility differences between p-OH PBI and para-PBI in phosphoric acid or due to the formation of a "blocky" copolymer rather than a random copolymer. All other films were transparent and red in color and did not appear to have any of the cloudiness as seen in the 50/50 copolymer system. This interesting observation in the 50/50 copolymer should be further investigated in the future. Figure 3.1 demonstrates the cloudiness seen in the 50/50 copolymer membrane.

Table 3.1: Monomer Ratios and Monomer/Polymer Concentrations for p-OH PBI and Para-PBI Copolymers

p-OH-PBI/para-PBI	TAB, g (mmol)	5-hydroxy T.A., g (mmol)	T.A., g (mmol)	PPA, g	Monomer concentration, wt%	Polymer concentration, wt%
100/0	1.892 (8.83)	1.609 (8.83)	--------	96.5	3.50	4.50
90/10	1.919 (8.96)	1.455 (7.99)	0.147 (0.88)	99.4	3.42	6.60
75/25	1.924 (8.98)	1.226 (6.73)	0.373 (2.25)	96.15	3.53	5.24
50/50	2.087 (9.74)	0.822 (4.51)	0.809 (4.87)	104.9	3.54	5.74
25/75	1.959 (9.14)	0.419 (2.30)	1.134 (6.83)	97.15	3.49	6.12
10/90	1.963 (9.16)	0.172 (0.94)	1.370 (8.25)	97.3	3.48	6.12

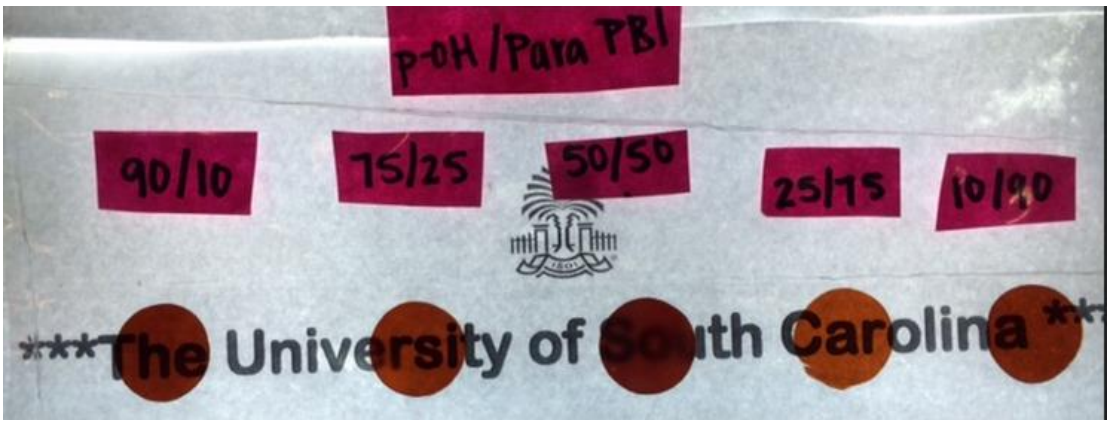

Figure 3.1: Copolymer Films Appearance

Inherent viscosity was tested on each of the copolymers to determine to ensure that films would be stable enough for testing as IV has a large effect on the mechanical properties of the film. Larger IVs typically lead to greater mechanical properties due to longer chains demonstrating greater entanglement. The IVs for this copolymer series ranged from 0.66 to 1.00 dL/g and are shown in Table 3.2. These IVs are not considered to be high; however, they were casted at appropriate solution viscosity. The IV could not have been increased by back-adding PA to dilute the polymer solution due to the insolubility of the p-OH PBI chemistry in PA. Though the films were not of high IV, they were stable enough to be handled for characterization.

Table 3.2: Inherent Viscosities of p-OH/Para copolymers

p-OH-PBI/para-PBI	Inherent Viscosity (dL/g)
90/10	0.66
75/25	1.00
50/50	0.91
25/75	0.77
10/90	0.99

The copolymer films were titrated to determine how the composition of the film would be affected by altering the ratios of the p-OH PBI to the para-PBI. It is known that both acid content and the chemistry of the film affect the membrane's conductivity. The membrane compositions for this copolymer series are shown in Table 3.3. The p-OH PBI and para-PBI homopolymers were included for reference and comparison value. It can be seen that acid content decreases as the amount of p-OH PBI character decreases with the exception of the 10/90 p-OH/para-PBI membrane. This trend is to be expected as hydroxy-PBI has previously shown a greater acid content than standard para-PBI and is capable of forming phosphate-esters and phosphate bridges between chains.

Table 3.3: Copolymer Membrane Compositions

p-OH-PBI/para-PBI	Acid Content (wt%)	Polymer Content (wt%)	Water Content (wt%)	Moles PA/ Mole PRU
100/0	49.90	4.50	45.60	36.5
90/10	65.20	6.60	28.2	32.6
75/25	50.70	5.24	44.06	31.9
50/50	51.70	5.74	57.44	29.6
25/75	55.13	6.12	38.75	29.0
10/90	60.76	6.12	33.12	31.9
0/100	38.84	6.35	54.81	19.3

The tensile properties of the copolymer films were tested to evaluate the strength of the films. Tensile strength, strain at break, and Young's modulus are shown in Table 3.4. No distinct correlation is seen between the membrane composition and the tensile properties, however, there is a slight correlation between the IV of the films and the tensile properties. It can be seen that out of the copolymer membranes, the 90/10 ratio has the lowest IV (0.66 dL/g) and also has the lowest tensile strength and strain at break. Alternatively, the 75/25 membrane which had the highest IV of the copolymers (1.00 dL/g) had the highest tensile strength and the second largest strain at break. All copolymers, with the exception of the 90/10 ratio exhibited better tensile properties than the p-OH PBI homopolymer. The poor mechanical properties of the 90/10 film can be attributed to the low IV of the polymer. Though this film demonstrated poor tensile properties, it was mechanically stable enough to be handled and further characterized.

Table 3.4: Tensile Properties of p-OH PBI/ Para-PBI Copolymers

p-OH PBI/para-PBI	Tensile Strength (MPa)	Strain at Break (mm/mm)	Young's Modulus (MPa)
100/0	0.29	0.52	0.93
90/10	0.20	0.14	1.22
75/25	0.58	0.75	1.31
50/50	0.35	0.49	1.07
25/75	0.51	1.00	1.02
10/90	0.36	0.62	0.96

The conductivity of each copolymer film was tested from 20-180 °C to evaluate conductivity over a range of temperatures. Each measurement was conducted after the oven was held at the reported temperature for 20 minutes to ensure accuracy. A first conductivity run was performed to remove water so the reported conductivity would only be dependent on the PA and PBI film. The conductivities of the p-OH homopolymer and the para-PBI homopolymers were included for comparison in Figure 3.2. The majority of the copolymers reach conductivities between 0.1 S/cm and 0.15 S/cm at 180°C which is low compared to other membranes prepared through the PPA Process. The 50/50 copolymer reached a much higher conductivity, 0.25 S/cm at 180 °C, than those of the other copolymer compositions. The conductivity was reproducible each time a new 50/50 composition was synthesized and tested. This conductivity cannot be attributed to the acid doping level of the film since the amount it contained was less than three of the other copolymers, however, it could potentially be attributed to the morphology of the membrane as it was visibly different from the other copolymers, though this difference has yet to be investigated. Although the 50/50 composition demonstrated a higher conductivity than the other copolymers, it had a conductivity similar to that of the para-PBI homopolymer and a conductivity far below that of the p-OH PBI homopolymer. One

possible reason the copolymers were lower in conductivity than the two homopolymers could be due to the low IVs of the copolymers. Low IV polymer could start solubilizing in PA as high temperatures were reached, thereby, leading to lower conductivities. Another explanation for the copolymer conductivities being lower than the p-OH PBI homopolymer is the lower acid loading in these membranes.

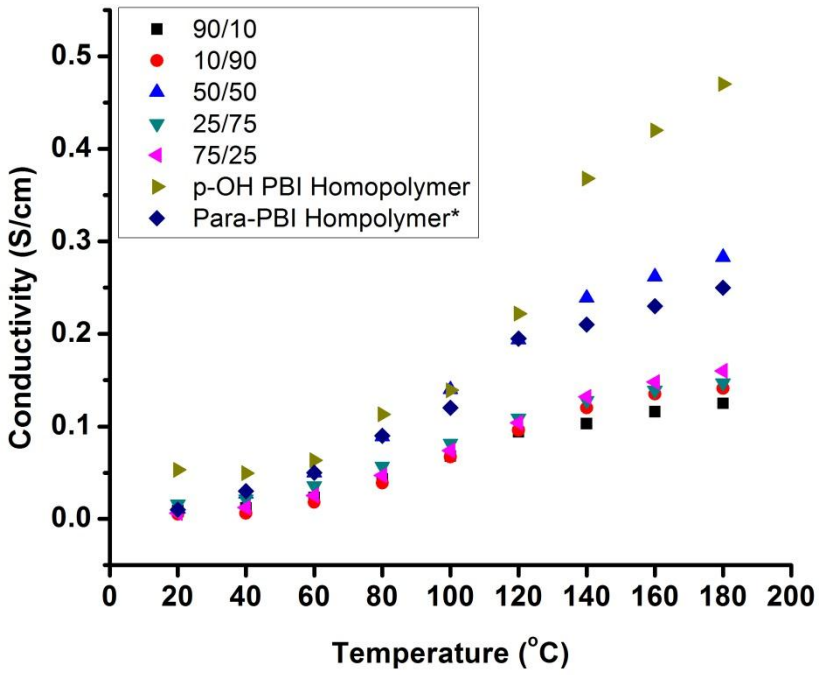

Figure 3.2: Conductivity of p-OH/Para PBI Copolymers and p-OH PBI and Para Homopolymers

Creep compliance is a known method of membrane failure in fuel cells. As the membrane starts to undergo creep, it causes thinning and loss of full contact with the electrodes which leads to fuel cell failure.[19] The compliance and creep rate of the membrane containing a 50/50 composition was tested and compared to films of p-OH

PBI and para-PBI. This chemistry was chosen to undergo creep testing since it demonstrated the highest conductivity and appeared to be the most promising for fuel cell testing. The membrane with the 50/50 composition demonstrated a lower creep than the p-OH PBI homopolymers. This could be due to the greater amount of polymer content in the 50/50 membrane than the homopolymer, as the copolymer was found to have a final polymer content of 11.27% and the p-OH PBI homopolymer was found to have a final polymer content of 8.77%. Many creep measurements have been conducted on para-PBI at various polymer contents.[19] The 50/50 composition had a compliance similar to that of a para-PBI membrane containing roughly twice the polymer content of the copolymer. This could be attributed to the crosslinks formed by the phosphate bridges between hydroxyl units leading to improved mechanical properties. A comparison of the creep in the 50/50 copolymer and the p-OH PBI homopolymer is shown in Figure 3.3.

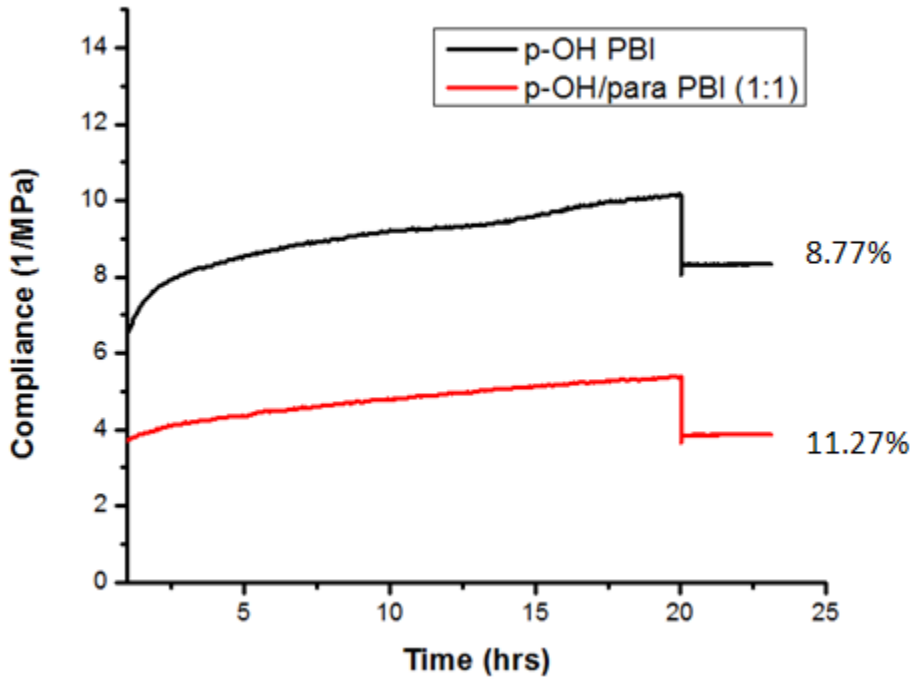

Figure 3.3: Compliance of p-OH PBI and 50/50 p-OH-r-Para PBI

Fuel cell performance was conducted on the 50/50 composition and the 25/75 (p-OH/para) composition to evaluate the membranes for use as the polymer electrolyte membrane. The polarization curves for the 25/75 composition are shown in Figure 3.4. Polarization curves were run at various temperatures and current densities to assess performance under different conditions. The fuel cell was able to reach a current density of 0.8 A/cm^2 at 160 °C and 180 °C. A current density of 0.6 A/cm^2 could be reached at both 120 °C and 140 °C. This performance is lower than the performances of both the p-OH and the para homopolymers. This could be due to the low IV of the polymer causing solubility issues at high temperatures. This is also consistent with the low conductivity of the membrane. Unfortunately, upon testing a fuel cell containing the 50/50 copolymer composition, the fuel cell was unable to reach 0.2 A/cm^2 and polarization curves were unable to be obtained. The membrane had appeared to have undergone creep as membrane could be seen in the sub-gaskets upon dismantling the fuel cell. This was unexpected as both the creep and conductivity of this film at high temperatures were good. Another possible contribution to the failure of the fuel cell could have been pinholes within the membrane that would have formed during casting, though none were visibly seen. This would have allowed for gas crossover and caused poor performance.

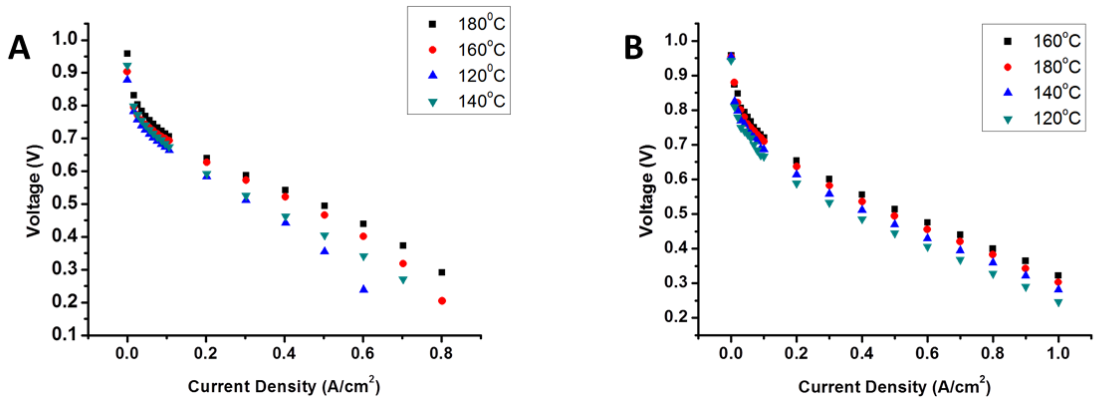

Figure 3.4: Polarization curves for a.) 25/75 p-OH/para PBI membrane b.) p-OH Homopolymer

3.6 Conclusion and Future Directions.

Five new random copolymer compositions containing p-OH PBI and para-PBI repeat units were able to be synthesized via the PPA Process and characterized to determine if they would be suitable for fuel cell membranes. Films were casted from the polymer solution once it visually hit an appropriate solution viscosity for film formation. All copolymer membranes demonstrated low inherent viscosities which were believed to contribute to the low tensile properties of the films. Unfortunately, the polymerizations could not have been conducted for longer period of time as the solutions would have been too viscous to cast. Conductivities were low for all copolymer compositions with the exception of the 50/50 composition. These low conductivities could be attributed to the low IV leading to solubility in PA at high temperatures.

The creep data of the 50/50 compositions appeared to be good under testing conditions, however, the membrane failed to operate in a fuel cell. This could have been due to creep within the film or pinholes that had formed during casting. The 25/75 p-

OH/para membrane had subpar performance compared with both the p-OH and para hompolymers. This could be attributed to the low IV and conductivity of the membrane.

In the future, investigating the morphology of the 50/50 membrane compared with the other copolymers would be beneficial to assess if the morphology plays a role in the higher conductivity seen and to determine if the polymer is "blocky" or random.

3.7 References.

(1) Xiao, L., Zhang, H., Scanlon, E., Ramanathan, L. S., Choe, E.W., Rogers, D., Apple, T., Benicewicz, B.C., *Chemistry of Materials* **2005**, *17*, 5328.

(2) Yu, S., Benicewicz, B.C., *Macromolecules* **2009**, *42*, 8640.

(3) Yu, S., Xiao, L., Benicewicz, B.C, *Fuel Cells* **2008**, *8*, 165.

(4) Li, Q., He, R., Gao, J., Jensen, J.O., Bjerrum, N. J., *Journal of The Electrochemical Society* **2003**, *150*, A1599.

(5) He, R., Li, Q., Xiao, G., Bjerrum, N. J., *Journal of Membrane Science* **2003**, *226*, 169.

(6) Wainright, J., Wang, J., Weng, D., Savinell, R., Litt, M., *Journal of Electrochemical Society* **1995**, *142*, L121.

(7) Hu, J., Zhang, H., Zhai, Y., Liu, G., Hu, J., Yi, B., *Electrochimica Acta* **2006**, *52*, 394.

(8) Li, Q., Hjuler, H. A., Bjerrum, N. J., *Journal of Applied Electrochemistry* **2001**, *31*, 773.

(9) Kongstein, O. E., Berning, T., Børresen, B., Seland, F., Tunold, R., *Energy* **2007**, *32*, 418.

(10) Yu , S., Zhang, H., Xiao, L., Choe, E., Benicewicz, B.C., *Fuel Cells* **2009**, *9*, 318.

(11) Mader, J., Xiao, L., Schmidt, T.J., Benicewicz, B.C., *Advances in Polymer Science* **2008**, *216*, 63.

(12) Mader, J., Xiao, L., Schmidt, T., Benicewicz, B.C., In *Fuel Cells II*; Scherer, G., Ed.; Springer Berlin Heidelberg: 2008; Vol. 216, p 63.

(13) Mader, J., Benicewicz, B.C., *Macromolecules* **2010**, *43*, 6706.

(14) Yu S, Ph. D. Thesis, Rensselaer Polytechnic Institute, 2006.

(15) Gulledge, A. L., Gu, B., Benicewicz, B.C. *Journal of Polymer Science Part A: Polymer Chemistry* **2012**, *50*, 306.

(16) Gulledge, A. L., Chen, X., Benicewicz, B.C. *Journal of Polymer Science Part A: Polymer Chemistry* **2014**, *52*, 619.

(17) Xiao, L., Zhang, H., Jana, T., Scanlon, E., Chen, R., Choe, E., Ramanathan, L., Yu, S., Benicewicz, B.C., *Fuel Cells* **2005**, *5*, 287.

(18) Mader, J. A., Benicewicz, B. C., *Fuel Cells* **2011**, *11*, 212.

(19) Chen, X., Qian, G., Molleo, M.A., Benicewicz, B.C., Ploehn, Harry J., *Journal of Polymer Science Part B: Polymer Physics* **2015**, *53*, 1527.

CHAPTER 4

SOLUTION POLYMERIZATION OF POLYBENZIMIDAZOLE

4.1 Abstract.

Polybenzimidazoles (PBI) are an important class of heterocyclic polymers that demonstrate high thermal and oxidative stabilities. The two dominant polymerization methods used for the synthesis of PBI are the melt/solid polymerization route and solution polymerization using polyphosphoric acid as solvent. Both methods have been widely used to produce high-molecular weight PBI, but also highlight the obvious absence of a practical organic solution based method of polymerization. This current work explores the synthesis of high-molecular weight meta-PBI in N,N-dimethyl acetamide (DMAc). Initially, model compound studies examined the reactivity of small molecules with various chemical functionalities that could be used to produce 2-phenyl-benzimidazole in high yield with minimal side reactions. ^{1}H-NMR and FTIR studies indicated that benzimidazoles could be efficiently synthesized in DMAc by reaction of an *o*-diamine and the bisulfite adduct of an aromatic aldehyde. Polymerizations were conducted at various polymer concentrations (2-26 wt% polymer) using difunctional monomers to optimize reaction conditions in DMAc which resulted in the preparation of high-molecular weight meta-PBI (IV>0.9 dL/g). TGA and DSC confirmed that meta-PBI produced via this route has comparable properties to that of commercial m-PBI. This method is advantageous in that it not only allows for high-polymer concentrations of m-PBI to be synthesized directly and efficiently, but can be applied to the synthesis of many PBI derivatives.

4.2 Introduction.

Polybenzimidazoles (PBIs) are an important class of heterocyclic polymers that were first reported in 1959[1] with the development of the first aromatic PBI shortly after, in 1961.[2] Polybenzimidazole was originally designed and investigated as a thermally stable, oxidative resistant material.[3] Since development, numerous variations of PBI derivatives have been reported.[4-6] Of all the derivations of polybenzimidazoles, aromatic

PBIs have received the most attention due to their excellent thermal stabilities and chemical resistances.[7-17]

Fully aromatic PBIs exhibit very high decomposition temperatures (>500˚C), and do not show melting points due to their lack of crystallinity or have melting points above their decomposition temperatures.[18] Since PBI demonstrates excellent thermal stabilities, it is especially suited for high-temperature fabric applications, and is commercially produced as a high-performance, thermally stable fiber.[19]

Polybenzimidazoles can be synthesized via a few different methods. One common synthetic route is through a polycondensation of diacid and tetra-amine monomers as shown in Scheme 4.1.Typical synthesis of bisbenzimidazoles involves a reaction between bis-*o*-phenylenediamines with a diacid in hydrochloric acid or polyphosphoric acid (PPA).[20] Synthesis of 2-substituted benzimidazoles from the reaction of *o*-phenylendiamine with an imidate are also well known.[21] Synthetic knowledge of these procedures can be applied to polymeric systems when di-functional monomers are incorporated, however, challenges arise when considering solubility and degree of polymerization. Although PBI is an alkaline polymer (pka ~5.25)[22] with both proton donor and acceptor sites that allow for specific interactions with polar solvents,[23-25] it is practically insoluble in most organic solvents.[26]

Scheme 4.1: Polybenzimidazole synthesis through polycondensation of diacid and tetraamine monomers

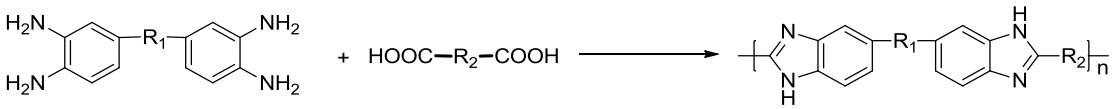

Many polymerization techniques have been investigated to develop high molecular-weight PBI including: Eaton's reagent as the polymerization solvent,[27,28] mixed solvent systems,[29] oxidative cyclization of corresponding polyamidines,[30] and Higashi phosphorylation techniques.[31] More commonly, PBI is synthesized with polyphosphoric acid as a solvent, and has proven to be quite advantageous for fuel cell applications.[32] Although PBI can be successfully prepared through these methods, none of the techniques mentioned provide an efficient route to the synthesis of high-molecular weight PBI in a common organic solvent suitable for commercial production of fibers, films, or coatings. PBI is commercially produced by PBI Performance Products using a two stage melt/solid phase polymerization method in which diphenyl isophthalate (DPIP) is condensed with tetraaminobiphenyl (TAB) to produce poly(2,2'-m-phenylene-5,5'-bibenzimidazole) (m-PBI).[33] The polymerized product is then dissolved and used to produce a high-performance thermal fiber, which is used for various fire resistant applications.

Herein, we report an efficient solution polymerization method for the synthesis of high-molecular weight m-PBI (up to 1.3 dL/g) in N,N-dimethylacetamide (DMAc) suitable for commercial production of m-PBI which can be applied to the synthesis of a variety of PBI derivatives. Model compound studies were conducted and monitored via GC/MS analysis to determine suitable candidates for the synthesis of m-PBI in DMAc. Using the bisulfite adduct of isophthalaldehyde, m-PBI was polymerized in DMAc as shown in Scheme 4.2. Polymerization parameters were optimized and the resulting polymer was confirmed via ^{1}H-NMR and FT-IR analysis. Further comparisons of the solution polymerized m-PBI product and the commercially produced m-PBI product were

conducted via differential scanning calorimetry (DSC) and thermogravimetric analysis (TGA) to confirm the solution polymerized m-PBI product met the material specifications of the commercially produced m-PBI.

Scheme 4.2: Polymerization of poly(2,2'-m-phenylene-5,5'-bibenzimidazole) (m-PBI) in DMAc.

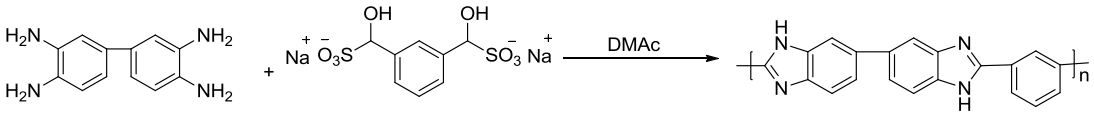

4.3 Experimental Section.

4.3.1 Materials

Isophthalaldehyde (98%) was purchased from Combi-Blocks. Sodium bisulfite ($NaHSO_3$) and Sodium metabisulfite ($Na_2S_2O_5$) were purchased from JT Baker. Diphenyl isophthalate (DPIP) was donated by PBI Performance Products. Isophthalic acid was purchased from Amoco. Lithium Chloride (LiCl, 99%) and phenyl benzoate (99%) were purchased from Acros. Benzaldehyde (99%) and o-phenylenediamine (99%) were purchased from Aldrich. TAB monomer, 3,3',4,4'-tetraaminobiphenyl (polymer grade, ~97.5 %) was donated by Celanese Ventures, GmbH (now, BASF Fuel Cell). Common solvents (e.g., DMSO, MeOH, EtOH etc.) and benzoic acid certified primary standard were purchased from Fisher Scientific. Sulfuric acid (96%) was purchased from Alfa Aesar. All chemicals were used as received unless otherwise stated.

4.3.2 Preparation of Isophthalaldehyde Bisulfite Adduct (IBA)

The procedure used for the synthesis of IBA was developed from Higgins et al.[34] Sodium bisulfite (22.5g, 0.216mol) was dissolved in 75mL deionized water. Isophthalaldehyde (14.5g, 0.108mol) was dissolved in 500mL of MeOH. Once dissolved, the solutions were combined in a 1000mL round bottom flask and stirred at room temperature for 24h. After

several hours, a white precipitate formed. This precipitate was confirmed via ^{1}H-NMR to be the bisulfite adduct of isophthalaldehyde (yield: 11.36g, 91.5%). Analysis: FT-IR: 1410w, 1350w, 1250w,1175s, 1000s, 650s cm^{-1}. ^{1}H-NMR (300 MHz, DMSO-d6) δ 7.7 (s, 1H), 7.5 (d, 1H, *J*=6.1), 7.3 (d, 1H, *J*=6.1), 6.0 (s, 1H), 5.1 (s, 1H).

4.3.3 Solution Polymerization of m-PBI

In a typical polymerization, 4.0g (11.6 mmols) of isophthalaldehyde bisulfite adduct, 2.504g (11.6 mmols) of tetraaminobiphenyl and 17.5mL of DMAc were added to a 3-neck 100mL round bottom flask under nitrogen. The flask was then equipped with a stir-rod and paddle and stir-rod adaptor in the center flask neck which was connected to an overhead mechanical stirrer. A reflux condenser with nitrogen outlet was then attached and the remaining flask neck was then fitted with a nitrogen inlet. A slow nitrogen flow rate, monitored by oil filled bubblers, was then established and maintained throughout the reaction. Once assembled, the apparatus was lowered into a temperature regulated silicone oil bath. The oil bath temperature was regulated with an IR^{2} thermal controller. Once the reaction was purged, the oil bath was heated to 180˚C , and maintained for the duration of the reaction. Upon refluxing of the solution, stirring was initiated at 60 RPM and maintained throughout the duration of the reaction. The polymerizations were allowed to proceed at reflux for 48-72 hours with the exception of the trials performed to determine the effect of time on inherent viscosity.

Polymerizations in which sodium metabisulfite was added to generate sulfur dioxide in situ were allowed to heat at reflux before the sodium metabisulfite was added. In these trials, 1 equivalent of sodium metabisulfite was added for every 3-6 equivalents

of isophthalaldehyde bisulfite adduct (0.371-0.741 g, 1.95-3.90 mmoles). The sodium metabisulfite was added over the duration of the polymerization (48-72 hours).

4.3.4 Polymer Isolation

Upon completion of the reaction, the polymer product was isolated by precipitation in deionized water. The polymer was blended in water and vacuum filtered 3x then blended in methanol and filtered 3x. Powders were then collected and dried under vacuum at 180 °C for 24 hours. Once dried, the polymer powder was used for product analysis.

4.4 Characterization Techniques

FT-IR spectra were recorded on a Perkin Elmer Spectrum 100. ^{1}H-NMR were recorded using a Varian Mercury 300 spectrometer. Thermal gravimetric analysis (TGA) of dried polymer samples was conducted using a TA Instruments Q5000 with nitrogen or air flow rates of 25mL/min and a heating rate of 10 ˚C/min.TGA was performed from room temperature to 750 ˚C. GC/MS analysis was used to monitor reaction products of small molecule analogs using a Shimadzu GCMS-QP2010S equipped with a Shimadzu SHRX1-5MS column. Samples were prepared in DMAc. The temperature program for the GC column oven ramped the oven temperature from 150˚C to 300˚C at 30˚C/min and then held at 300˚C for 6 minutes. Differential scanning calorimetry (DSC) was conducted using a TA Instruments Q2000 with 50 mL/min nitrogen flow and a heating rate of 5 °C/min.

Inherent viscosity (IV) measurements were conducted using a Cannon Ubbelohde (200 μm) viscometer at a concentration of 0.2 g/dL in sulfuric acid (H_2SO_4) at 30.0 ˚C. Samples were prepared by dissolving the dried polymer powders in sulfuric acid using a

mechanical shaker. Reported IV values are an average of three separate measurements and were calculated as previously reported.[35]

4.5 Results and Discussion.

4.5.1 Model compound studies

Model compound studies were conducted in which GC/MS analysis was used to evaluate the reactivity of various chemical functionalities with *o*-phenylenediamine in 1:1 ratios in DMAc for the production of 2-phenyl benzimidazole as shown in Figure 4.1.

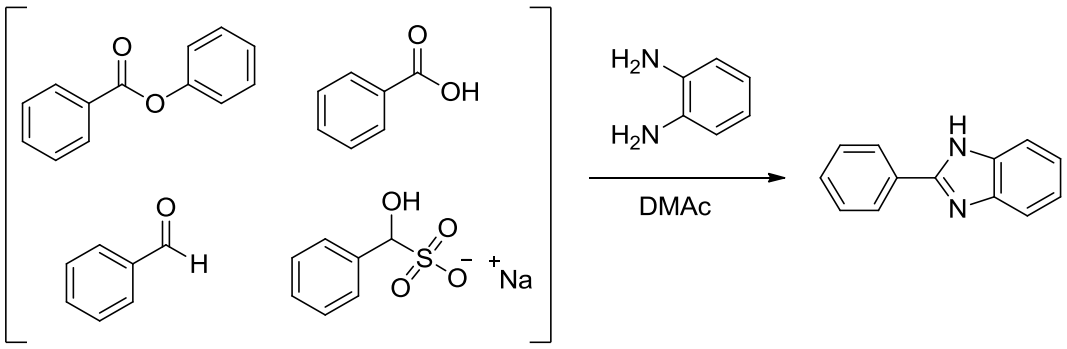

Figure 4.1: Chemical functionalities evaluated for the synthesis of 2-phenyl benzimidazole in DMAc.

Initially, the reaction of phenyl benzoate with *o*-phenylenediamine was evaluated because of the commercial utilization of DPIP, however, even at reflux conditions, the reaction was unsuccessful and yielded no 2-phenyl benzimidazole. Studies were then conducted with benzoic acid, as PBIs are commonly synthesized using diacid monomers.[7,14,36] GC/MS analysis of the reaction of *o*-phenylenediamine showed multiple reaction products. After 48hrs of reaction, less than 10 % of the desired 2-phenyl benzimidazole product was obtained. Efforts then proceeded to the evaluation of the aldehyde functionality. The reaction of benzaldehyde and *o*-phenylenediamine was then evaluated as shown in Figure 4.2.

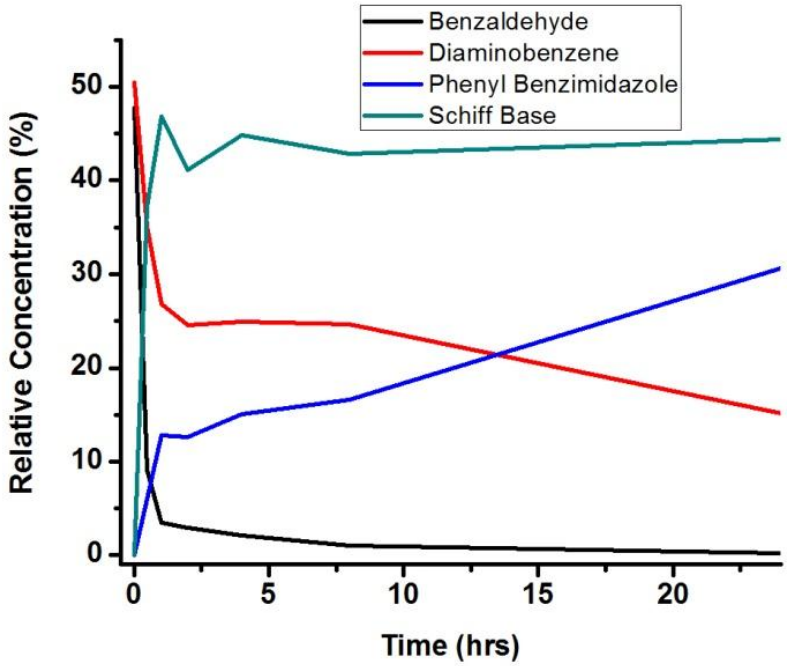

Figure 4.2**:** GC/MS analysis for the reaction of benzaldehyde and o-diaminobenzene in DMAc at 160˚C

A higher yield of the desired product was obtained (~30 % after 24h), however, the reaction system was quickly dominated by an m/z 284 signal which was later determined to be the bisimine or schiff-base product (N1E,N2E)-N1,N2-dibenzylidenebenzene-1,2-diamine.

An earlier literature report of an isophthalaldehyde bisulfite adduct used to produce polybenzimidazole was found in which low-molecular weight PBI was obtained in DMAc at low concentration.[34] Analysis was then conducted via GC/MS for the reaction of the bisulfite adduct of benzaldehyde with *o*-phenylenediamine in DMAc. GC/MS analysis revealed a very efficient reaction with high yield of 2-phenylbenzimidazole and no unwanted byproducts as shown in Figure 4.3. It is important to note that the bisulfite adduct of benzaldehyde and *o*-phenylenediamine were used in a

1:1 equivalent even though it appears at the beginning of the GC/MS spectra that less of the bisulfite adduct of benzaldehyde was used. This is due to the low solubility of the bisulfite adduct of benzaldehyde in DMAc.

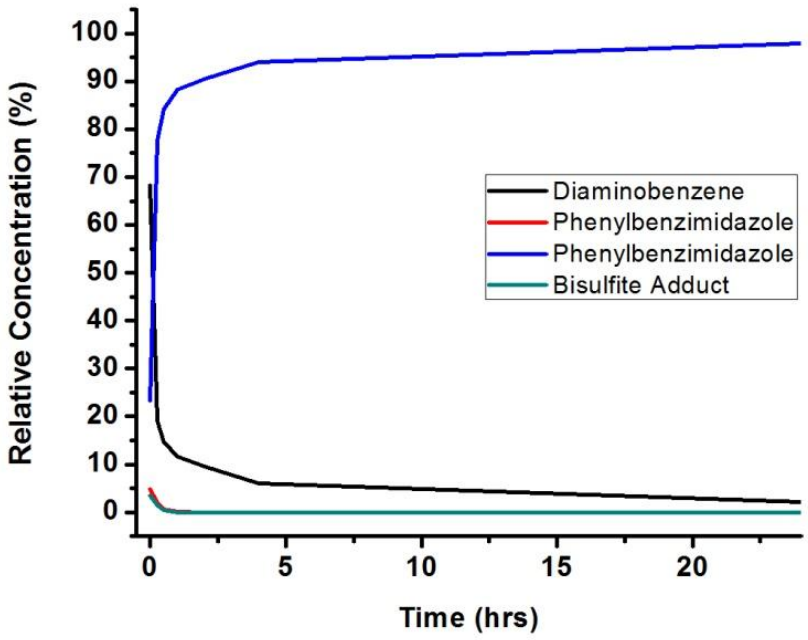

Figure 4.3: GC/MS analysis for the reaction of the bisulfite adduct of benzaldehyde and o-diaminobenzene in DMAc at 160˚C.

4.5.2 Polymerization Trials

To be thorough, and ensure nothing was overlooked, polymerization trials were conducted using difunctional monomers corresponding to those used in the model compound studies. Evaluating the polymerization of DPIP and TAB, polymer product was not obtained as the small molecule study had suggested. Polymerization trials with isophthalic acid and TAB yielded some reaction products, however polymer was not obtained. Trials involving isophthalaldehyde and TAB quickly resulted in a cross-linked products which were insoluble in all solvents tested. This is attributed to the formation of

the imines, which were previously observed and reported by Higgins and Marvel.[34] Finally, polymerization trials using isophthalaldehyde bisulfite adduct and TAB were conducted and shown by ^{1}H-NMR, TGA, and DSC to produce m-PBI which was studied in further detail and reported herein.

4.5.3 Synthesis of Isophthalaldehyde Bisulfite Adduct (IBA)

IBA was synthesized using mild reaction conditions as described previously. Monomer scale up was achieved on the kilogram scale to allow for detailed polymerization studies. This was performed by dissolving 498.64 g of isophthalaldehyde in 17.5 L of MeOH in a 7 gallon plastic pail. An overhead stirrer was used at a stir rate of approximately 250 RPM. Sodium bisulfite (781.0 g) was then dissolved in 2.6 L of distilled water. Once both the sodium bisulfite and the isophthalaldehyde, the sodium bisulfite solution was added to the bucket over a 5 minute period and vigorous stirring was continued. After 5h, a large amount of white precipitant was obtained in high yield (> 90%) and purity (> 98%). Monomer was purified via a methanol wash to remove residual isophthalaldehyde before drying under vacuum at 80 °C. Purity was assessed by monitoring the aldehyde impurity peak at 9.9 ppm in the ^{1}H-NMR spectrum. It was found that monomer batches containing < 3% aldehyde resulted in the highest IV polymers. In order to be certain that additional salt was not present from the sodium bisulfite reactant, TGA was performed to assess the char yield. Monomer batches that contained < 33% char at 400 °C yielded the highest IV polymer. It is important to note that impurities in monomer can affect the IV of the polymer by disrupting stoichiometry during weighing, as explained by Carother's equation.

4.5.4 Polymerization studies of m-PBI

Detailed polymerization experiments were conducted for m-PBI using IBA and TAB in DMAc to study the effects of LiCl addition, monomer concentration, and polymerization time on final polymer molecular size as indicated by IV measurements. Investigations were conducted with and without the addition of LiCl, a solution stabilizer for m-PBI in DMAc, at various polymer concentrations as shown in Figure 4.4.

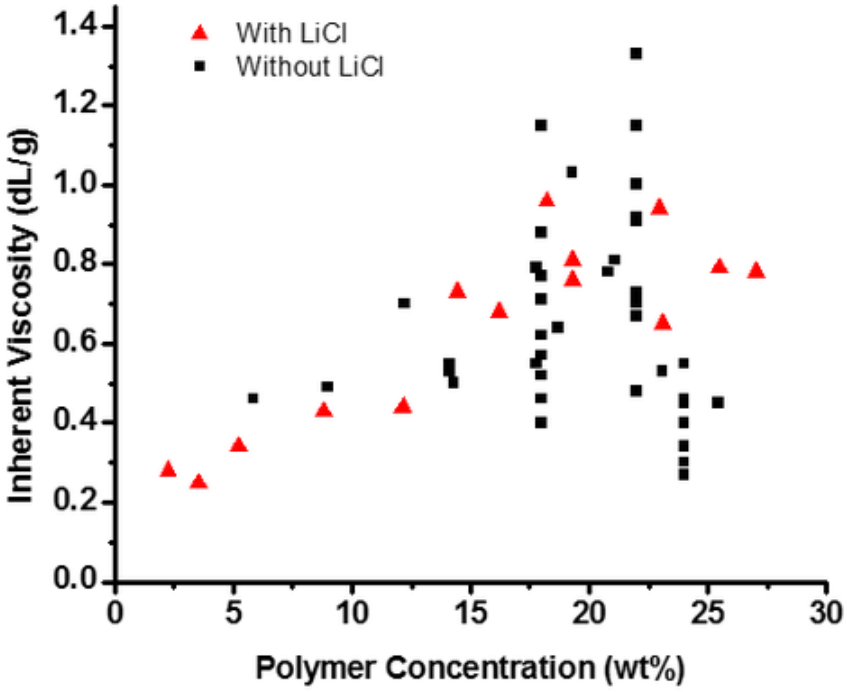

Figure 4.4**:** Optimization study for the synthesis of m-PBI in DMAc with and without the presence of LiCl. A solution of 2% LiCl in DMAc was used.

Experiments were also performed to assess the effect of time on inherent viscosity at various polymer concentrations as seen in Figure 4.5. No direct correlation was observed between inherent viscosity and time when polymerizations were conducted greater than 24 hours.

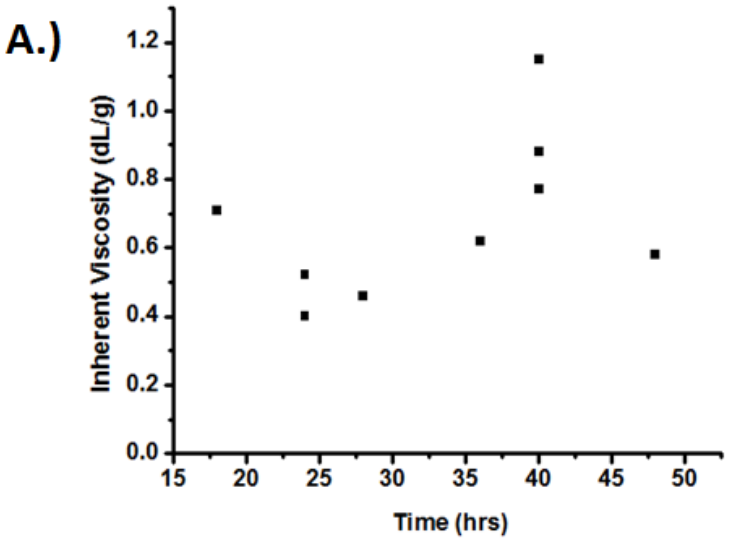

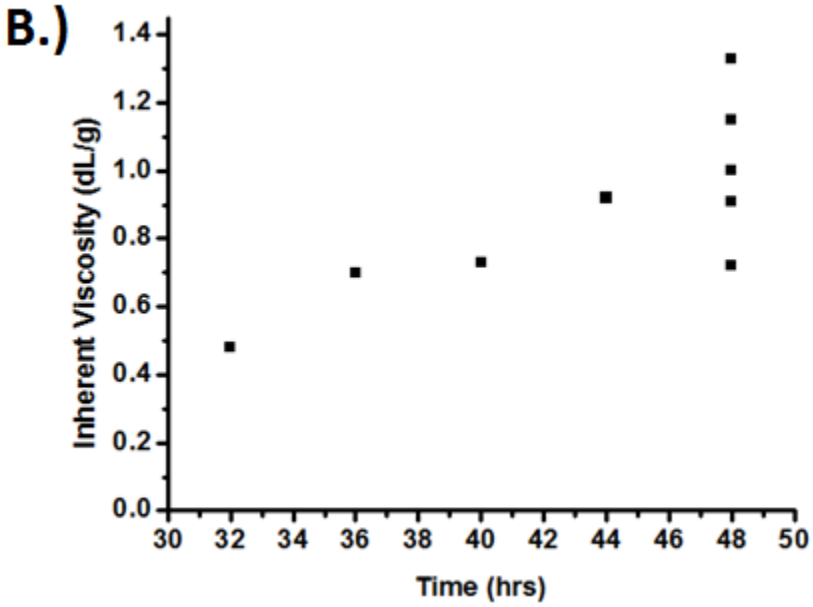

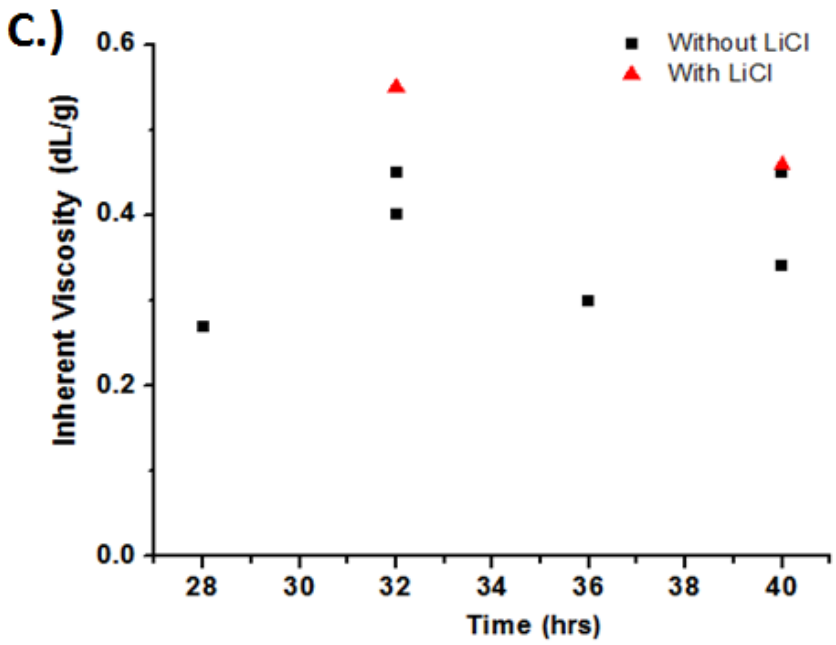

Figure 4.5: Inherent viscosity as a function of time: A.) 18 wt % polymer B.) 22 wt% polymer C.) 24 wt% polymer

Due to the variation in polymer IV values obtained in polymerizations that were performed under similar reaction conditions, the monomer purity of isophthalaldehyde bisulfite adduct was reassessed. Variations in monomer purity were found among different monomer batches and thus, a more dilute monomer synthesis procedure than previously reported was followed (as reported in the experimental section) that produced high-purity monomer. The m-PBI product was investigated via ^{1}H-NMR and compared to a reported literature spectra for m-PBI[37] as shown in Figure 4.6. FT-IR spectral comparisons of the solution polymerized product and commercially produced m-PBI also confirmed the synthesis of m-PBI.

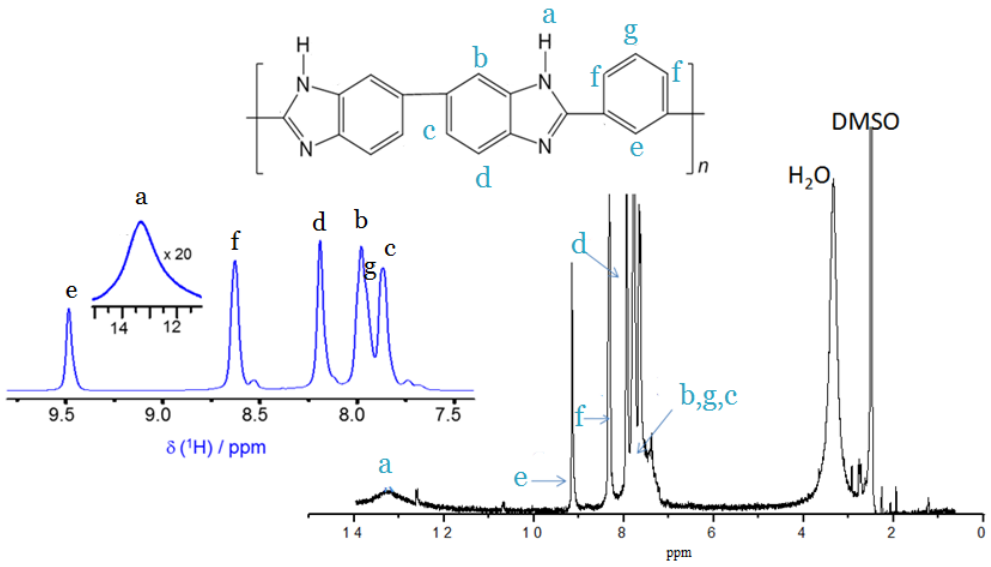

Figure 4.6: 1) Reported literature for the 1H-NMR of m-PBI[36], 2) 1H-NMR of solution polymerized m-PBI.

To further understand what factors are involved in obtaining high molecular weight PBI via this solution polymerization method, the final step of the mechanism (dehydrogenation) leading to imidazole formation was investigated. Starshikov and Romero both report the synthesis of heterocyclic aromatic molecules that are similar in structure to benzimidazole.[38,39] In both cases, sulfur dioxide is generated in situ and is used as the oxidant for the final dehydrogenation step with the concomitant generation of sulfurous acid.[38,39] To test the effects of sulfur dioxide on imidazole formation and final IV of the polymer, polymerizations were conducted with the in situ generation of sulfur dioxide. Sodium metabisulfite, which thermally decomposes into sulfur dioxide and sodium sulfite, was added to these polymerizations over the duration of the reaction. Figure 4.7 shows a variety of polymerization trials, some with and without the addition of sodium metabisulfite. Scheme 4.3 shows the proposed reaction mechanism in which

sulfur dioxide is generated in situ. The highlighted area shows how SO_2 oxidizes the heterocyclic ring to the benzimidazole while the sulfur is reduced to sulfurous acid.

Scheme 4.3: Proposed mechanism of ring closure in the presence of sulfur dioxide

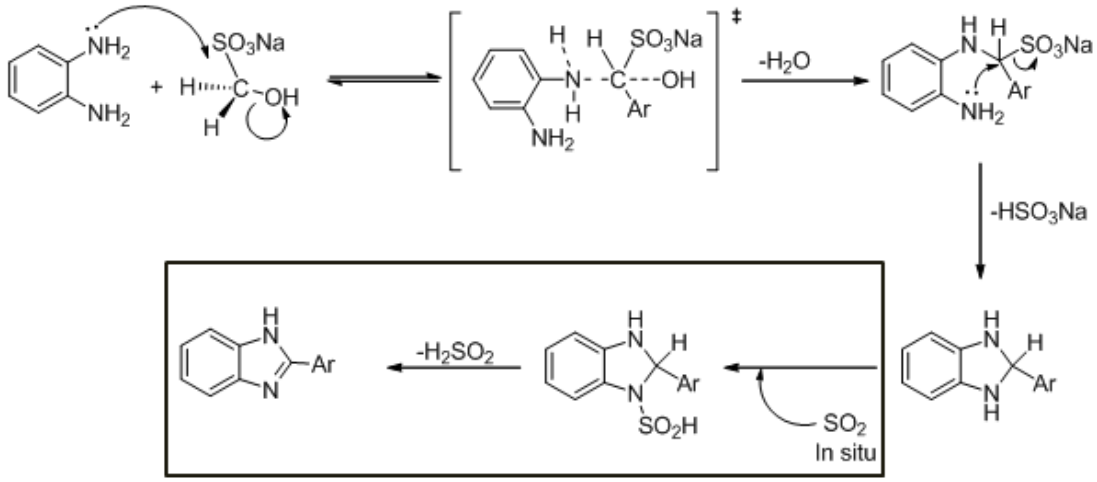

Figure 4.7 shows the results of the polymerizations conducted over a variety of experimental conditions with and without the addition of sodium metabisulfite. The overwhelming correlation on final polymer IV was the introduction of sodium metabisulfite during the polymerization. Polymer IVs in excess of those found commercially (>0.5-0.7 dL/g) were routinely prepared under different conditions.

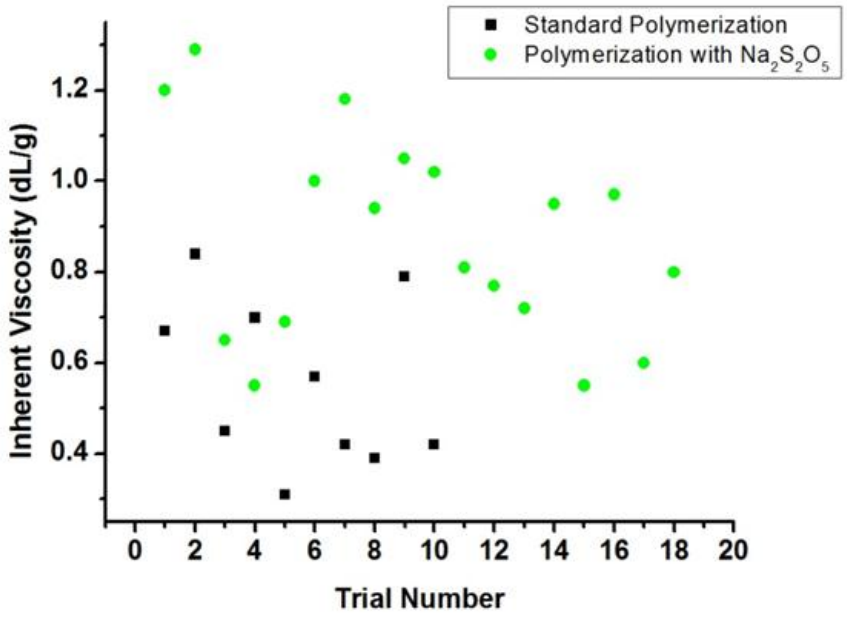

Figure 4.7**:** Polymerization trials with and without the addition of sodium metabisulfite for SO_2 generation in situ.

4.6 Thermal Analysis.

Thermal analyses of the solution polymerized m-PBI and the commercially produced m-PBI were conducted via DSC and TGA. Modulated DSC analysis was conducted from ambient temperature to 500˚C with 50 mL/min nitrogen flow and a heating rate of 5 °C/min. The glass transition temperature (T_g) of the solution polymerized m-PBI was determined to be ~430˚C as indicated by a baseline shift. Analysis of the commercially produced m-PBI also indicated a corresponding T_g. A modulated DSC comparison of the solution polymerized m-PBI and commercially produced m-PBI as shown in Figure 4.8.

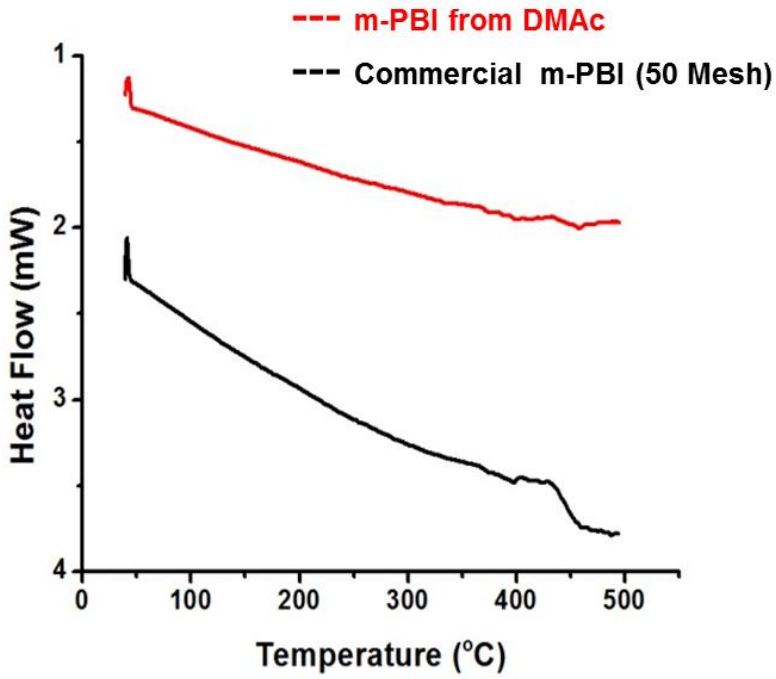

Figure 4.8: Modulated DSC analysis for the solution polymerized m-PBI and commercially produced m-PBI.

PBI type polymers are well-known for their high thermal stabilities resulting from their fully aromatic structure and polymer chain rigidities.[40-42] TGA analysis was conducted from ambient temperature to 800˚C with a heating rate of 10˚C/min. TGA analysis was conducted on the solution polymerized m-PBI and the commercially produced m-PBI as shown in Figure 4.9. Both materials show more than 90% weight retention at 600˚C, a known thermal characteristic of PBI.[43] The commercially produced m-PBI sample shows water an dimethyl acetamide loss between 100 and 200°C, which is to be expected as PBI is very hygroscopic and has been shown to retain up to 15% (by weight) of water even in short handling times.[44] The solution polymerized m-PBI product also shows gradual weight loss between 200-500˚C which was attributed to residual DMAc within the polymer sample.

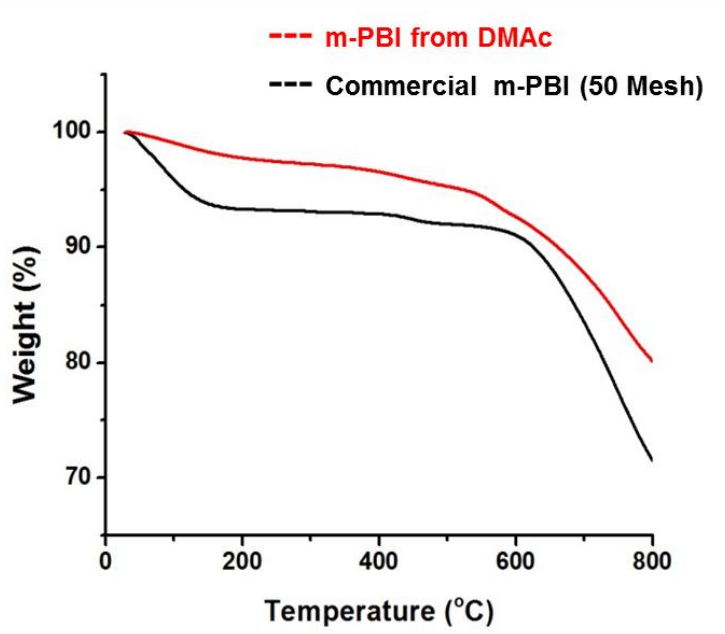

Figure 4.9: TGA analysis of the solution polymerized m-PBI and commercially produced m-PBI.

4.7 Conclusions.

Model compound studies were conducted with mono-functional reagents and monitored via GC/MS to determine which chemical functionalities would be suitable for benzimidazole formation in DMAc. Studies on the reaction of phenyl ester, carboxylic acid, aldehyde, and a bisulfite adduct of the aldehyde functionalities with *o*-phenylenediamine in DMAc showed that only the bisulfite adduct was capable of producing a high yield of the desired 2-phenylbenzimidazole.

Polymerizations were conducted with all difunctional counterparts, and again, reaction of the bisulfite adduct of isophthalaldehyde with TAB was the only pair of monomers that showed successful conversion to m-PBI. Monomer scale-up was conducted for the isophthalaldehyde bisulfite adduct (IBA) to allow for further polymerization studies. Detailed polymerization experiments with IBA and TAB were

conducted in DMAc for concentrations ranging from 2 to 26 weight % polymer. These studies established polymerization conditions that produced high IV polymers (up to 1.3 dL/g) at high polymer concentrations in the range suitable for the direct processing of solutions into films, coatings, and fibers. Additional mechanistic studies on the benzimidazole ring formation showed that *in situ* generation of sulfur dioxide (to ensure complete oxidative dehydrogenation) led to routine and consistent syntheses of high IV polymers.

The chemical structure of the solution polymerized m-PBI was confirmed via ^{1}H-NMR and FT-IR analysis. DSC showed the T_g of both the solution polymerization product and the commercially produced m-PBI to be approximately 430˚C. The thermal stability of the solution polymerized m-PBI was also comparable to that of the commercially produced m-PBI. Overall, a new, convenient, commercially viable solution polymerization method was developed for the synthesis of m-PBI in DMAc solutions. This new polymerization method is reported as a viable means for both laboratory scale and large scale production of high-molecular weight m-PBI and is applicable to the synthesis of a variety of PBI derivatives.

4.8 Acknowledgments.

We gratefully acknowledge the support of PBI Performance Products Inc.

4.9 References.

(1) Brinker, K. C., Cameron, D. D., Robinson, I. M., U.S. Patent #2904537, 1959.

(2) Vogel, H., Marvel, C.S. *Journal of Polymer Science, Part A: Polymer Chemistry* **1961**, *34*, 511.

(3) Powers, E. J., Serad, G.A. In *High Performance Polymers: Their Origin and Development* 1986, p 355.

(4) Mader, J., Xiao, L., Schmidt, T.J., Benicewicz, B.C. *Advanced Polymer Science* **2008**, *216*, 63.

(5) Li, Q., Jensena, J.O., Savinell, R.F., Bjerrum, N. *Journal of Progress in Polymer Science* **2009**, *34*, 449.
(6) Seel, D. C., Benicewicz, B.C., Xiao, L., Schmidt, T.J. In *Handbook of Fuel Cells* 2009; Vol. 5, p 300.
(7) Gulledge, A. L., Chen, X., Benicewicz, B.C. *Journal of Polymer Science Part A: Polymer Chemistry* **2014**, *52*, 619.
(8) Perry, K. A., More, K.L, Payzant, A., Meisner, R.A., Supter, B.G., Benicewicz, B.C. *Journal of Polymer Science Part B: Polymer Physics* **2014**, *52*, 26.
(9) Li, X., Qian, G., Chen, X., Benicewicz, B. C. *Fuel Cells* **2013**, *13*, 832.
(10) Li, X., Chen, X., Benicewicz, B.C. *Journal of Power Sources* **2013**, *243*, 796.
(11) Jayakumar, J. V., Gulledge, A., Staser, J.A., Kim, C., Benicewicz, B.C., Weidner, J.W. *ECS Electrochemistry Letters* **2012**, *1*, F44.
(12) Neutzler, J., Qian, G., Huang, K., Benicewicz, B.C. *Journal of Power Sources* **2012**, *216*, 471.
(13) Seel, D. C., Benicewicz, B.C. *Journal of Membrane Science* **2012**, *405–406*, 57.
(14) Gulledge, A. L., Gu, B., Benicewicz, B.C. *Journal of Polymer Science Part A: Polymer Chemistry* **2012**, *50*, 306.
(15) Mader, J. A., Benicewicz, B. C. *Fuel Cells* **2011**, *11*, 212.
(16) Yu, S., Benicewicz, B.C. *Macromolecules* **2009**, *42*, 8640.
(17) Molleo, M., Schmidt, T., Benicewicz, B.C. In *Encyclopedia of Sustainability, Science and Technology*; Meyers, R. A., Ed.; Springer Science + Business Media LLC: New York, 391-431, 2013.
(18) Bingham, M. A., Hill, B. J. *Journal of Thermal Analysis* **1975**, *7*, 347.
(19) Coffin, D. R., Serad, G.A., Hicks, H.L., Montgomery, R.T. *Textile Research Journal* **1982**, *52*, 466.
(20) Berrada, M., Anbaoui, Z., Lajrhed, N., Knouzi, N., Vaultier, M., Sekiguchi, H., Carrière, F. *Chemistry of Materials* **1997**, *9*, 1989.
(21) Holan, G., Samuel, E. L. *Journal of the Chemical Society C: Organic* **1967**, 25.
(22) Sannigrahi, A., Ghosh, S., Maity, S., Jana, T. *Polymer* **2010**, *51*, 5929.
(23) Kojima, T. *Journal of Polymer Science: Polymer Physics Edition* **1980**, *18*, 1685.
(24) Shogbon, C. B., Brousseau, J., Zhang, H. Benicewicz, B. C., Akpalu, Y.A. *Macromolecules* **2006**, *39*, 9409.
(25) Sannigrahi, A., Arunbabu, D., Sankar, R. M., Jana, T. *Macromolecules* **2007**, *40*, 2844.
(26) Stuetz, D. E., Diedwardo, A. H., Zitomer, F., Barnes, B. P. *Journal of Polymer Science: Polymer Chemistry Edition* **1980**, *18*, 987.
(27) Borjigin, H., Stevens, K. A., Liu, R., Moon, J.D., Shaver, A.T., Swinnea, S., Freeman, B.D., Riffle, J. S., McGrath, J.E., *Polymer* **2015**, *71*, 135.
(28) Li, X., Singh, R. P., Dudeck, K. W., Berchtold, K. A., Benicewicz, B.C., *Journal of Membrane Science* **2014**, *461*, 59.
(29) Hedberg, F. L., Marvel, C. S. *Journal of Polymer Science: Polymer Chemistry Edition* **1974**, *12*, 1823.

(30) Dudgeon, C. D., Vogl, O. *Journal of Polymer Science: Polymer Chemistry Edition* **1978**, *16*, 1831.
(31) Yamazaki, N., Higashi, F. *Journal of Polymer Science: Polymer Letters Edition* **1974**, *12*, 185.
(32) Xiao, L., Zhang, H., Scanlon, E., Ramanathan, L. S., Choe, E.W., Rogers, D., Apple, T., Benicewicz, B.C. *Chemistry of Materials* **2005**, *17*, 5328.
(33) Sandor, R. B. *PBI (Polybenzimidazole): Synthesis, Properties, and Applications* **1990**, *2*, 25.
(34) Higgins, J., Marvel, C. S. *Journal of Polymer Science Part A-1: Polymer Chemistry* **1970**, *8*, 171.
(35) Mader, J. A., Benicewicz, B. C. *Macromolecules* **2010**, *43*, 6706.
(36) Qian, G., Benicewicz, B. C. *ECS Transactions* **2011**, *41*, 1441.
(37) Conti, F., Willbold, S., Mammi, S., Korte, C., Lehnert, W., Stolten, D. *New Journal of Chemistry* **2013**, *37*, 152.
(38) Starshikov, N., Pozharskii, A., *Chemistry of Heterocyclic Compounds* **1980**, *16*, 81.
(39) Romero, A., Salazar, J., Lopez, S. *Journal of Synthetic Organic Chemistry* **2013**, *45*, 2043.
(40) Neuse, E. In *Synthesis and Degradation Rheology and Extrusion*; Springer Berlin Heidelberg: 1982; Vol. 47, p 1.
(41) Buckley, A., Stuetz, D.E., Serad, G.A. *Encyclopedia of Polymers Science and Technology*; Wiley: New York, 1998; Vol. 11.
(42) Chung, T. S. *Plastics Engineering* **1997**, *41*, 701.
(43) Choe, E. W., Choe, D.D. *Polybenzimidazoles (overview)*; CRC Press: New York, 1996; Vol. 7.
(44) Li, Q., He, R., Berg, R. W., Hjuler, H. A., Bjerrum, N. J. *Solid State Ionics* **2004**, *168*, 177.

CHAPTER 5

ETHER POLYBENZIMIDAZOLES VIA SOLUTION POLYMERIZATION

5.1 Abstract.

Herein, two ether-containing polybenzimidazoles, poly[2,2'-(p-oxydiphenylene)-5'5-benzimidazole] (P,P-Ether PBI) and poly[2,2'-(m,p-oxydiphenylene)-5'5-benzimidazole] (M,P-Ether PBI), were synthesized directly in dimethyl acetamide (DMAc) via a new solution polymerization method. In order to polymerize these ether-containing polymers, new monomers containing sodium bisulfite adduct functional groups were first synthesized and characterized. The thermal stability of the polymers was evaluated using thermogravimetric analysis (TGA). Solubility studies were also performed in order to further characterize these ether-PBI analogs.

5.2 Introduction.

Polybenzimidazole (PBI), a class of heterocyclic aromatic polymers, has long been known for its thermal and chemical stabilities which are greatly attributed to its aromatic backbone.[1] PBI has proven useful in many high temperature applications such as polymer electrolyte membrane fuel cells,[2-8] hydrogen pumping devices,[9,10] and high performance fibers.[11] Though PBI's excellent thermal stability gives it many advantages in these high temperature applications, its high glass transition temperature makes processing difficult.

A library of PBI analogs has been synthesized in order to alter the properties of the polymer.[2,6] For example, pyridine PBI analogs have been incorporated into PBI copolymer systems to increase the polymer content in gel membranes.[12] In another study, hydroxyl functional units are incorporated into PBI copolymer systems to increase conductivity.[13] In the past, ether linkages have been incorporated into rigid polymers in order to increase backbone flexibility and the overall processability of the polymer. The incorporation of aryl ether linkages into the backbones of thermally stable polymers has

been heavily explored. Polybenzoxazoles,[14] polyimides,[15] polyquinoxalines,[16,17] polybenzothiazoles,[18] and polybenzimidazoles[19,20] have all been studied when aryl ether linkages are introduced in the polymer backbone to increase flexibility and to lower the T_g.

The previously reported ether-PBI analogs were prepared in many different research groups via a few different methods and were synthesized primarily to target more flexible PBI films for fuel cell applications.[21-24] The synthesis of P,P-Ether PBI has been performed under microwave irradiation using polyphosphoric acid and phosphorous pentoxide between 40-200°C.[21] While in another study, this same analog was synthesized in Eaton's reagent (methane sulfonic acid and phosphorous pentoxide) at 140°C.[22] A similar para-oriented PBI analog that contains an additional ether-phenyl linkage per repeat unit has also been reportedly synthesized in Eaton's reagent, however, films were reportedly too brittle to undergo mechanical and conductivity testing.[23] P,P-Ether PBI has also been used in a copolymer system with para-PBI to study the effects the ether linkage had when incorporated in varying amounts.[24]

A new method for polymerizing high inherent viscosity PBI from sodium bisulfite adduct monomers and tetraamines was recently discovered, however, the study focused strictly on the synthesis of meta-PBI. The research herein discusses the polymerization of two ether containing PBI moieties, poly[2,2'-(p-oxydiphenylene)-5'5-benzimidazole] (P,P-ether PBI) and poly[2,2'-(m,p-oxydiphenylene)-5'5-benzimidazole] (M,P-ether PBI), directly in dimethyl acetamide. The repeat units of these ether-PBIs are shown in Figure 5.1. Though P,P-Ether PBI has been synthesized a number of times, synthesis has always been performed using dicarboxylic acid monomers with a tetraamine in an

inorganic solvent. No studies involving M,P-Ether PBI have been reported. This study first includes the synthesis of bisulfite adduct monomers to be used in the ether-PBI synthesis with the goal of producing a more processable polymer directly in organic solvent. The solubilities and thermal stabilities of the resulting polymers are explored and discussed and comparisons between the two chemistries are made.

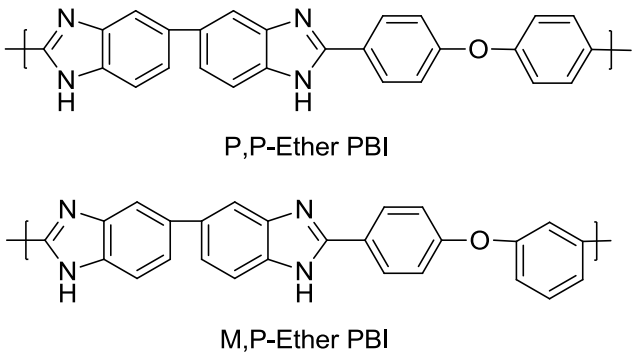

Figure 5.1 Ether-PBI Chemistries

5.3 Experimental

5.3.1 Materials.

4-Fluorobenzaldehyde (98%), 3-hydroxybenzaldehyde (>99%), and 4-hydroxy benzaldehyde (97%) were purchased from Sigma Aldrich. Sodium bisulfite was purchased from JT Baker. TAB monomer, 3,3',4,4'-tetraaminobiphenyl (polymer grade, ~97.5 %) was donated by Celanese Ventures, GmbH. Methanol, dimethyl sulfoxide (DMSO), tetrahydrofuran (THF), dichloromethane (DCM), dimethyl formamide (DMF), and potassium carbonate were purchased from Fisher Scientific. Dimethyl acetamide (DMAc) was purchased from Oakwood Products. All chemicals were used as received unless otherwise stated.

5.3.2 Synthesis of 3-(4-formylphenoxy)benzaldehyde.

4-Fluorobenzaldehyde (20.0g, 0.163 mol), 3-hydroxybenzaldehyde (20.3g, 0.163 mol), potassium carbonate (11.3g, 0.082 mol), and dimethyl acetamide (DMAc) (150 mL) were charged to a 500 mL 3-neck round bottom flask equipped with a magnetic stir bar, reflux condenser, and nitrogen inlet and outlet. The reaction was heated to 140 °C for 4-8 hours at which point the solution turned dark purple/brown in color. Upon cooling to room temperature, the solution was poured into 1.0 L of distilled water. A sludgy brown layer formed on the bottom of the beaker and was scratched with a metal spatula in order to initiate nucleation. Upon scratching for ~15 minutes, brown solid precipitated out. The brown solid was collected via vacuum filtration and was washed with distilled water. The product was allowed to dry in the air for 2 days. Product was confirmed via ^{1}H-NMR and melting point comparison.[25] ^{1}H-NMR: (300 MHz, DMSO-d6) δ 9.9 (s, 1H), 7.9 (d, 1H), 7.8 (s,1H), 7.6 (t, 1H), 7.5 (s, 1H), 7.4 (d, 1H), 7.2 (d, 1H). Lit melting point[25]: 58-59°C Actual melting point: 58-59°C. (Yield= 24.3g, 66%)

Scheme 5.1: Synthesis of 3-(4-formylphenoxy)benzaldehyde

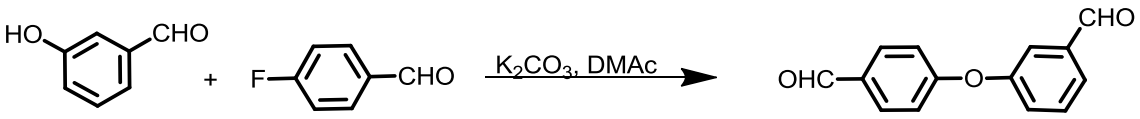

5.3.3 Synthesis of 4,4'-oxydibenzaldehyde.

4-Fluorobenzaldehyde (20.0g, 0.163 mol), 4-hydroxybenzaldehyde (20.3g, 0.163 mol), potassium carbonate (11.3g, 0.082 mol), and dimethyl acetamide (DMAc) (150 mL) were charged to a 500 mL 3-neck round bottom flask equipped with a magnetic stir bar, reflux condenser, and nitrogen inlet and outlet. The reaction was heated to 140 °C for 4-8 hours at which point the solution turned dark purple/brown in color. The solution was

then allowed to cool to room temperature. Contents were poured into 750 mL of distilled water at which point a sludgy, brown layer formed on the bottom of the beaker. A metal spatula was used to scratch the sludgy layer in order to initiate nucleation. Upon scratching for ~15 minutes, tan solid precipitated out. The tan solid was collected via vacuum filtration and washed with water. The product was allowed to dry in the air for 2 days. Product was confirmed via ^{1}H-NMR and melting point comparison.[26] ^{1}H-NMR: (300 MHz, DMSO-d6) δ 9.9 (s, 1H), 7.9 (d, 1H), 7.3 (d, 1H). Lit melting point[26]: 59-64 °C. Actual melting point: 53-55 °C. (Yield= 22.0g, 59%)

Scheme 5.2: Synthesis of 4,4'-oxydibenzaldehyde

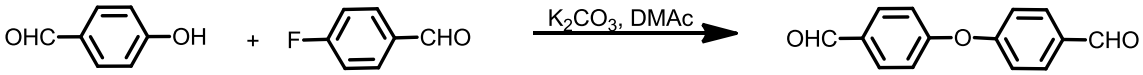

5.3.4 Synthesis of M,P-Ether Bisulfite Adduct (sodium hydroxy(3-(4-(hydroxy(sulfonato)methyl) phenoxy) phenyl) methane sulfonate)

3-(4-formylphenoxy)benzaldehyde (7.08 g, 0.031 mol) was dissolved in methanol (704 mL) in a 1 L resin kettle equipped with an overhead stirrer. Sodium bisulfite (6.45 g, 0.062 mol) was dissolved in water (107 mL) in a 250 mL beaker. Upon each solid dissolving in the respective solvent, the sodium bisulfite solution was added to the methanol solution over a ten minute period. After approximately 15 minutes, the solution turned from a transparent amber color to an opaque, light brown color and tan solid had precipitated. Precipitate was collected via vacuum filtration, washed with methanol, and dried under vacuum at 80 °C. Product was confirmed via ^{1}H NMR: (300 MHz, DMSO-d6) δ 7.4 (d, 1H), 7.2 (d, 1H), 7.1 (s, 1H), 6.9 (d, 1H), 6.8 (t, 2H), 5.9 (s, 1H), 5.8 (d, 1H), 4.9 (d, 2H). (Yield= 10.4g, 77%)

Scheme 5.3: Synthesis of M,P-Ether Bisulfite Adduct

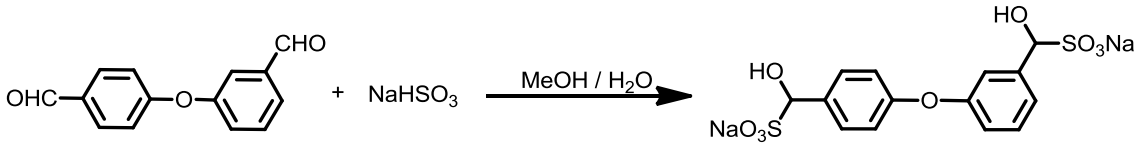

5.3.5 Synthesis of P,P-Ether Bisulfite Adduct (sodium (oxybis(4,1-phenylene))bis(hydroxy methanesulfonate))

4,4'-Oxydibenzaldehyde (7.08g, 0.031 mol) was dissolved in methanol (704 mL) in a 1 L resin kettle equipped with an overhead stirrer. Sodium bisulfite (6.45g, 0.062 mol) was dissolved in water (321 mL) in a 500 mL beaker. Upon each solid dissolving in the respective solvent, the sodium bisulfite solution was added to the methanol solution over a 10 minute period. After approximately 15 minutes, the solution turned from a transparent amber color to an opaque tan color and white solid had precipitated. Precipitate was collected via vacuum filtration, washed with methanol, and dried under vacuum at 80 °C. Product was confirmed via ^{1}H NMR: (300 MHz, DMSO-d6) δ 7.5 (d, 1H), 6.9 (d, 1H), 5.9 (d, 1H), 4.9 (d, 1H). (Yield= 11.2g, 83 %)

Scheme 5.4: Synthesis of P,P-Ether Bisulfite Adduct

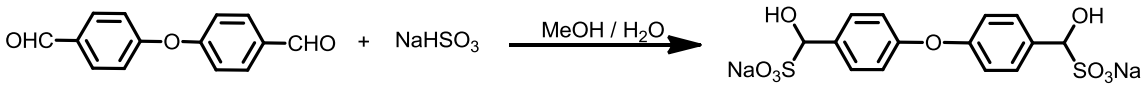

5.3.6 Synthesis of Ether PBIs.

The bisulfite adduct (M,P-ether bisulfite adduct or P,P-ether bisulfite adduct) (4.30g, 9.89mmol) and 3,3',4,4'-tetraaminobiphenyl (TAB) (2.11g, 9.89mmol) were charged to a 100 mL 3-neck flask in a nitrogen environment. Dimethyl acetamide (25 mL) was then added to the flask before being placed in a silicone oil bath. The flask was

equipped with a reflux condenser, overhead stirrer, and nitrogen inlet. Polymerizations took place at reflux for 48 hours with a stir rate of 60 RPM. Upon reaching reflux, P,P-Ether PBI was an opaque mint green color and M,P-Ether PBI was a light orange. Polymer had appeared to begin crashing out of solution even at reflux and solution was slightly viscous. After 48 hours, the polymer solution was allowed to cool to room temperature. It was poured into distilled water and chopped using a blender. This was repeated 3x followed by blending 3x in methanol. Polymer was collected using vacuum filtration then dried under vacuum at 150 °C. ^{1}H-NMR was performed using both polymers. The polymers were soluble in DMSO-d6 at low concentrations. P,P,-Ether PBI could be more clearly seen than M,P-Ether PBI in the spectra. ^{1}H-NMR for P,P-Ether PBI: (300 MHz, DMSO-d6) 13.1 (s, 1H), 8.3 (s, 1H), 8.1 (s, 1H), 7.9 (d, 1H), 7.6 (d, 1H), 7.3 (s, 1H). Unfortunately, the M,P-Ether PBI was difficult to see, however, a broadening of the baseline at ~13 ppm, indicative of the benzimidazole[27], could be seen in spectra as well as other aromatic peaks between 7 and 8 ppm. Unfortunately, the polymer's limited solubility made it difficult to interpret the spectra any further. Lithium chloride was added to the samples to assist with solubility; however, it did not enhance solubility enough to report a clear spectra.

Scheme 5.5: Synthesis of Ether PBI

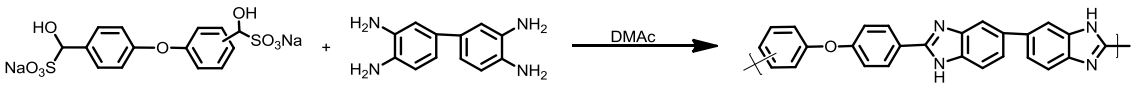

5.4 Characterization Techniques.

5.4.1 Thermal Gravimetric Analysis (TGA). TGA of dried polymer samples was conducted using a TA Instruments Q5000 with nitrogen or air flow rates of 25mL/min and a heating rate of 20 ˚C/min. TGA was performed from room temperature to 800 ˚C.

Differential scanning calorimetry (DSC) was conducted using a TA Instruments Q2000 with 50 mL/min nitrogen flow and a heating rate of 10 °C/min.

5.4.2 Inherent Viscosity. Inherent viscosity (IV) measurements were conducted using a Cannon Ubbelohde (200 μm) viscometer at a concentration of 0.2 g/dL in sulfuric acid (H_2SO_4) at 30.0 ˚C. Samples were prepared by dissolving the dried polymer powders in sulfuric acid using a mechanical shaker. Reported IV values are an average of three separate measurements and were calculated as previously reported.[28]

5.4.3 Solubility Testing. Solubility testing was performed by first weighing the polymer sample and allowing it to stir in a scintillation vial in various solvents. All solubility tests were performed at both room temperature and at reflux at a concentration of 1 wt% polymer.

5.4.4 Film Preparation. The general membrane preparation procedure for M,P-Ether PBI and P,P-Ether PBI was as follows: 1.000 g PBI powder was mixed with approximately 30 ml DMAc in a 100 ml round-bottom flask and then refluxed for 3-4 hours until most polymer solids were dissolved. The solution was cooled to room temperature and centrifuged at 5500 RPM for 30 minutes. The solution was then decanted to remove insoluble particles. The PBI membrane was then cast in a glove bag under dry nitrogen atmosphere. The PBI solution was poured onto a clean glass plate which was taped with glass slides on each side to restrain the movement of the solution. After casting, the membrane was pre-dried inside the glove bag with a hotplate temperature of 40-50℃ overnight to remove most dimethyl acetamide. The film was then transferred to the vacuum oven and dried at 110℃ overnight to obtain the PBI membrane.

5.4.5 Tensile Testing. The tensile properties of the membranes were tested at room temperature using an Instron Model 5543A system with a 10 N load cell and crosshead speed of 5 mm/min. Strips of film were cut to 5 cm x 1 cm and preloaded to 0.1 N prior to testing.

5.5 Results and Discussion.

Two novel ether bisulfite adduct monomers were synthesized by first undergoing nucleophilic aromatic substitution between the hydroxy-aldehyde and the fluoro-aldehyde compounds as seen in Scheme 1 and Scheme 2. Upon pouring the solution mixture into water, a great amount of scratching had to be done to initiate the nucleation. 3-(4-formylphenoxy)benzaldehyde was much more difficult to precipitate than 4,4'-oxydibenzaldehyde and required a more dilute mixture. Both compounds were confirmed via ^{1}H-NMR and through comparison to the melting points of these molecules that were previously published. Figure 5.2 shows the spectra of 3-(4-formylphenoxy)benzaldehyde and Figure 5.3 shows the spectra of 4,4'-oxydibenzaldehyde.

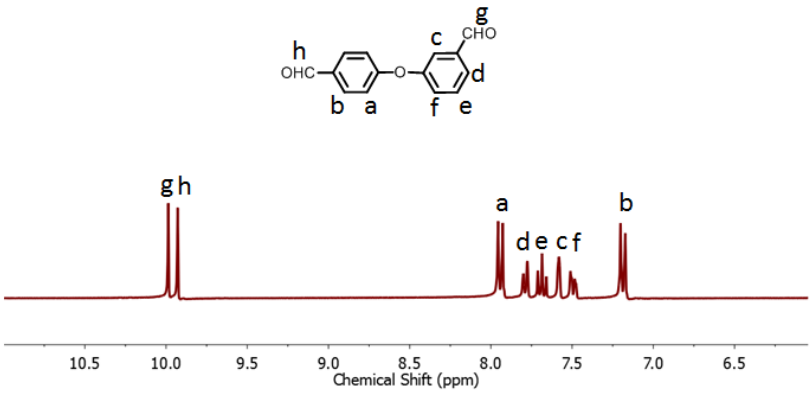

Figure 5.2: ^{1}H-NMR Spectra of 3-(4-formylphenoxy)benzaldehyde in DMSO

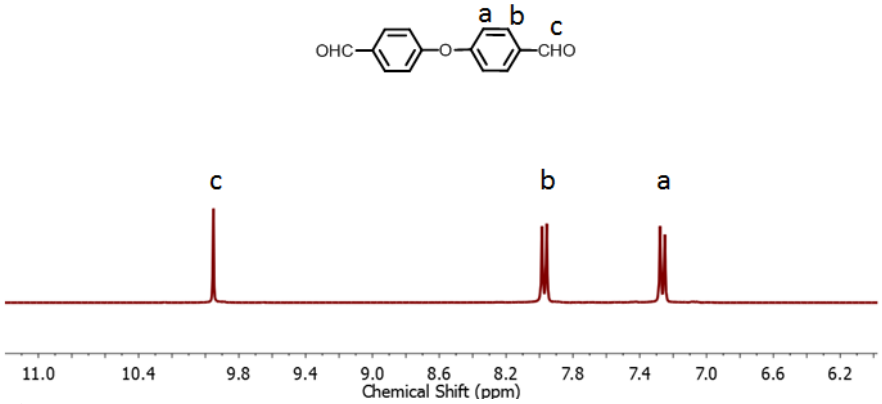

Figure 5.3: ^{1}H-NMR of 4,4'-oxydibenzaldehyde in DMSO

The ether dialdehydes were then converted to ether bisulfite adducts using sodium bisulfite in a water/methanol mixture as seen in Schemes 5.3 & 5.4. Both new dialdehydes had a significantly lower solubility in methanol than the previously discussed isophthalaldehyde bisulfite adduct which could be attributed to the additional phenyl ring in each dialdehydes. ^{1}H-NMR was used to characterize the new bisulfite adduct monomers. Figure 5.4 and 5.5 show the spectra of M,P-Ether bisulfite adduct and the P,P-ether bisulfite adduct, respectively. It is important to note the impurities seen in the spectra are attributed to the conversion of a single aldehyde to the bisulfite adduct rather than conversion of both aldehydes. It has been found in the past that monomer containing >3% aldehyde leads to a noticeable decrease in inherent viscosity due to the imbalance in stoichiometry which can be explained using Carother's equation.

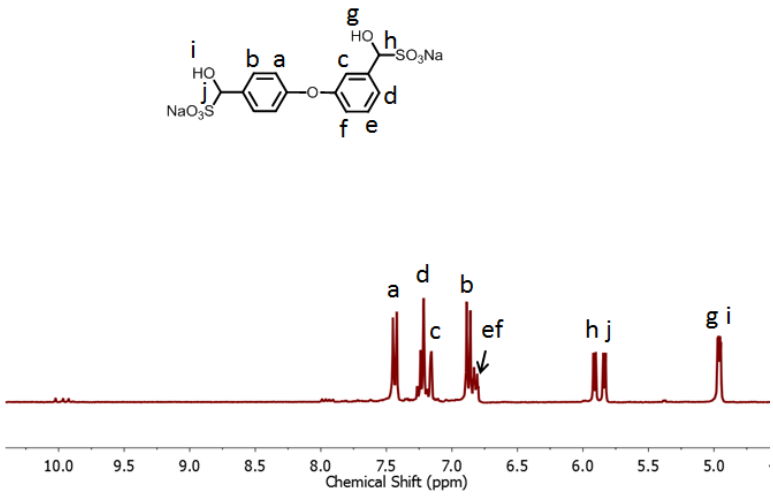

Figure 5.4: [1]H-NMR of M,P-Ether Bisulfite Adduct in DMSO-d6

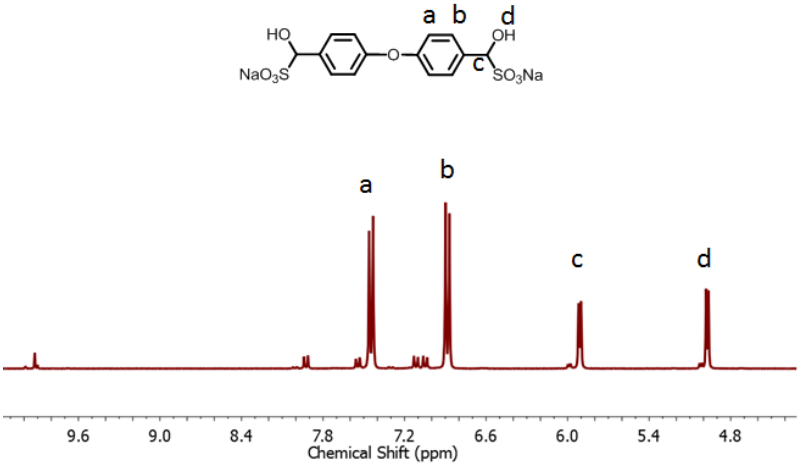

Figure 5.5: [1]H-NMR of P,P-Ether Bisulfite Adduct in DMSO-d6

These new bisulfite adduct monomers were able to successfully produce ether-PBI analogs through a new solution polymerization method in dimethyl acetamide. Inherent viscosities of the M,P-Ether PBI and the P,P-Ether PBI were found to be 0.50 dL/g and 0.55 dL/g, respectively. These inherent viscosities were potentially limited by the solubility of the polymer at this concentration since polymer began crashing out of

solution at reflux. This indicates that the polymerization concentration was too high and higher IV polymer could be targeted using a more dilute synthesis. Though the polymer was not of high IV, the polymer powders were still useful in the characterization of these new PBI analogs produced via a new synthetic method. ^{1}H-NMR was used to confirm that PBI had been synthesized and the benzimidazole peak was found at ~13.0 ppm for both polymers.

Thermogravimetric analysis was performed in order understand the thermal stability of these new PBIs containing ether linkages. Figure 5.6 shows the weight loss of the polymers at various temperatures. Meta-PBI prepared through the solution polymerization method was also included so the thermal stabilities of these polymers could not only be compared to each other to determine how backbone orientation affected decomposition, but also to determine what affect the ether linkage had on thermal decomposition. It can be seen under nitrogen conditions that both M,P-Ether PBI and P,P-Ether PBI exhibit a decrease in weight at the up to 200 °C which can be attributed to water and residual dimethyl acetamide loss. Also, the bisulfite adduct end groups decompose between 120-140°C which could further explain some of the weight loss at these temperatures. From 200-300°C, M,P-Ether PBI exhibits a 10% weight loss while P,P-Ether PBI only exhibits a 3% weight loss, while both polymers exhibit ~ 5% weight loss from 300-500°C. In a previous study, the thermal degradation mechanism of poly(ether ether ketone) (PEEK) was explored.[29] The aryl ether linkages were found to begin decomposition to phenol-containing units around 450°C.[29] Chain scission of the aryl-ether linkages is also found to cause crosslinking around this temperature. Though these ether-PBIs are not identical in structure to PEEK, their similar aryl-ether units can

explain some of the weight loss up to 500°C. Potential rearrangement within the M,P-Ether PBI backbone could also explain some of the loss seen from 200-300°C and could be a result of the more flexible backbone than that of the P,P-Ether PBI. Around 550°C, all three polymers produced through the solution polymerization method start to undergo a more rapid weight loss. Since meta-PBI contains no ether linkages, this weight loss can be attributed to the decomposition of the benzimidazole units. Overall, the ether-PBIs were found to have a lower thermal stability than that of meta-PBI prepared via the solution polymerization method.

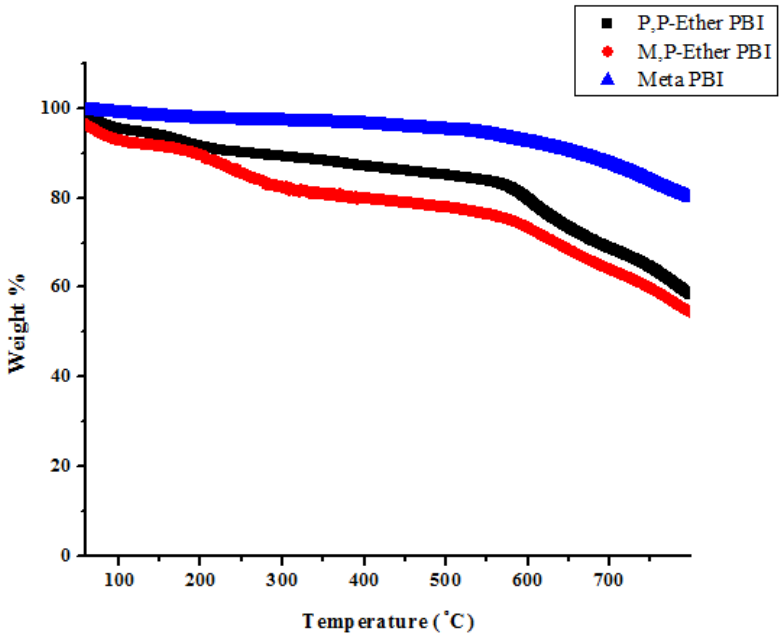

Figure 5.6: TGA of PBI Analogs Prepared Via Solution Polymerization Method

In order to understand the solubility of these newly synthesized polymers, various organic solvents were investigated. It is well-known that fully aromatic PBIs exhibit an extremely low solubility in organic solvents, hence the motivation to develop the solution polymerization method discussed in the previous chapter. Since these are not fully aromatic polybenzimidazoles, they could potentially demonstrate different solubility

characteristics. In order to determine the solubility of these polymers, five different solvents were chosen and tests were conducted on both M,P-Ether PBI and P,P-Ether PBI at 1 wt% polymer. Tests were performed at both room temperature and at the solvents' boiling points. Table 5.1 shows the solubility of these polymers in the various solvents.

Table 5.1: A.) Solubility of P,P-Ether PBI, B.) Solubility of M,P-Ether PBI

A.)

P,P-Ether PBI	DMSO	DMAc	DMF	THF	DCM
Room temp.	++	+	+	N	+
Heated	++	++	++	N	+

B.)

M,P-Ether PBI	DMSO	DMAc	DMF	THF	DCM
Room temp.	++	++	+	N	+
Heated	++	++	++	N	+

++ means completely soluble, + means slightly soluble, and N means insoluble

Both chemistries were soluble in dimethyl sulfoxide at both room temperature and at reflux. These ether-PBIs also demonstrated similar solubility trends in DCM, DMF, and THF. Both polymers were slightly soluble in DCM and fully soluble in DMF at reflux, however, neither demonstrated solubility in THF. The only solubility difference seen within the polymers was in DMAc. P,P-Ether PBI was only slightly soluble in DMAc at room temperature, however, M,P-Ether PBI was completely soluble in DMAc at room temperature. This could in part be attributed to the structure of the backbone since M,P-Ether is less rigid than P,P-Ether PBI. Molecular size would not be a factor in this study considering the IVs were relatively the same (0.50 dL/g and 0.55 dL/g,

respectively). Both polymers are soluble in DMAc at reflux which is to be expected considering DMAc was used as the polymerization solvent.

Since polybenzimidazole films produced through different polymerization methods are commonly characterized, a film was formed from the M,P-Ether PBI in order to assess mechanical properties. Films were able to be formed; however, they were too brittle to undergo mechanical testing. The M,P-Ether PBI film, which can be seen below, was transparent and yellow in color, and extremely brittle. The film was cut into strips to be used for tensile testing, however, the film cracked when the clamps of the Instron closed. Films were synthesized through the same method for P,P-Ether PBI and were red in color, however, they were also brittle and were unstable to undergo mechanical testing.

Figure 5.7: M,P-Ether PBI Film

Differential scanning calorimetry (DSC) was performed on these samples with the goal of determining the glass transition temperature (T_g) of each of these polymers to compare it to other PBI chemistries. It was hypothesized that the ether linkage, which would allow for a more flexible backbone than that of the fully aromatic PBI chemistries,

could lead to a lower T_g and a potentially more processable chemistry of PBI. Although other researchers have synthesized ether-containing PBI, none have reported the glass transition temperatures (T_g) or DSC results. Upon testing the ether-PBIs using both standard DSC and modulated DSC, the spectra revealed a large amount of noise and no T_g was conclusive from any of the runs. Although this was initially disappointing, this noise could potentially be explained by the rearrangement of the aryl-ether units in the backbone that have been reported in previous studies.[29]

5.6 Conclusion.

In this study, it was found that new bisulfite adduct monomers containing ether linkages could be synthesized in order to successfully synthesize two ether-containing PBIs, M,P-Ether PBI and P,P-Ether PBI. All steps of the synthesis were confirmed via ^{1}H-NMR. These ether-containing PBIs were assessed through solubility studies and thermogravimetric analysis. They indicated they had a greater solubility in organic solvents than most fully aromatic PBIs and also a lower thermal stability than that of meta-PBI prepared via the solution polymerization method. DSC was inconclusive; however, this could be attributed to the rearrangements exhibited in aryl-ethers at high temperatures.

5.7 Future Work.

In the future, polymerization trials for both polymers should be conducted at a range of polymer concentrations to determine the optimal polymerization concentration for obtaining high IV polymer. A higher IV polymer could increase the thermal stability of the polymer and could potentially lead to more stable films for mechanical testing due to greater chain entanglement. Copolymer systems containing ether-PBI could also be studied to assess structure-property relationships.

5.8 References.

(1) Bingham, M. A., Hill, B. J. *Journal of Thermal Analysis*.**1975**, *7*, 347.

(2) Mader, J., Xiao, L., Schmidt, T.J., Benicewicz, B.C. *Advances in Polymer Science*.**2008**, *216*, 63.

(3) Mader, J. A., Benicewicz, B. C. *Fuel Cells*.**2011**, *11*, 212-221.

(4) Gulledge, A. L., Gu, B., Benicewicz, B.C. *Journal of polymer Science Part A: Polymer Chemistry*.**2012**, *50*, 306.

(5) Gulledge, A. L., Chen, X., Benicewicz, B.C. *Journal of polymer Science Part A: Polymer Chemistry*.**2014**, *52*, 619.

(6) Molleo, M., Schmidt, T., Benicewicz, B.C. In *Encyclopedia of Sustainability, Science and Technology*; Meyers, R. A., Ed.; Springer Science + Business Media LLC: New York, 391-431, 2013.

(7) Li, Q., Jensena, J.O., Savinell, R.F., Bjerrum, N. *Progress in Polymer Science*.**2009**, *34*, 449.

(8) Li, Q., He, R., Berg, R. W., Hjuler, H. A., Bjerrum, N. J. *Solid State Ionics*.**2004**, *168*, 177.

(9) Perry, K., Eisman, G., Benicewicz, B.C. *Journal of Power Sources*.**2008**, *177*, 478.

(10) Huth, A., Schaar, B., Oekermann, T. *Electrochimica Acta*.**2009**, *54*, 2774.

(11) Coffin, D. R., Serad, G.A., Hicks, H.L., Montgomery, R.T. *Textile Research Journal*.**1982**, *52*, 466.

(12) Molleo, M. A., Chen, X., Ploehn, H. J., Benicewicz, B. C. *Fuel Cells*.**2015**, *15*, 150.

(13) Yu, S., Benicewicz, B.C. *Macromolecules*.**2009**, *42*, 8640.

(14) Hilborn, J. G., Labadie, J.W., Hedrick, J.L. *Macromolecules*.**1990**, *23*, 2854.

(15) White, D. M., Takekoshi, T., Williams, F. J., Relles, H. M., Donahue, P. E., Klopfer, H. J., Loucks, G. R., Manello, J. S., Matthews, R. O., Schluenz, R. W. *Journal of Polymer Science: Polymer Chemistry Edition*.**1981**, *19*, 1635.

(16) Hergenrother, P. M., Kiyohara, D. E. *Macromolecules*.**1970**, *3*, 387.

(17) Wrasidlo, W., Augl, J. M. *Macromolecules*.**1970**, *3*, 544.

(18) Hedrick, J. L. *Macromolecules*.**1991**, *24*, 6361-6364.

(19) Twieg, R., Matray, T., Hedrick, J. L. *Macromolecules*.**1996**, *29*, 7335.

(20) Foster, R., Marvel, C. S. *Journal of Polymer Science Part A: General Papers*.**1965**, *3*, 417.

(21) Kang, Y., Zou, J., Sun, Z., Wang, F., Zhu, H., Han, K., Yang, W., Song, H., Meng, Q. *International Journal of Hydrogen Energy*.**2013**, *38*, 6494.

(22) Li, J., Li, X., Zhao, Y., Lu, W., Shao, Z., Yi, B. *ChemSusChem*.**2012**, *5*, 896.

(23) Henkensmeier, D., Cho, H., Brela, M., Michalak, A., Dyck, A., Germer, W., Duong, N., Jang, J.H., Kim, H.J., Woo, N.S., Lim, T.H. *International Journal of Hydrogen Energy*.**2014**, *39*, 2842.

(24) Kim, T. H., Kim, S.K., Lim, T.W., Lee, J. *Journal of Membrane Science*.**2008**, *323*, 362.

(25) Gawroński, J., Brzostowska, M., Kwit, M., Plutecka, A., Rychlewska, U. *The Journal of Organic Chemistry*.**2005**, *70*, 10147.

(26) Guilani, B., Rasco, M., Hermann, C., Gibson, H.W. *Journal of Heterocyclic Chemistry*.**1990**, *27*, 1007.

(27) Conti, F., Willbold, S., Mammi, S., Korte, C., Lehnert, W., Stolten, D. *New Journal of Chemistry*.**2013**, *37*, 152.

(28) Mader, J. A., Benicewicz, B. C. *Macromolecules*.**2010**, *43*, 6706-6715.

(29) Patel, P., Hull, T., McCabe, R., Flath, W., Grasmeder, D., Percy, M. *Polymer Degradation and Stability*.**2010**, *95*, 709.

CHAPTER 6

SUMMARY AND OUTLOOK

6.1 Summary and Outlook.

Polybenzimidazoles (PBI), a class of condensation polymers which has long been known for its thermal and chemical stabilities, has proven useful in high temperature applications, such as, fuel cell membranes and high performance fibers. Due to the need of alternative energy sources, PBI has the opportunity to continue being heavily investigated for use as a polymer electrolyte membrane in fuel cell applications. New, efficient methods for the polymerization of polybenzimidazole are always of interest as PBI is a versatile polymer and is useful in many applications.

In the first part of this dissertation, two novel PBI homopolymers, each containing one hydroxyl unit per polymer repeat unit, were synthesized via the PPA Process and evaluated as possible candidates to be used as the polymer electrolyte membrane in high temperature polymer electrolyte membrane fuel cells (HTPEMFC). 2-Hydroxyterephthalic acid, a diacid monomer, was synthesized to be used in the polymerization of p-OH PBI. These two homopolymers were chosen for investigation due to the interesting properties previously exhibited in PBI chemistries containing hydroxyl functional units. Both polymers were found to contain phosphate-ester linkages and phosphate bridges between polymer chains after undergoing polymerization in polyphosphoric acid (PPA). The p-OH PBI chemistry had a slightly higher solubility in PPA than the previously studied 2OH-PBI chemistry and a lower solubility than the m-OH PBI chemistry.[1] This was to be expected as the p-OH PBI had less opportunity to form phosphate bridges (physical crosslinks) between chains since it contained fewer hydroxyl units than the 2-OH PBI. It was also hypothesized that p-OH PBI would have a lesser solubility than the m-OH PBI which has a more flexible backbone. The conductivity of the p-OH PBI was very high compared to many of the PBI chemistries

previously studied which could be attributed to both the chemistry of the polymer and the great amount of phosphoric acid (PA) present within the membrane. The m-OH PBI membrane had a higher conductivity than standard meta-PBI but did not exhibit the high conductivity seen in the p-OH membrane. Mechanical properties indicate low tensile properties overall but good compliance creep properties compared to some of the other PBI chemistries that have been study for use in fuel cells. Fuel cell performance was evaluated for each membrane. The p-OH PBI was able to operate at a current density up to 1.0 A/cm^2 and is considered to be a good candidate for use in these high temperature fuel cells, however, the m-OH PBI was unable to operate at high current densities and started to show performance loss as temperature was decreased. The poor performance of the m-OH PBI can be attributed to solubility issues within the PA at high temperatures.

Next, a copolymer system involving the p-OH PBI chemistry and para-PBI was investigated at five different compositions of these two analogs. The properties of these membranes were compared to both the p-OH PBI and para-PBI homopolymers to understand how properties of these copolymer systems were different from the homopolymers. All resulting copolymers were casted at what appeared to be an optimal solution viscosity, however, all membranes in the copolymer series were found to have relatively low inherent viscosities (IV). Membranes were transparent and red in color with the exception of the 50/50 p-OH/para composition which was a cloudy red membrane. Acid contents ranged from 20-32.6 moles PA/ mole polymer repeat unit. The conductivities of these copolymer membranes were relatively similar (0.1-0.15 S/cm) which the exception of the 50/50 chemistry which demonstrated a higher conductivity at 0.25 S/cm. This conductivity is close to that of the para-PBI homopolymer but still

significantly lower than that of the p-OH PBI homopolymer. Potential reasons for the low conductivities seen within these films could be attributed to the low IV which could lead to solubility issues in PA at high temperatures. Fuel cell performance was tested on the 50/50 and the 25/75 p-OH PBI/para PBI membranes. These were selected in order to use the membrane that exhibited the highest conductivity and another membrane was chosen since the other four exhibited similar properties. Upon testing the 50/50 composition, the fuel cell immediately died. This could be attributed to potential solubility issues as the membrane had a low IV. The 25/75 film performed better than the 50/50 composition, however, past a current density of 0.4 A/cm^2, the fuel cells voltage quickly dropped. In the future, investigations on these polymers' morphologies could be investigated to determine how the two chemistries interact and to determine if they are random or blocky in nature.

In the fourth chapter, a new method for synthesizing polybenzimidazole directly in organic solution was investigated. Many methods of synthesizing PBI have been reported; however, due to the limited solubility of PBI in organic solvent, no previous reports of high IV polymer produced directly in organic solvent had been reported. This project was geared originally toward fiber applications of meta-PBI as the fiber itself is spun from a dimethyl acetamide (DMAc) and LiCl solution. Small molecule studies were evaluated to determine the reactivity of the functional units with the intention of forming phenyl benzimidazole. It was found that of the four small molecules screened, that the bisulfite adduct of the aldehyde and the ortho-diamine produced phenyl benzimidazole effectively and with no obvious side products from competitive reactions. This was previously reported in 1970 by Higgins and Marvel to synthesize meta-PBI, however,

they were only able to perform the reaction at low concentrations and produced low IV polymer.[2] The IV as a function of polymer concentration was studied ranging from 1-26 wt% polymer and it was found that the optimal polymerization concentration was between 18 and 22 wt%. Time studies were performed to assess how IV was affected over a range of times and at various polymer concentrations, however, no correlation seemed present in any of the studies. At this point monomer purity was reevaluated and a new, more dilute monomer synthesis was employed. Along with a better procedure for monomer synthesis, investigations into literature indicated that sulfur dioxide that was generated through the reaction itself was used as the oxidant in the final ring closure of the benzimidazole. Sodium metabisulfite, which decomposes to sulfur dioxide and sodium sulfite at high temperatures, was used as additional oxidant in these polymerizations to target higher IV. It was found that by generating sulfur dioxide in situ, the IV of the polymer increased significantly compared to the polymerizations conducted without additional sulfur dioxide. In the future, a better understanding of how much sodium metabisulfite needs added to the polymerization and over what time period should be investigated to gain better control of the IV.

It is important to note that although the solution polymerization method previously discussed was focused on the synthesis of meta-PBI, this solution polymerization method is not limited to just one chemistry of PBI. Chapter 5 investigates two PBI chemistries, each containing an ether linkage, which were synthesized via the solution polymerization method. In order to produce PBI containing an ether linkage, monomers first needed to be synthesized. This was done in a two-step process. In the first step, a fluorbenzaldehyde was reacted with a hydroxylbenzaldehyde to generate a

dialdehyde containing an ether linkage between phenyl rings. This was done to produce both a para/para dialdehyde and a meta-para dialdehyde. These dialdehydes were then dissolved in methanol and a solution of sodium bisulfite in water was added to produce the new bisulfite adduct monomers. These new monomers were then used to make P,P-ether PBI and M,P-Ether PBI. Since these were new chemistries to this polymerization method, solubility testing was performed. Thermogravimetric analysis was also performed to determine if the ether linkage would lower the thermal stability. It was found that compared to standard meta-PBI prepared through via solution polymerization, the ether PBIs exhibited a lower decomposition temperature than the meta-PBI. DSC was performed in order to assess the polymers' glass transition temperatures (T_g) to determine if the ether linkage lowered the T_g below that of meta-PBI. Using both modulated DSC and standard DSC, a T_g on these polymers was inconclusive due to the noise of the spectra, however, this noise could potentially be explained by the aryl ether rearrangement at high temperatures. Films were formed from both polymers, however, they were too brittle to undergo mechanical testing. This could potentially be caused from the low inherent viscosity of the polymers. In the future, optimal polymerization concentrations should be performed on these polymers in order to produce a higher IV polymer and to understand more about the solubility of these polymers in DMAc.

6.2 Conclusion.

In conclusion, various chemistries of PBIs were investigated to understand how the chemistry of the polymer affects the polymer's properties. In the future, new chemistries and copolymer systems should be assessed to continue optimizing fuel cell membranes. With the ability to synthesize polymers directly in DMAc, new chemistries of PBI should be investigated through this process which could potentially be useful in a

variety of applications. Comparisons could also be made between polymers of the same chemistry produced through both the PPA Process and the solution polymerization method to determine how process affects the polymer.

6.3 References.

(1) Yu, S., Benicewicz, B.C. *Macromolecules* **2009**, *42*, 8640.
(2) Higgins, J., Marvel, C. S. *Journal of Polymer Science Part A-1: Polymer Chemistry* **1970**, *8*, 171.

APPENDIX A – PERMISSION TO REPRINT

Thank you for your order! A confirmation for your order will be sent to your account email address. If you have questions about your order, you can call us at +1.855.239.3415 FREE Toll Free, M-F between 3:00 AM and 6:00 PM (Eastern), or write to us at info@copyright.com. This is not an invoice.

Confirmation Number: 11464857
Order Date: 10/11/2015

If you paid by credit card, your order will be finalized and your card will be charged within 24 hours. If you choose to be invoiced, you can change or cancel your order until the invoice is generated.

Payment Information

Kayley Fishel
fishel@email.sc.edu
+1 (412)6077402
Payment Method: n/a

Order Details

High Temperature Polymer Electrolyte Membrane Fuel Cells : Approaches, Status, and Perspectives

Order detail ID: 68620647
Order License Id: 3726061289724
ISBN: 9783319170817
Publication Type: Book
Publisher: Springer International Publishing

Permission Status: Granted
Permission type: Republish or display content
Type of use: Thesis/Dissertation
View details

Note: This item will be invoiced or charged separately through CCC's **RightsLink** service. More info **$ 0.00**

This is not an invoice.

Total order items: 1

Order Total: 0.00 USD